IFPRI 2022 Project and Review Proposals

New Projects

1. Aeration of Geldart Type C Powders
    a. Olivier Pouliquen, Aix Marseilles University, France
2. Drying of Powders with Shear
    a. Heather Emady, Arizona State University, USA
    b. Alban Sauret, University of California at Santa Barbara, USA
3. Spray Drying of Pastes
    a. Volker Gaukel, Karlsruhe Institute of Technology, Germany
4. Numerical Modeling of Spray Droplet Formation
    a. Olivier Desjardins, Cornell University, USA
    b. Meng Wai Woo, University of Auckland, New Zealand

Collaborations

1. Dynamic Powder Flow: Karen Daniels (North Carolina State University) and Prabhu Nott (India Institute of Science Bangalore)

Renewals

1. Characterization of Spray-Drying Nozzles at Industrially Relevant Conditions, Nasser Ashgriz, University of Toronto, Canada
2. Wetting and Dispersion of Powders, Claire Gaiani, University of Lorraine, France
3. Slurry and Paste Rheology, Erin Koos, University of Leuven, Belgium

Reviews

1. Dynamic Powder Flow: Nico Gray, University of Manchester, UK
2. Particle Simulations Beyond DEM: Farhang Radjai, University of Montpellier, France

IFPRI BRIEF TEMPLATE

Check One: ☐**Project** ☐**Review** ☒**Collaboration**
☐**Workshop** ☐**Other**

Descriptive Title	Collaboration: Karen Daniels & Prabhu Nott on non-local rheology
Working Title[1]	Non-local rheology of dry flows: from experiments to practical model
Technical Area[2]	Dry Systems
Date	June 22, 2021
Short Description	Collaboration between Daniels and Nott to compare experimental data and repair non-local rheology models with dilatancy and wall effects
Objectives	Repair models of non-local rheology with dilatancy and wall effects
Scope	The past decade has seen multiple nonlocal rheological models proposed, all of which need to be tested against experimental data. As an IFPRI grantee, Karen Daniels (NCSU) has produced detailed data on the kinematics and internal stresses in sheared granular flows, and compared to two different models so far. Prabhu Nott (IISc) has recently published an alternative nonlocal rheological model that accounts for dilatancy (which the others do not). As an IFPRI grantee, he is currently working on experiments and model of screw feeders, but has not yet tested the model on simple experimental geometries such as the NCSU annular rheometer. This collaboration grant would facilitate the efforts of Daniels and Nott to elucidate (1) the effects of walls on the kinematics, and (2) the coupling between packing fraction and shear rate (dilatancy), and (3) internal stress fields. The key laboratory measurements needed to compare to the model are the stress profiles, velocity profiles, and packing fraction profiles. NCSU has an existing dataset from the main project (rheology as a function of wall roughness) which will be the starting point for our comparisons. It will likely be necessary to supplement that dataset with improved packing fraction and particle-tracking measurements in the vicinity of both walls. IISc has working code to make predictions from the model, and compare to experimental results. A particularly important variable to measure is the slip velocity at the wall (proportional to the angular velocity of the

[1] Title used in meeting agendas and file archives
[2] One or more from the following list: W = wet systems; D = dry systems; F = particle formation; SR = size reduction; M = modeling; SE = systems engineering

	particles, which is important for identifying Cosserat effects). It may be possible to directly test these assumptions.

Recommended Contractors (2 or 3)		
Name	**Institution**	**Email Address**
Karen Daniels	NC State University	kdaniel@ncsu.edu
Prabhu Nott	Indian Institute of Science	prnott@chemeng.iisc.ernet.in

Submitted By:	
Name	**Organization**
Michel Louge	IFPRI consultant, dry systems
Massih Pasha	Chemours
Simon Greener	P&G
Jarrod Hart	Imerys
Rohit Kumar	Alkermes

Detailed Research Description

The past decade has seen multiple nonlocal rheological models proposed, all of which need to be tested against experimental data. To date, two models (Kamrin, Andreotti) have been well-tested in experiments and perform equivalently; this work was funded by IFPRI during Years 1-6 of Karen Daniels' grant (1,2). As the Kamrin ("cooperative") model has one fewer free parameter, it is the preferred model and has been pursued in more detail. A key limitation of both of these nonlocal models is that they do not account for dilatancy explicitly, and therefore will always be limited in their ability to predict mass flux. In addition, questions remain about how to appropriately set the boundary conditions from first principles. Therefore, it is prudent to continue to examine other nonlocal models. Prabhu Nott (separately from his IFPRI funding) has recently published an alternative nonlocal rheological model that accounts for dilatancy inherently; the model has been validated by DEM simulations, but remains to be tested against experimental measurements (3).

Conveniently, the methods that Daniels has used for validating nonlocal models are quite general: particle-scale kinematics and internal stresses. Sample data collection and coarse-graining of a single image is shown at right (from ARR-12-05). These methods require movies of the dynamics to be taken until mixed lighting (unpolarized light in the red channel for particle-tracking and polarized light in the green channel for internal stress measurements), and the required equipment is already present in her lab. The resulting images (panel b) can be fit to known photoelastic responses (panel c) to provide particle-scale contact force measurements. From this type of data, it is possible to coarse-grain the results to extract the packing fraction, velocity, strain rate fields, and stress fields (both shear and pressure). Nott's nonlocal model is similarly flexible: it can be written in cylindrical coordinates and solved for the annular rheometer geometry that currently exists in Daniels' lab (the same rheometer which has been used to test the other two models).

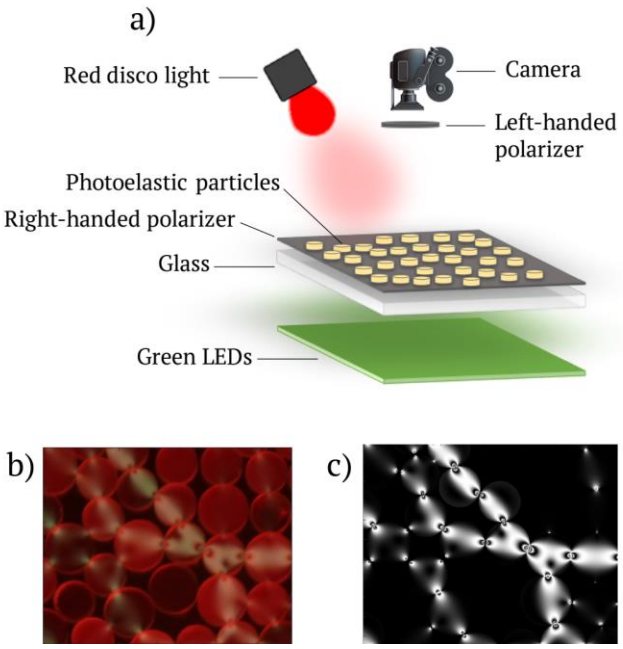

Therefore, we propose to complete the following aims:

- Aim 1: using realistic experimental conditions, determine the appropriate material parameters and solve Nott's nonlocal model. Make a comparison between

measurements from the experiments and predictions from the model, iterating to elucidate the conditions under which agreement is achievable for both strain rate and stress fields
- Aim 2: test the functional form of the coupling between packing fraction and shear rate, the behavior formally known as dilatancy
- Aim 3: use the experiments with different wall-roughness to test the effects of walls on the kinematics

The key laboratory measurements already exist (see ARR-12-06) – stress profiles, velocity profiles, and packing fraction profiles – for experimental runs with a variety of wall-roughnesses. It will likely be necessary to supplement that dataset with improved packing fraction and particle-tracking measurements in the vicinity of both walls, as these were not fully-resolved in previous experiments. A particularly important variable to measure is the slip velocity at the wall (proportional to the angular velocity of the particles, which is important for identifying Cosserat effects). In addition to the aims above, it may be possible to directly test these assumptions if the data is well-enough resolved.

IISc has working code to make predictions from the model and compare to experimental results. Apart from making predictions of the steady state, the model can also make predict the (unsteady) evolution of all the fields starting from a (roughly) uniform packing fraction – this will serve to validate the coupling between the shear rate and packing fraction fields.

This project will proceed by IISc graduate student Gautam making a monthlong visit to work NCSU to work closely with graduate student Fazelpour to establish the best parameters for the model. During this time, Fazelpour would take any additional data that is needed to establish the model and boundary conditions. The second two months would allow for analyzing any additional experimental runs, fine-tuning the model, and writing up the results. This work would need to begin approximately June 1 in order to align with Fazelpour's estimated completion of her PhD during May/June 2022.

Budget: $25000

NCSU: $19000
- 3 month NCSU postdoc: 1/4 ($60k annual salary + 9.05% fringe rate) = $16500
- experimental supplies/machining = $1000
- campus housing for visiting student @ $50/night, 1 month = $1500

IISc: $6000
- Travel for 1 person, 1 month, from India: $2000 transportation + $50 per diem ($1500) = $3500
- 3 month IISC graduate student stipend: $700/month = $2100
- management fees = $400

References:

(1) Zhu Tang, Theodore A Brzinski, Michael Shearer, and Karen E Daniels. Nonlocal rheology of dense granular flow in annular shear experiments. *Soft Matter*. 14:3040-3048 (2018)

(2) Farnaz Fazelpour, Zhu Tang, and Karen E. Daniels. The effect of grain shape and material on the nonlocal rheology of dense granular flows (2021) https://arxiv.org/abs/2108.11369.

(3) Peter Varun Dsouza and Prabhu R. Nott. A non-local constitutive model for slow granular flow that incorporates dilatancy. *Journal of Fluid Mechanics*. 888: R3 (2020)

IFPRI

International Fine Particle Research Institute

Research Project Brief

Aeration and Deaeration of Geldart Type C Powders

The International Fine Particle Research Institute (IFPRI) wishes to fund a research project on aeration and deaeration of Geldart Type C powders that occurs in bulk handling operations such as packaging. Controlled fluidization (i.e., fluidized bed operation or pneumatic conveying) is out of scope of this project.

Geldart Type C powders – fine and cohesive – exhibit unpredictable packaging behavior, for example highly variable packing rates and densities. This is especially true at large-scale production rates, > 100 kg/hour. Different powders behave qualitatively and quantitatively differently, and it is difficult to characterize them in a way that is predictive of their aeration and deaeration behavior. This project should focus on this problem: development of reliable characterization methods for Group C powders that enable prediction of packaging behavior (rate, density, variability) when the material is aerated during handling processes. The work should investigate the effects of single particle properties and particle interactions such as size distribution, surface roughness, particle cohesivity, and electrostatics. Ideally, the proposal should include a representative validation system.

In the packaging operations of interest, the powder is loaded into (semi) bulk containers (flexible or hard walled), 5-20 kg bags, or 1–4-liter bottles. Dosing into small packages (die filling, encapsulation) is out of scope, as this is the subject of other IFPRI projects. Uncontrolled aeration takes place during flow into the package, for example gravity flow in a chute or in a high-speed screw conveyer. Deaeration in the package is time-dependent and often is influenced by compaction (due to the weight of powder in a package or by stacking of multiple packages). Vibration is sometimes used to increase bulk density.

IFPRI
Research Project Brief
Aeration and Deaeration of Geldart Type C powders

Controlling Adhesion between Particles for a better understanding of Compaction and Aeration of Powders.

CAPCAP

- **Principal investigator (PI):** Olivier Pouliquen
- **Host institution:** Aix Marseille University-CNRS, France

- **Proposal duration:** 36 months

To address the problem of powder packaging raised by the IFPRI research program, we propose a fundamental approach consisting in using a model material, for which the inter-particle adhesion can be precisely controlled. We believe that being able to tune the cohesion at will is a necessary condition to develop a fundamental understanding of the flow of cohesive materials and powders. In our group we have recently developed a technics to coat silica particles with polymers and we are able by controlling the coating thickness to continuously varies the cohesion properties, and goes from a cohesionless to a highly cohesive medium. The proposed project consists in using this material to investigate the packaging process. We will first study the rheology of the model material, before analysing a simplified version of a packaging process. We should be able to investigate the role of cohesion and of the rheology of the material in the different steps of the process, from the flow in the hopper to the formation of the deposit, looking also at the stability of the final packing to tap perturbations.

A. General context and state of art

Powders are omnipresent in many industrial processes but predicting their behavior still represents a challenge (Schulze 2008). Whereas the description of coarse granular media has notably progressed during the last 20 Years (Andreotti et al. 2013), our understanding of the physical mechanisms involved during powder flow remains sparse, which represents a real challenge both for engineers designing new industrial processes and for physicists seeking for a unified framework to predict particulate flows. The difficulty comes from the presence of adhesion forces between the grains at the origin of problems of clogging, flow heterogeneities, agglomeration, intermittent flows encountered during the storage, the transportation, the processing of the material. No unified framework exists that can predict and describe the rich variety of behaviors observed with powders, and industry relies on empirical characterization to measure the so-called "flowability", the ability of powders to flow (Castellanos 2005; Tay et al. 2016). This concept that lacks solid physical bases, consists in estimating different properties (compaction, heap angles ...) mostly related to static properties. Recently, powder rheometers have been developed based on the measurement of the torque experienced by a helix rotating in the powder (Hare et al. 2015). All these measurements are of crucial importance in many industrial processes, but do not not have a predictive power, and no framework is nowadays relevant to describe and capture the complex properties of cohesive granular media. Understanding the concept of ”flowability” from a physical point of view is still a challenge.

The challenge posed by IFPRI in this call concerns the aeration and deaeration of fine particles encountered when handling powders and particularly during the filling and packaging process (Rathbone et al. 1987). The control and the reproducibility of the filling process pose major problems such as intermittent flow rates, air trapping, intempestive recompaction of the material during manipulation. Despite the apparent simplicity of the configuration of filling a bag with powders, the process involves different physical phenomena, from the rheology of powders to two-phase flow when the interaction between the powder and the air is important. To improve our fundamental understanding of the mechanics controlling the packaging processes, I think three main questions need to be addressed: the role of particle properties and of the rheology of the powder, the role of the feeding process, and the role of air.

The rheology of powder flows

The first and perhaps most important question concerns the role of the grain properties on the flow characteristics and in particular understanding the crucial role of the adhesion forces. Characterising the rheology of powders and its links to the grain properties is to my opinion a necessary step to progress in our understanding of the aeration problem. We need a detailed knowledge of the powders rheology in the regime encountered during packaging, which is a regime where the material is dense but flow rapidly under low level of stress, typically its own weight. This is a regime not captured by the classical characterisation of quasi-static properties of powders as measured in a Schulze’s shear cell, and there is a need for a controlled and relevant rheological protocol to characterize the "fluid regime". This question is currently motivating numbers of fundamental studies in the granular community (Vo et al. 2020). In absence of adhesion between particles, i.e for dry granular material made of grains interacting through frictional contacts only, a lot of progresses have been achieved. A key property of these materials is that in the limit of rigid particles, no internal stress scale exists in the system. This dimensional argument fully constrains the constitutive relations, leading to the writing of a rheology in terms of a friction law, relating the shear stress to the pressure through a macroscopic friction coefficient function of a single dimensional number called the inertial number I (Jop et al. 2006). This approach and its tensorial extension predict flows in many configurations like silo, avalanches, drums,..and can be enriched to capture transient effects due to dilatancy. One would like to get the same level of description with powders. However, adding adhesion between the grains dramatically changes the problem, as it introduces a new internal force scale, which modifies the scaling laws.

Recent numerical studies based on DEM simulations have shown that in presence of adhesion, the same framework might be relevant, but that a new dimensionless parameter has to be taken into account in addition to the inertial number to describe the rheology (Rognon et al. 2008; Vo et al. 2020). This number called the cohesion number measures the relative importance of adhesion and confining forces. Numerically, we have recently shown in my group that the story is more complex, that other parameters like stiffness and dissipation play also a crucial role when adhesion is present (Mandal et al. 2020), and that the rheological laws are non monotonic, leading to shear banding (Mandal et al. 2021) and instabilities that may be crucial to understand the concept of "fluidity". These results open new ideas to try do describe from a continuum perspective the flow of powders, and any advance in this direction will help in better understand the dynamics observed in packaging processes.

The role of the feeding technics

The second question of importance in the packaging process concerns the influence of the mode of supply. One would like to understand how powders flow from a hopper, on a chute, from a screw, how the flow characteristics change when changing the powders properties, and how the final deposit obtained in the container depends on the way the powder has been transported. This challenge, which is about to be achieved for simple granular materials are still fully open for cohesive materials, and there is a real need for controlled experiments in simplified flow configurations. One of the main question would be to understand to which extend the heterogeneities observed in the final bag are related to heterogeneities developing during the flow. Looking at the different instabilities that may arise in the different flow configurations is a way to improve our understanding of the origin of the variability in packaging processes.

The role of Air

Finally, a last crucial point for the dynamics at high flow rates and using fine particles concerns the coupling with air. Air might be entrained during the flow, and get trap in the deposit. It may then affect the structure of the deposit, and also can be a source of strong instabilities during the manipulation of the filled container. If mechanical perturbations of vibration are imposed, for exemple during transportation, the packing initially in a very loose state might be destabilized, and dramatic phenomena, including sudden fluidisation and compaction, may occur. This phenomenon similar to the well-know liquefaction in soil mechanics, is not really studied in details for powders, and a challenge would be to understand the role of the cohesion in this transient fluidisation process.

Our approach

The ambition of the CapCap Project is to study a simplified version of a packaging process on a model material, for which cohesion is controlled. We believe that being able to tune the cohesion at will is a necessary condition to develop a fundamental understanding of the flow of cohesive materials. We just develop in our group a method to coat in a control manner particles with polymers, a promising way to tune at will the adhesion. We should then be able to go from cohesionless particles to very cohesive material, and study how the rheology, the flow in a hopper and chute, and the resulting deposit in the bag varies with inter-particle adhesion.

B. Research Program

Ideally to understand the role particle interaction in the flow of cohesive materials, one would like to be able to experimentally tune the cohesion at will, in order to follow how the dynamics is modified when increasing gradually the inter-particle adhesion from the well known case of granular materials. Whereas in suspensions, playing with the chemical properties of the solvent is a way to change the interaction from repulsive to attractive (Van De Laar et al. 2016; Clavaud et al. 2017), for grains in air, the task is more difficult. Fundamental studies on cohesive granular media have then focused

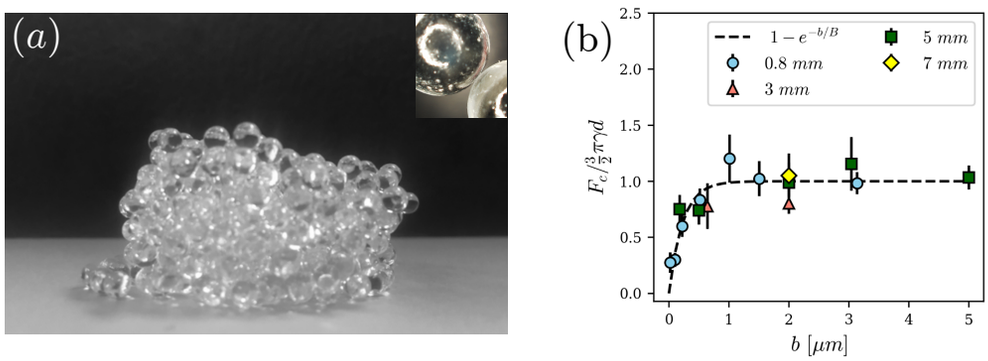

Figure 1: The model material: a) exemple of cluster formed by the coated particles b) rescaled interparticle adhesion force as a function of the averaged coating thickness.

on mixture of grains and liquid, in which cohesion is controlled by the amount of liquid through the formation of capillary bridges (Scheel et al. 2008). However, capillary bridges appear to migrate during flows, leading to strong heterogeneities (Badetti et al. 2018). Humid sand is thus of interest per se, but does not represent a model material to understand powders. Working with real powders is also a challenge as they are very sensitive to environment (humidity, temperature) preventing a precise characterization of their rheology. To circumvent this difficulty, we have recently developed in our group a simple method to introduce controlled adhesive forces between silica beads (Gans et al. 2020). The idea is inspired by the "kinetic sand", a toy for kids made of a mixture of sand and polymers which can be moulded and sculpted at will indefinitely. Our recipe is based on a mixture of PDMS, acid boric and water, mixed and heated with the particles during one hour. After cooking, the particles are coated with a layer of PolyBoroSiloxane (PBS), which makes them sticky (see Fig. 1a). The stickiness is stable, remains after many contacts, is present on every particle. The adhesion force is controlled by the thickness of the coating (see Fig. 1b). We have shown that this system is very stable in time, can be re-used with the same properties, making it an ideal material to study how adhesion may change the flowing properties of granular media, and thus a relevant model for powders. The research program proposes to use this new and unique model material to investigate how in the process of filling a container adhesion changes the dynamics and the deposit. Three main tasks are planned. First, the rheology of this model material will be analysed. Once the rheology characterized, we plan to study the flow in a simplified filling process consisting in emptying a silo in container. The aim is to understand how cohesion modifies the flow in the hopper, the heterogeneities at the exit, the formation and the structure of the resulting deposit. Finally the role of air will be studied in a second step using fine particles, with a focus on the stability of the packing submitted to tap perturbations.

Rheology of the model material

As a first task, we aim at characterizing the rheology of our model cohesive granular material. We will use the pressure imposed rheometer build in my group (Tapia et al. 2019) (Fig. 2a), where the grains are confined under a controlled pressure in an annular cell and sheared by a rotating top cover. The torque and position of the top plate provide accurate measurement for the shear stress and the volume fraction and thus a measure of the friction law and the volume fraction law. Our aim is to understand the role of the coating and how it changes the rheology under steady shear. The questions we would like to answer are : does adhesion induce a shear weakening branch in the friction law as observed in simulation (Mandal et al. 2021)? Can we put in evidence some scaling with adhesion as suggested in the literature (Vo et al. 2020) ? How transient flows starting from different controlled volume fraction are affected by adhesion and how it may affect dilatancy or compaction ? The results of the rheological study will serve as a base to analyse the flow characteristic in a filling process.

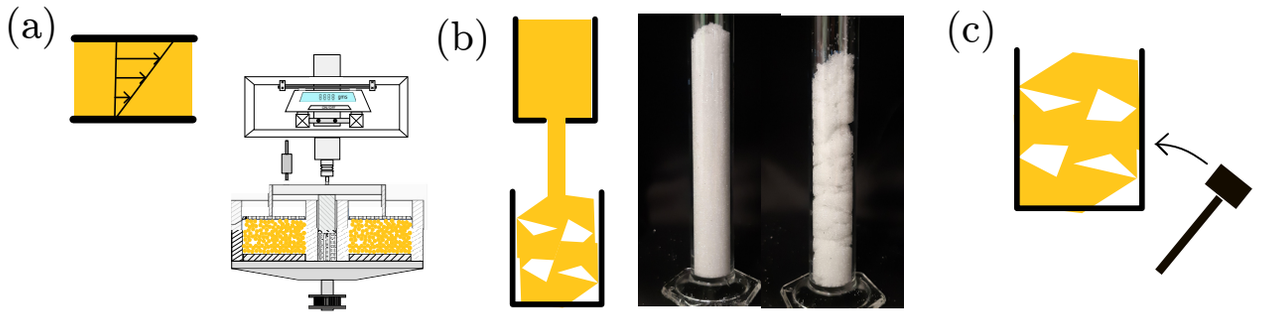

Figure 2: The three proposed tasks: a) Rheological characterisation of the model material; b) Studying a simplified feeling process (pictures show packings obtained for a low cohesion (left) and high cohesion(right) material; c) Compaction of a cohesive material.

Filling a container from a hopper

Once the rheology of the model cohesive material characterized, we plan to study the emptying of a silo in a container as sketched in Fig. 2b. The presence of cohesion is known to dramatically affect the flow in hopper, leading to channellisation and clogging (Schulze 2008). The ability to continuously modify the adhesion between the particles in our model material, gives us the opportunity to study and understand what controls the flow regime and when clogging appears. We will also carefully look at the heterogeneities that may appear at the exit of the hopper, to understand how cohesion affects the formation of clusters at the exit. Lastly we will study how the deposit is created from the flow. When preparing this proposal, we have conducted preliminary experiments to test the feasibility and check the interest of the proposed approach. Results of the filling of a tank is shown in Fig 2b for two different levels of cohesion. One clearly observes that the packing looks homogenous and dense when cohesion is low (left picture), whereas strong heterogeneities are observed at high level of cohesion (right picture), with the formation of clusters at the exit of the silo that keep their identity in the final deposit, trapping air. A detailed analyse of the formation of the deposit, of its structure (we have access in our university to an X-Ray microtomographe to measure the 3D structure of granular packing), of its stability during the feeling process should provide important information about the dynamics at work during the process and the role of cohesion.

Compaction of a cohesive material

The last task we would like to investigate in a longer term is the coupling of the packing with air. In the limit of very cohesive materials, the packing resulting from the emptying of the hopper is very loose. A perturbation, a shock or a vibration might destabilize the deposit and compact it. During compaction, the trapped air escapes. If the particles are coarse, air flows easily through the pores and the dynamics of compaction is simply controlled by the inertia of the particles. When the grains are fine, the air flow induces additional stresses due to viscous drag, which fluidizes the powder. This phenomenon called liquefaction when the fluid is water has been intensively studied in soil mechanics community. We propose to try to understand the role of cohesion in the his transient fluidisation of powders, using our model material. Traina et al (Traina et al. 2013) have shown that tap experiments, which consists in imposing a sudden acceleration to the packing, is an interesting test to discriminate between different powders. With our new model material, playing with both the adhesion force between particles and the particle size, we should be able to disentangle the role of cohesion and the role of air in the compaction under tap, by performing controlled experiments measuring simultaneously compaction and evolution of the air pressure during the dynamics.

C. Expected achievements

This experimental project focus on the understanding of the role of cohesion in the packaging process. We hope to be able to improve our physical understanding of the flowability of cohesive granular materials, to evidence how inter-particle adhesion influences flow in a hopper and the formation of heterogeneous structures during the filling procedure. This experimental project is part of a wider project in our group, with also numerical and theoretical approaches on the powder rheology, with the ultimate goal being to be able to propose relevant continuum description of the flow of powders.

D. Risks and critical unknowns

One of the main unknown of this research program is the use of the model granular material. Our first studies have shown its potential in controlling cohesion, a key challenge to improve our understanding of cohesive granular media. However, the coating of the particles might introduce more complexity than expected, for example one risk being that it might introduce also lubrification effects. This will be checked in our rheological investigation. We are also currently investigated other ways of controlling particle properties in collaboration with chemists, based on the click chemistry technics, which alow to graft almost any kind of molecules at the interface of polymer particles.

E. The team

Our group in Marseille has a strong expertise in granular flows, suspensions and in the rheology of complex fluids. With Maxime Nicolas and Pascale Aussillous, both professors at Aix Marseille University, we started four years ago a long term program on cohesive granular materials, with the hope that the recent progress on dry granular flows we have achieved in the last decade will help us to tackle the much more difficult challenge of the rheology of powders. Beside the fact that we believe that our fundamental approach based on the design of a model material to control adhesion might provide useful information in the aeration problem raised in the IFPRI call, we are convinced that our research program would strongly benefit from the IFPRI Community. It would give us the opportunity to share our results with imminent colleagues working in the field, but also and more importantly would provide contacts and discussion with engineers from various industries and learn from their unique knowledge of the rich and complex behaviour of powders.

Bibliography

Andreotti, B., Y. Forterre, and O. Pouliquen (2013). *Granular media: between fluid and solid*. Cambridge University Press.

Badetti, M., A. Fall, D. Hautemayou, F. Chevoir, P. Aimedieu, S. Rodts, and J.-N. Roux (2018). "Rheology and microstructure of unsaturated wet granular materials: Experiments and simulations". In: *Journal of rheology* 62.5, pp. 1175–1186.

Castellanos, A. (2005). "The relationship between attractive interparticle forces and bulk behaviour in dry and uncharged fine powders". In: *Advances in physics* 54.4, pp. 263–376.

Clavaud, C., A. Bérut, B. Metzger, and Y. Forterre (2017). "Revealing the frictional transition in shear-thickening suspensions". In: *Proceedings of the National Academy of Sciences* 114.20, pp. 5147–5152.

Gans, A., O. Pouliquen, and M. Nicolas (2020). "Cohesion-controlled granular material". In: *Physical Review E* 101.3, p. 032904.

Hare, C., U. Zafar, M. Ghadiri, T. Freeman, J. Clayton, and M. Murtagh (2015). "Analysis of the dynamics of the FT4 powder rheometer". In: *Powder Technology* 285, pp. 123–127.

Jop, P., Y. Forterre, and O. Pouliquen (2006). "A constitutive law for dense granular flows". In: *Nature* 441.7094, pp. 727–730.

Mandal, S., M. Nicolas, and O. Pouliquen (2020). "Insights into the rheology of cohesive granular media". In: *Proceedings of the National Academy of Sciences* 117.15, pp. 8366–8373.

– (2021). "Rheology of Cohesive Granular Media: Shear Banding, Hysteresis, and Nonlocal Effects". In: *Physical Review X* 11.2, p. 021017.

Rathbone, T., R. Nedderman, and J. Davidson (1987). "Aeration, deaeration, and flooding of fine particles". In: *Chemical engineering science* 42.4, pp. 725–736.

Rognon, P., J. Roux, M. Naaim, and F. Chevoir (2008). "Dense flows of cohesive granular materials". In: *Journal of Fluid Mechanics* 596, pp. 21–47.

Scheel, M., R. Seemann, M. Brinkmann, M. Di Michiel, A. Sheppard, B. Breidenbach, and S. Herminghaus (2008). "Morphological clues to wet granular pile stability". In: *Nature Materials* 7.3, pp. 189–193.

Schulze, D. (2008). "Powders and bulk solids". In: *Behaviour, characterization, storage and flow. Springer* 22.

Tapia, F., O. Pouliquen, and É. Guazzelli (2019). "Influence of surface roughness on the rheology of immersed and dry frictional spheres". In: *Physical Review Fluids* 4.10, p. 104302.

Tay, J. Y. S., C. V. Liew, and P. W. S. Heng (2016). "Research Article Powder Flow Testing: Judicious Choice of Test Methods". In: *AAPS PharmSciTech* 18.5, pp. 1–12.

Traina, K., R. Cloots, S. Bontempi, G. Lumay, N. Vandewalle, and F. Boschini (2013). "Flow abilities of powders and granular materials evidenced from dynamical tap density measurement". In: *Powder technology* 235, pp. 842–852.

Van De Laar, T., R. Higler, K. Schroën, and J. Sprakel (2016). "Discontinuous nature of the repulsive-to-attractive colloidal glass transition". In: *Scientific reports* 6.1, pp. 1–7.

Vo, T., S. Nezamabadi, P. Mutabaruka, J.-Y. Delenne, and F. Radjai (2020). "Additive rheology of complex granular flows". In: *Nature Communications* 11.1, pp. 1–8.

IFPRI

International Fine Particle Research Institute

Research Project Brief

Drying Wet Powders With Shear to Prevent Agglomerate Formation

The International Fine Particle Research Institute (IFPRI) wishes to fund a research project on elucidating how the method of drying, and more specifically the intensity of shear in a dryer, affects the state of agglomeration of the dried product and its redispersibility.

IFPRI has supported strong work on spray drying in recent years which has provided insight into the mechanisms of atomisation (affects granule PSD) as well as the dewatering modes of the droplets (drying outside-in vs inside out) and how they affect the granule strength and porosity. However, industrially, drying is diverse, with tray and belt dryers at low/no shear, fluid bed and rotary dryers at medium shear, and flash and agitated dryers at high shear - with diverse mechanisms of heat exchange. The choice of the right dryer for a given situation is multifactorial - it can be driven by cost (capex/energy efficiency), by the delicacy of the material, or by the resulting bulk density, flowability or dustiness of the product.

The state of agglomeration of the dried powder, and the ability to redisperse the powder later is also very important. For many fine materials, drying results in unavoidable agglomeration, sometimes this is beneficial, sometimes it presents problems. The degree and nature of this agglomeration is influenced by the particle's surface chemistry and morphology (size and shape) but is also strongly influenced by the type of dryer used, as well as the presence or absence of solutes in the water. The intensity of shear in the dryer clearly is a key variable that influences both agglomeration and granule attrition in conjunction with the time-temperature history of the powder and understanding interplay between these variables in controlling the ultimate particle structure of the *dried* powder is the general objective of this project.

While we expect this project to be largely experimental, we place no restriction on the approach. For example, development of a regime map in terms of fundamental variables (e.g., time, temperature, moisture content, shear stress) would be acceptable, as would be a focused study on drying of particle clusters under appropriate mechanical stresses. IFPRI is interested in drying of both organic and inorganic powders, so the primary restriction of material system is that the powders be fine (volume mean particle size smaller than 100 microns) and hydrophilic. Drying in the presence of soluble species is in-scope as well.

A REGIME MAP APPROACH FOR PREDICTING THE AGGLOMERATION OF FINE WET POWDERS AFTER DRYING UNDER VARYING LEVELS OF SHEAR

IFPRI Research Project Proposal: Drying Wet Powders with Shear to Prevent Agglomerate Formation

Dr. Heather Emady, Associate Professor of Chemical Engineering, Arizona State University

BACKGROUND

Wet powder drying is a unit operation used in a variety of industries, yet the many variables involved in this process make it very difficult to predict the dried powder product attributes. A particular concern for drying of fine powders is the tendency for agglomerate formation and also attrition, which are highly dependent upon the level of shear in the dryer. The extents of both agglomeration and attrition can be characterized by the change in particle size and size distribution between the initial powder and the dried powder product.

Important dried powder product attributes include particle size and size distribution, particle shape, and bulk density. Formulation properties (e.g., particle size and size distribution, particle shape, particle density, bulk and tapped density) and process variables (e.g., liquid content, temperature, shear rate, time) can all influence the product attributes.

A regime map can be a useful tool to guide formulation choices and process operation, and is an improvement upon just performing many experiments to test variables, and is a positive step toward predictive model development.[1] Regime maps for wet granulation (the process of adding a liquid binder to a powder bed, usually with some level of agitation, for particle size enlargement) were established over 20 years ago, with separate regime maps for nucleation[2] and growth.[3,4] More recently, we expanded this regime map framework for single drop granule formation in static powder beds (see **Figure 1**).[5] Two distinct mechanisms and corresponding granule shape regimes were discovered, based upon the powder bed porosity and the granular Bond number. Spreading occurred with granular Bond numbers <65,000 (roughly corresponding to surface mean particle sizes >30 μm) for all bed porosities below the minimum fluidization porosity and formed flat granules, while Tunneling occurred with granular Bond numbers >65,000 (roughly corresponding to surface mean particle sizes <30 μm) for all bed porosities and formed round granules. These two regimes in particle size, from coarser particles that naturally form a smooth, packed bed of individual particles, down to finer particles that form a fluffy powder bed comprised of dry agglomerates, are expected to be critical components in the development of a drying regime map for this proposed work.

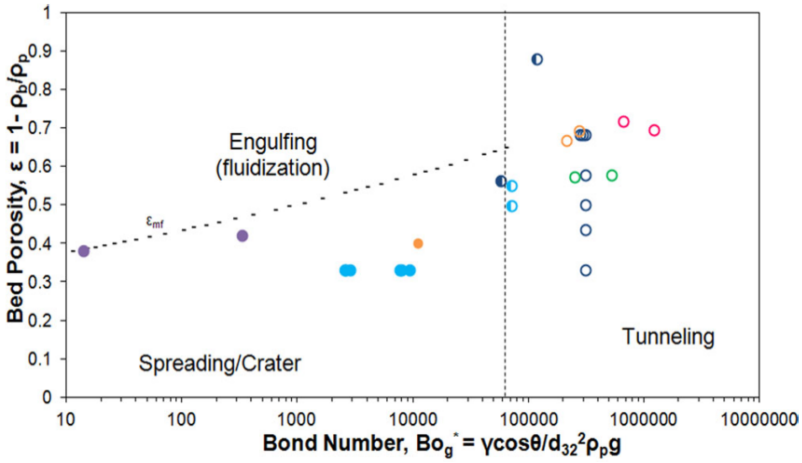

Figure 1. Granule formation mechanism regime map.[5]

PROPOSED RESEARCH PLAN

The overall goal of this research is to develop a particle drying regime map that determines the conditions under which agglomerate formation will occur in drying processes with varying shear rates. Toward this end, the following research objectives will be explored:

(**RO 1**) Raw Material Characterization and Preparation of Wet Particle Assemblies;
(**RO 2**) Tray Drying of Wet Particles [***no shear***];

(**RO 3**) Rotary Drying of Wet Particles [***low-medium shear***];
(**RO 4**) Jet Milling of Wet Particles [***high shear***];
(**RO 5**) Dried Product Characterization; and
(**RO 6**) Regime Map Development.

Details of each objective are provided in the subsequent sections, and a proposed timeline for carrying out the work for all objectives is included at the end of the proposal, in **Table 3**. More details are given for **RO 3** to demonstrate the capability of our in-house rotary drum dryer system, while the drying tests for **RO 2** and **RO 4** use standard commercial equipment.

(RO 1) Raw Material Characterization and Preparation of Wet Particle Assemblies:

The selection of materials will be done with the input of IFPRI members and will cover the two important particle size regimes (e.g., <30 μm and 30-100 μm). In addition to particle size, thorough raw material characterization is essential for elucidating the powder properties that will be relevant for regime maps. The techniques available in our powder characterization lab, outlined in **Table 1**, will be utilized for this purpose.

Table 1. Equipment and corresponding measurements used for material characterization.

Equipment	Measurement
Malvern Morphologi G3 Automated Particle Characterization System with Automated Sample Dispersion Unit	Particle size and shape, and their distributions
AccuPyc II 1340 Automatic Gas Pycnometer	Particle density
SOTAX Tap Density Tester	Bulk and tapped density

The wet particle assemblies will be prepared by mixing the powder with the desired amount of liquid and kneading until the mixture appears homogeneous. The mixtures will be prepared immediately before each test in order to minimize evaporation.

(RO 2) Tray Drying of Wet Particles [no shear]:

Oven tray drying will be performed in order to have a control drying case without shear. We have a Fisher Scientific 60L Gravity Oven in our lab that is capable of operating at temperatures up to 250°C.

(RO 3) Rotary Drying of Wet Particles [low-medium shear]:

Rotary drying will be performed in order to test the low-medium shear regimes. We will use our in-house rotary drum experimental setup that is designed for conductive and convective granular heat transfer, with particle temperature quantification via a thermal IR camera. Rotary drum systems have been used to explore mixing of fine particles, as characterized by the axial dispersion coefficient,[6,7] but little experimental work on the heating and drying of this class of materials in rotary drums is available in the literature.

Details of our experimental rotary drum setup and thermal IR camera are presented in Adepu et al.[8] The setup consists of a stainless-steel cylinder (ID = 15.24 cm, OD = 16.51 cm, L = 7.62 cm) that is closed on each end by 6 mm

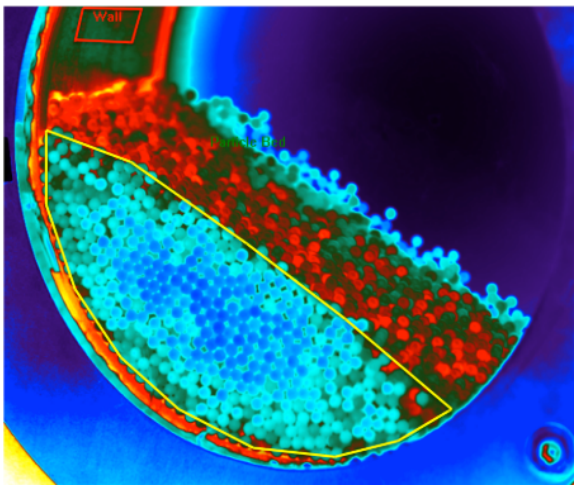

Figure 2. Sample IR camera image, with region of interest selection for the drum wall (red) and the particle bed (yellow).

thick windows. One end of the drum is closed by a sapphire window (D = 15.24 cm) that provides optical and thermal access to the interior particle bed, and the other side of the drum is closed by a quartz window (D = 16.51 cm) that provides optical access to the particle bed. Both windows are held in place using 1.27 cm thick titanium rings that are specifically chosen due to the low conductivity, thereby preventing direct contact of the drum walls with the rollers used for rotating the drum and reducing heat loss through any contact. The sapphire window is held using a 14.478 cm ID, 27.94 cm OD titanium ring, and the quartz glass is held using a 15.24 cm ID, 27.94 cm OD titanium ring. The drum rotates on the two 27.94 cm OD titanium wheels using rollers with variable rotational speed. Three heat guns are placed with equal spacing, at 120° apart, around the drum, to provide effective uniform heating. An infrared radiation (IR) camera (FLIR A6701SC) is used to capture the temperature profile through the sapphire window (see **Figure 2)**. Therefore, the sapphire window is specifically chosen to give a high transmittance to IR light, with a transmission range from 0.17 μm to 5.5 μm.

This rotary drum system was designed for conduction heat transfer via the drum walls. However, to incorporate convection heat transfer, the setup has been modified to introduce forced convection into the drum system. For the conduction setup, one side of the drum is closed using a quartz window and another side is covered using a sapphire window. For convection, besides the sapphire window that is used for IR imaging, a quartz window with holes to pump hot air into the drum is used. The quartz window used features a central inlet hole for hot air to be forced into the drum for internal heating. It also has four smaller holes around the edge to let air outside, in order to release the pressure from inside the drum. The internal heat gun is attached to an air duct that connects with pipe fittings to a temperature sensor and the air inlet port. This heat gun serves to insert a hot air stream into the drum to heat the particle bed inside the drum via forced convection. The rotary drum experimental setup, showing the placement of all four heat guns, is provided in **Figure 3**.

(a) 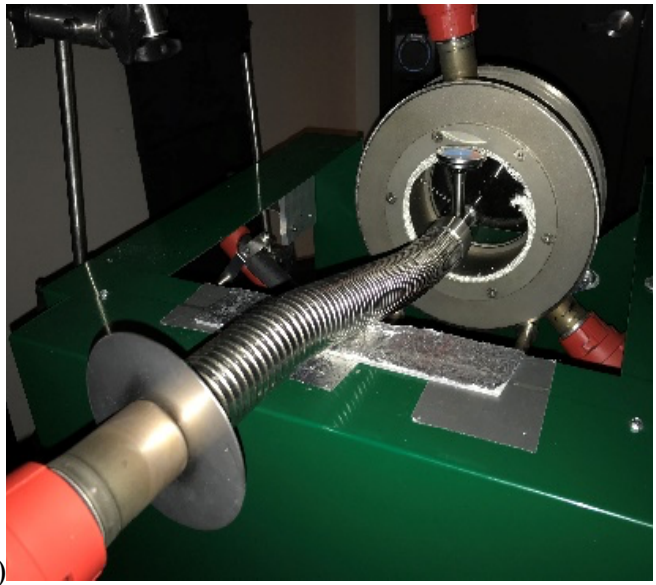 (b) 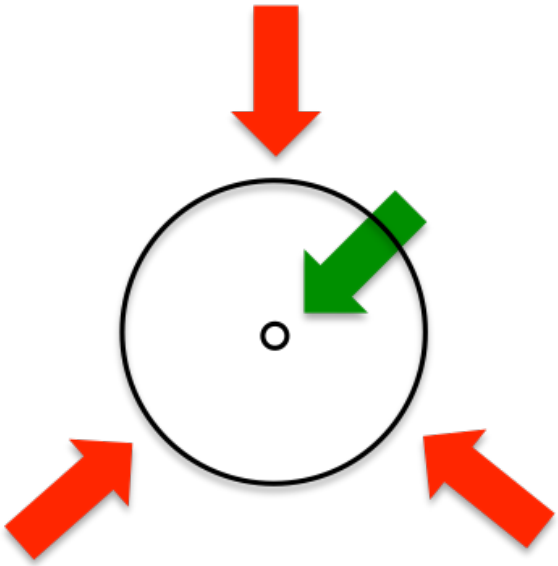

Figure 3. Rotary drum experimental setup. (a) Rear view of empty drum with air inlet duct and quartz window. The opposite end of the drum is enclosed with a sapphire window, where the thermal IR camera is positioned in order to obtain the particle temperature profile within the drum. (b) Schematic of the heat addition to the rotary drum, with the red arrows indicating external heat guns, and the green arrow indicating an internal heat gun.

(RO 4) Jet Milling of Wet Particles [high shear]:

Jet milling will be performed in order to test the high shear regime. We have a Fluid Energy Model 00 Jet-O-Mizer Mill in our lab, which can process 0.75-15 g/min of material.

(RO 5) Dried Product Characterization:

The dried powder will be characterized using the same techniques outlined in **RO 1**. A key attribute of the dried powder product is the extent of agglomeration. The product particle size, shape, and their distributions will be measured using the Malvern Morphologi G3. These product size and shape characteristics will then be compared with those of the original powder, as obtained in **RO 1**, to quantify the extent of agglomeration.

(RO 6) Regime Map Development:

The regime map will incorporate fundamental properties of the particles (e.g., particle size and shape), as well as process conditions (e.g., moisture content and shear rate), into dimensionless groups. **Table 2** provides a summary of all of the variables that will be tested, and the results will be obtained from **RO 1-5**, which will be used for derivation of the dimensionless groups and development of the regime map that will predict agglomerate formation upon drying under shear.

Table 2. Tested variables for inclusion in regime map.

	Variable
Formulation	Particle size and size distribution
	Particle shape
	Tapped and bulk density
Process	Temperature
	Shear rate
	Mass of material
	Moisture content
Product	Particle size and size distribution
	Particle shape
	Tapped and bulk density

CRITICAL UNKNOWNS

The primary uncertainties in the proposed work are: (1) the quantification of the shear rate, and (2) determination of the dimensionless groups to be used in the resulting regime map. Shear rate is variable across various equipment designs, but we strive to develop a single dimensionless group that quantifies shear rate across a variety of process equipment. For example, in the rotary drying process, there will be a balance between the shear of drum rotation versus the shear of air flow into the drum. We will not have an understanding of what this balance looks like until we actually perform the experiments. Additionally, we do not know the dominating variables in each of these drying processes before we do the experiments, so our experimental results will dictate the formation of the dimensionless groups for the regime map. Despite these unknowns, we have experience using this framework of characterizing the feed material, performing experiments looking at the effects of varying process variables, and characterizing the product material; then, we combine all of these components to determine the dominating dimensionless groups and corresponding regime map.

INTEGRATION INTO EXISTING RESEARCH PROGRAM

The proposed research combines our lab's two main research thrusts, namely single drop granulation and granular heat transfer. The regime map framework comes from the granulation project, which is currently funded by the NSF CAREER award. However, we do not currently have external funding for our granular heat transfer project, and the proposed work can leverage our existing infrastructure for this project, namely the rotary drum with the thermal IR camera.

OPPORTUNITIES FOR IFPRI MEMBER SUPPORT

The proposed research would benefit from the supply of appropriate particulate materials from IFPRI members. The two categories of particles needed are as follows: particles with surface mean sizes <30 μm, and those between 30-100 μm. Beyond these size requirements, we would be open to any type of particulate materials from relevant industries.

In addition to the supply of test materials, we would appreciate the input of IFPRI members for industrially relevant drying conditions (e.g., liquid saturation levels, temperature, drum rotation rate, etc.) to test in our setups.

PROPOSED TIMELINE

The proposed research will take place in Dr. Heather Emady's laboratory at ASU from August 1, 2022 – July 31, 2025, and the details are provided in **Table 3**.

Table 3. Timeline of research activities for the proposed work.

	Year 1	Year 2	Year 3
RO 1: Raw Material Characterization and Preparation of Wet Particle Assemblies			
Select materials of the following surface mean particle sizes: (1) <30 μm binary, and (2) 30-100 μm Characterize materials: particle size and size distribution, particle shape, particle density, bulk and tapped density Prepare wet particle assemblies for each drying test	■	■	■
RO 2: Tray Drying of Wet Particles [***no shear***]			
Perform oven tray drying experiments and test for the effects of: (1) temperature, (2) mass of material, and (3) moisture content	■		
RO 3: Rotary Drying of Wet Particles [***low-medium shear***]			
Perform rotary drying experiments and test for the effects of: (1) temperature, (2) mass of material, (3) moisture content, and (4) shear rate	■	■	
RO 4: Jet Milling of Wet Particles [***high shear***]			
Perform jet milling experiments and test for the effects of: (1) mass feed rate, (2) moisture content, and (3) air pressure/shear rate			■
RO 5: Dried Product Characterization			
Measure dried powder product properties, including size, shape, and their distributions, in order to quantify the extent of agglomeration	■	■	■
RO 6: Regime Map Development			
Develop regime maps that predict agglomerate formation after drying based on dimensionless groups involving the formulation properties and the process variables			■

REFERENCES

1. Kayrak-Talay, D., Dale, S., Wassgren, C. & Litster, J. Quality by design for wet granulation in pharmaceutical processing: Assessing models for a priori design and scaling. *Powder Technol.* **240**, 7–18 (2013).
2. Hapgood, K., Litster, J. D. & Smith, R. Nucleation regime map for liquid bound granules. *AIChE J.* **49**, 350–361 (2003).
3. Iveson, S. M. & Litster, J. D. Growth regime map for liquid-bound granules. *AIChE J.* **44**, 1510–1518 (1998).

4. Iveson, S. M. *et al.* Growth regime map for liquid-bound granules: further development and experimental validation. *Powder Technol.* **117**, 83–97 (2001).
5. Emady, H. N., Kayrak-Talay, D. & Litster, J. D. A regime map for granule formation by drop impact on powder beds. *AIChE J.* **59**, 96–107 (2013).
6. Koynov, S. *et al.* Measurement of the axial dispersion coefficient of powders in a rotating cylinder: Dependence on bulk flow properties. *Powder Technol.* **292**, (2016).
7. Paredes, I. J. *et al.* Measurement of the residence time distribution of a cohesive powder in a flighted rotary kiln. *Chem. Eng. Sci.* **191**, 56–66 (2018).
8. Adepu, M., Boepple, B., Fox, B. & Emady, H. Experimental investigation of conduction heat transfer in a rotary drum using infrared thermography. *Chem. Eng. Sci.* **230**, 116145 (2021).

DEVELOPMENT OF INNOVATIVE TOOLS TO CHARACTERIZE THE DRYING OF WET POWDERS UNDER SHEAR

Alban Sauret
Department of Mechanical Engineering, UC Santa Barbara
asauret@ucsb.edu (805) 518-6318 https://sauretlab.me.ucsb.edu/

1 PROBLEM STATEMENT AND PROJECT OBJECTIVES

▷ **Granular matter and powders** are widely used in the manufacturing of numerous products and in many industries. In particular, powders are used as intermediate products but are also products consumed as such or, most often, after rehydration in the food industry [1]. They are also omnipresent in pharmaceutical products, but also in building materials as the PI has experienced with Saint-Gobain. Despite this intense utilization, their behavior is still poorly understood and empirical [2]. One significant difficulty in developing a general understanding is the range of possible powder properties (size, shape, wettability, etc.), the key role of the moisture and electrostatic force, and the flow conditions.

▷ **Drying of powders and formation of agglomerates.** Developing final products with powders often involves a wet agglomeration process, which is still very empirical [3]. Wet agglomeration of powders consists of coupling the agitation of solid particles to an operation of adding water or a binder to form granular structures of larger size, which after drying modify the properties of the final powder (flowability, rehydration properties, density, etc.) [4, 5]. At the industrial level, there is a great diversity of equipment (configuration, agitation mode) and modes of water supply (pulverization, flow...) allowing to realize this operation. The drying of wet powders ultimately leads to agglomerate formation because of solid bonds formed between the particles [3, 6]. The average size of the agglomerates produced can vary from ten to a few hundred microns. Nevertheless, in all cases, one can expect that two different drying techniques will lead to different final granules in terms of strength, size, compressibility, flowability, and ultimately result in products of varying quality and properties.

▷ **A complex (and impossible?) prediction.** As mentioned in the project brief, the question on how the intensity of the shear in a dryer affects the state of agglomeration of the dried product, and its redispersibility is broad and fascinating because of all the different physical and chemical ingredients involved. An approach to provide some first answers useful to a broad community would be to perform some real-scale experiments with a few selected powders and build a regime map for some well-chosen variables. However, this approach would have limited interest since the degree and nature of the agglomeration is influenced by the particle's surface chemistry and morphology (size and shape) but is also strongly influenced by the type of dryer used, as well as the presence or absence of solutes in the water. As a result, any particular characterization obtained may not be appropriate to describe or predict other configurations.

▷ **Should we give up? Towards a predictive tool.** The goal of this project is to develop two innovative experimental tools that will allow easy implementation and quick testing of a large variety of powders and liquid while controlling the input energy and/or shear rate during the drying process. We will base our approach on our expertise in granulation and blending of liquid and grains performed in the past with an industrial collaborator, Saint-Gobain. Deliverables will be the tools developed within this project from which we will obtain the final size distribution, but also the time evolution, of the agglomerates formed. The capabilities of such tools will be demonstrated through experiments with model powders, from which the PI will gain some fundamental insights into potential optimization properties (evolution of the final size distribution of the agglomerate with the shear rate).

▷ **Research objectives.** A schematic of the research objectives, tasks, and deliverables is shown in figure 1, highlighting the nature of the project and the cross-talk between the different stages. In particular,

once the tools have been developed, the PI will seek powders of interest among the IFPRI members to leverage these characterizing tools while simultaneously running experiments with model materials. The proposed research will lead to the development of two characterizing tools, (i) oscillating box for high-shear rate and (ii) rotating drum for medium shear rate, that could be used on any powders to provide the time-varying and final size distribution of the agglomerates formed upon the drying of wet powders with shear. These tools will provide a first, quick, and cheap estimate of the influence of the different controlling parameters (shear rate, relative humidity, nature of the powders, etc.) prior to running more elaborate tests in industrial settings.

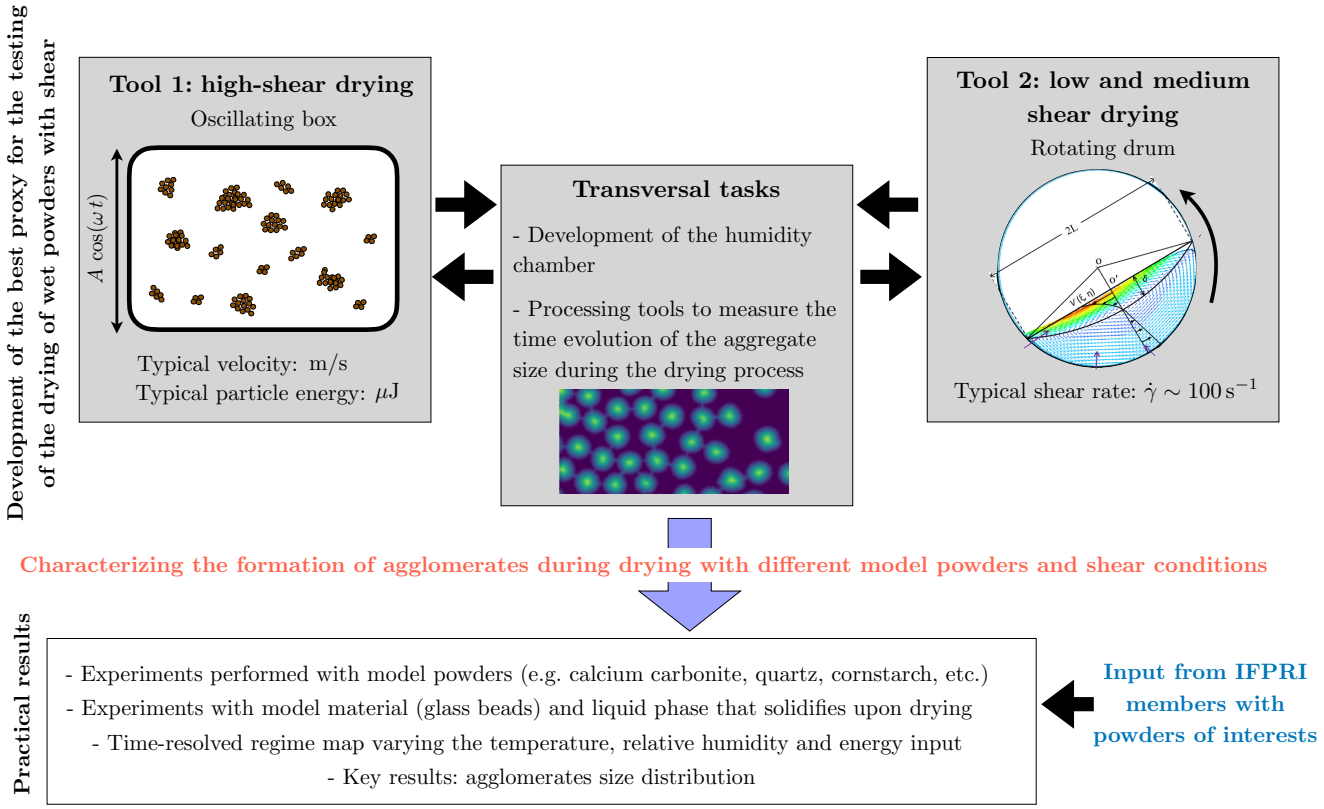

Figure 1: Schematic overview of the proposed research.

2 EXPERTISE OF THE PI AND RELEVANCE TO ITS OWN RESEARCH

▷ **Background of the PI.** The PI, Alban Sauret, is a faculty in the Department of Mechanical Engineering at UC Santa Barbara (USA) since 2018. He leads the Multiphase and Multiscale Flow Laboratory (*website*), which consists of 10-15 researchers. His group tackles problems in the area of fluid mechanics, soft matter, and granular materials. In particular, topics of current interest in the group include capillary flows of suspensions (dispensing of suspensions through nozzles, dip coating of suspensions, etc.), clogging in confined systems, rheology and properties of granular material and powders, blending of liquid and grains. Before joining UCSB, the PI was a CNRS Researcher between 2014 and 2018 in SVI (*website*), a joint academic-industrial laboratory between the CNRS and Saint-Gobain located in the Saint-Gobain Research center in Aubervilliers (France). In addition, he was a scientific consultant for Saint-Gobain Research in the field of granular materials, powders, and coating processes.

▷ **Why is PI well-qualified to develop new diagnostic tools for powders?** In the past, the PI, in collaboration with Saint-Gobain and Dr. Pierre Jop (SVI), has developed model approaches to gain some

fundamental insights into the wet granulation processes. In these past projects, the goal was to work at constant water content and thus prevent any evaporation and drying of the liquid phase. However, similar approaches could easily be used and extended to control the drying of the liquid phase and provide relatively quick insights into the size distribution of the agglomerates resulting from the drying of wet powders. In addition, since 2019, the PI has started to investigate constitutive laws to provide a physical understanding of the concept of flowability of powders by studying the rheology of powders in various configurations in collaboration with researchers in France (Dr. Olivier Pouliquen and Prof. Maxime Nicolas, IUSTI, Marseille, France). Interestingly, whereas powders are handled at large scales, different simple tools have been developed to characterize powders in industrial environments (see for instance *Granutools*). The spirit of the present project is similar, *i.e.*, developing experimental tools to provide insights into the formation of agglomerates during the drying of wet powders under shear.

▷ **Why focusing on an oscillating box and a rotating drum as model configurations?** We have performed similar work leveraging the simplicity of an oscillating box in the past with a postdoctoral student and an MS student at CNRS and Saint-Gobain (France) to mimic the wet granulation process using controlled granular systems (spherical glass beads and polystyrene beads, both monodisperse in size). We thus believe that combining this approach with a control of the relative humidity, temperature, water content, and nature of the powders could lead to the development of an innovative tool for characterizing wet powders drying under controlled shear. Similarly, the PI has also considered the rotating drum configuration during the Ph.D. thesis of G. Saingier (funded by Saint-Gobain). We have used this approach to model wet granulation processes at low shear rates [7,8]. More specifically, we have considered the growth of a single wet aggregate rolling in a dry granular flow inside a rotating drum. We have been able to measure the time evolution of its diameter for different grains and liquids and various shear rates. Using X-ray tomography, we were also able to characterize the internal structure of the granular aggregate at different times during the process. Therefore, extending this approach to provide a tool to build a regime diagram of the drying of wet powders at low shear rates is feasible.

The proposed project relies on the expertise of the PI and controlled flow configurations and drying kinetics. The goal is the development of innovative tools for characterizing the drying of wet powders with shear and the resulting formation of agglomerates. The tools that will be developed could be used with any powders and binding agents at high shear rates (oscillating box) and medium shear rates (rotating drum).

3 RESEARCH WORK-PLAN

Objective 1: Drying powders at high-shear

The first objective in this project will be to investigate and characterize the drying dynamics and the resulting agglomerates formed under *high-shear drying*, typically as encountered in flash and agitated dryers [9]. A large part of this process is controlled by the impact of the agglomerates with the impellers during the drying process [10]. Performing such an approach with an actual high-shear drying system would only result in the characterization of a specific situation (specific powder, for given relative humidity and temperature). However, these kinds of tests could be pretty time-expensive while only providing limited opportunities for optimizing the formation of the agglomerates. We, therefore, aim to develop a more controlled setup where we will be able to visualize the drying agglomerate both during the drying process using high-speed visualization and post-mortem (either with microscopy or X-ray tomography). During the drying process under agitation, the visualization of the agglomerates and the dynamic evolution of the size distribution may provide previous information on what controls the final size distribution (collision of agglomerates between themselves, on the solid boundaries, leading to the

formation of larger agglomerates or break-up in smaller agglomerates).

▷ **From wet granulation to drying with shear.** Beyond the difference due to the drying phase, the wet granulation process [11] and the drying of wet powder under high shear rates share common key features. In the context of high shear wet granulation, the process often takes place in a tank in which rotating blades set the material in motion. The shape of the blades only impacts the intensity of the velocity field within the granulator, and they serve to set the material in motion and to give it enough energy for shocks to occur. Indeed, during the granulation stage, it is assumed that it is the shocks between agglomerates that will determine the average value of the final diameter of the latter [12]. It is, therefore, possible to assume that such an analogy can be made with the shear drying process. The approach is to use a large-amplitude vibrating pot where the two main control parameters to impose the shear are the amplitude of oscillation A and the frequency of oscillation $f = 2\pi/\omega$ [see figure 2(a)].

▷ **A simplified approach.** Although a vibrated box seems to be a simple system, in the context of wet granulation, the size distribution of the final agglomerate size with the water content have shown that the data obtained with this system are similar to data from high-shear granulation systems at an impeller rotation speed that would lead to a similar input energy in the system (close to 1 m/s with a typical size of the impeller of 10 cm and a typical particle size 10 μm) [13] although the details of the process are different. Moreover, it is worth mentioning that the effects of the typical velocity on the final size are also similar in industrial processes, suggesting that this setup was a promising model system to understand high-shear granulation, but also high-shear drying of powders [14].

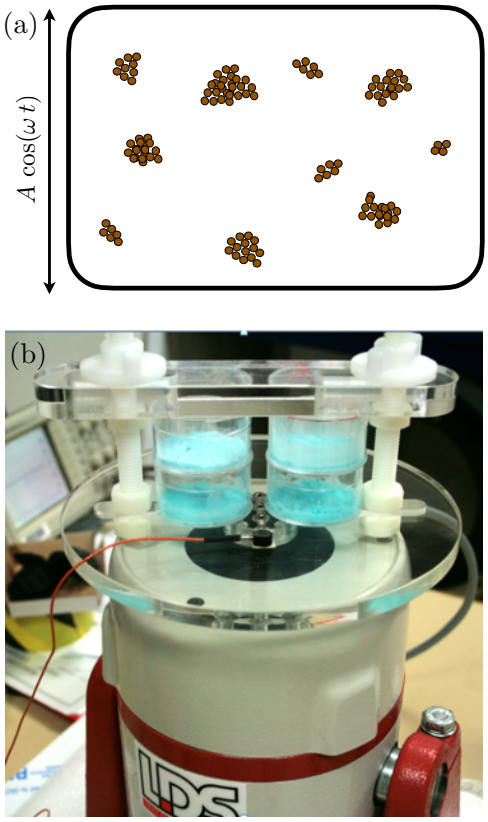

Figure 2: (a) Schematic and (b) picture of the oscillating box experiment.

▷ **The apparatus.** We will initially base our approach on a setup similar to the one we used in the past, shown in figure 2(b). A small amount of the initial powder, mixed with the liquid, will be placed in a rectangular plastic box of typical dimensions $10 \times 3 \times 5$ cm. Within this box, shocks between agglomerates will also take place, similar to what would be observed in other high-shear drying processes. In addition, the agglomerates will also impact the solid boundaries during the entire drying process. This experiment should allow us to reach comparable values for the acceleration, velocity, and input with those obtained using a tank (the frequency and amplitude of the oscillations could be extended to reach a different range of shear). The mechanisms involved are likely similar, and this procedure seems to be a good alternative to provide a benchmark to test different powders, liquid, initial moisture, time variation, etc. To make this box oscillate, we will use a vibrating pot. The amplitude and frequency will be controlled by an amplifier and a low-frequency generator. We will also add an accelerometer on this plate to measure the acceleration experienced by the box, thus estimating the input energy in our system.

▷ **Preparation of the initial sample.** We will initially use a plastic bag in which we will weigh the desired quantity of powders, and the volume of liquid will then be added to obtain the desired liquid content with a pipette, and the bag will be sealed, the powder homogenized, and then place in the plastic box to run a test.

▷ **Environmental chamber: control of the temperature and the relative humidity.** An important modification to this setup will be to implement a control in temperature and relative humidity in the box. Since our system is quite simple, this will be easily done by connecting on the side of the box an inlet a full range humidity control with an elevated temperature that would allow control from 10 to 98% RH (at 20°C) and a temperature from ambient to 55°C. We have used such a system in the past, purchased from Electro-Tech Systems, within an environmental chamber, to study the drying dynamics in fibrous media [15]. The airflow can then be exchanged between this environmental chamber and the test box. An alternative will be to place the entire setup within the environmental chamber since its footprint is moderate. In both cases, we will have a total control over the temperature and the relative humidity. Furthermore, we would also be able to investigate the influence of the time-temperature history on the agglomerate.

▷ **Micro-High-Speed Imaging.** A specialty of our group is to characterize high-speed phenomena, such as, for instance, the formation of droplets of suspensions for manufacturing application [16, 17] or the blending of grains and liquids [18, 19]. These situations require reaching a recording speed of typically 10,000 frames per second and a spatial resolution of order 5 µm/pixels. We will use a similar approach here, where the motion and evolution of the agglomerate inside the oscillating box will be recorded using a Phantom VEO 710 high-speed camera (already available in our laboratory), equipped with a macro lens (Nikkor 200 mm), on which, if we need to reach a higher resolution, we could add a microscopic lens (Mitutoyo) as we have done in the past to study the coating of tubings by suspensions [20]. Even if high-speed imaging is not intended to record an entire drying under shear process, we will record a few seconds at different times along the process so that it will give us a picture of the entire drying dynamics, as well as crucial information on the state of the agglomerate at a given time. This approach is particularly unique, as it provides a direct visualization *in situ* of the dynamical process.

▷ **Image analysis.** For each experiment, the analysis of the size distribution of the agglomerates over time will be done using methods commonly used in our group (via custom-made routines). From the videos obtained with the high-speed camera during the dynamics drying process, we will detect the agglomerates as distinct "objects" to obtain each equivalent diameter (defined through the surface area A by $D_{eq} = \sqrt{(4\,A/\pi)}$). The different steps are illustrated in figure 3 with an example for polystyrene beads [figure 3(a)]. The images of the agglomerates are first thresholded to differentiate the agglomerates from the background of the image [figure 3(b)]. Then a segmentation allows us to separate the agglomerates [figure 3(c)]. This step being done, the next step, the label, allows us to number these different objects to define each agglomerate as an object from which we can recover some characteristics, the diameter being the one we are interested in [figure 3(d)]. This method also has the advantage of following the fragmentation and coalescence processes of agglomerates and thus obtaining unique information on the dynamics during drying, such as, for instance, the time evolution of the agglomerate size distribution.

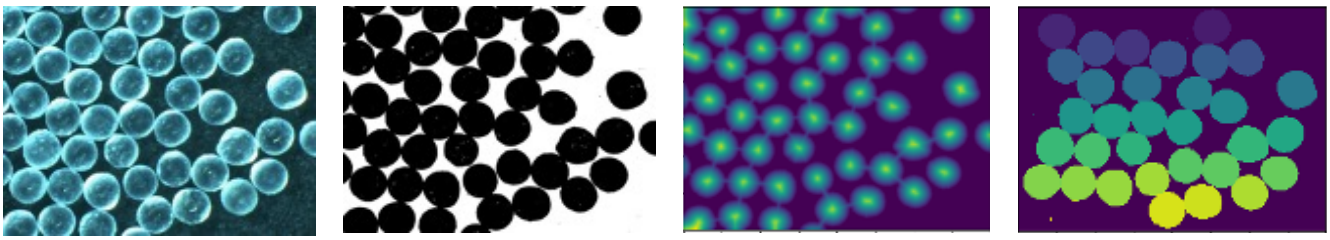

Figure 3: (a) Example of a zoomed picture of agglomerate of glass beads and water formed during the model granulation process. (b) Example of resulting probability ditribution function of the agglomerate sizes and (c) Example of the evolution obtained when varying the size of the beads (blue: 60 µm, green: 200 µm)

Post-mortem characterization. Once the drying process is over, we expect to have a distribution of agglomerate that will depend on the particle's surface chemistry and morphology but also on the temperature, shear stress, and other physical parameters. We will be able to collect the samples and measure the relevant powder properties such as the bulk density and the flowability. In addition, we will image the resulting agglomerate using a Nikon Eclipse Microscope that will allow us to characterize more finely the final agglomerate size distribution as we have done for the granulation process, as illustrated in figure 4.

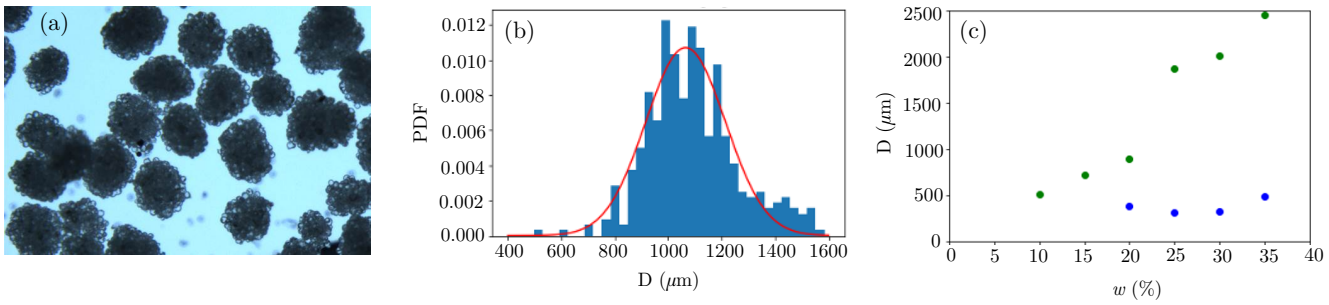

Figure 4: (a) Example of a zoomed picture of aggregate of glass beads and water formed during the model granulation process. (b) Example of resulting probability ditribution function of the aggregate sizes and (c) Example of the evolution obtained when varying the the water content w for two different size of beads (blue: 60 μm, green: 200 μm)

Expected outcome of objective 1. The development of the experimental setup and the characterization methods. The successful completion of this task will provide a unique tool to provide the final aggregate size distribution but also the evolution during the process to identify which steps may be the more important. This tool will then be used to characterize some powders and develop regime maps to identify the role of the time, temperature, relative humidity, and high shear stress on the drying of wet powders.

Objective 2. Drying at low and medium shear

Industrially, the processes of drying wet powders in the presence of shear to avoid agglomeration are diverse. The tool that will be developed in objective 1 aims at reaching high-shear and input energy, similar, for instance, to an agitated dryer. However, other methods, such as belt or rotation dryers, involve low or medium shear that will not be captured with the previous approach. The second main objective of the proposed project will rely on the development of a thin experimental drum, shown in figure 5(a), in which the shear will be imposed by the rotation rate, and the temperature and ambient humidity will be controlled in a similar approach while allowing in the same time to observe the drying dynamics.

▷ **Why is a rotating drum a good approach to model medium shear rates?** The rotating drum is one of the classical experimental configurations for the study of granular flows, which allows obtaining a stationary and cyclic flow. This system can also be used as a mixer [21] and has been shown to provide relevant information regarding the flow of powders [22]. In our study, the interest of the rotating drum lies in the periodicity of the flows that it generates, which makes it possible to observe the evolution of the agglomerates over long times, *i.e.*, during the entire drying process. The flows encountered in a rotating drum depend on the rotational speed of the cylinder, Ω. We will work in the continuous regime characterized by a stationary flow of grains at the surface. The flow of grains in the continuous regime occurs in two stages: (1) a rotation phase where the grains are at the bottom of the pile and have a solid

rotational motion following the cylinder wall and then (2) an avalanche flow phase when the grains reach the surface. These two phases can be seen in figure 5(b). Models of the velocity field in a granular drum flow are well-known in the literature. The flow field exhibits a linear profile in the active layer (region II in figure 5(b)), which concentrates most of the shear, and a tail of exponentially zero-trending profile in the passive zone, having a solid-body rotation with the cylinder. The shear rate in the linear part is approximately constant and its amplitude is of the order of $\dot{\gamma} \simeq \sqrt{g/(4\,d)}$ [23], where d is the size of the particle or agglomerate. Since the velocity profile is linear in this region, the shear rate can be written as $\dot{\gamma} = V_{max}/h_0 = \bar{V}/(2h_0)$, where $\bar{V}$ is the average velocity in the layer and h_0 the thickness of the flowing layer that can be controlled with the rotation rate and the filling rate of the drum [24]. We will work in the situation where the thickness of the flowing layer is larger than the mean radius of the agglomerate so that it will be advected by the granular flow and subject to a controlled shear. We plan to perform the first tests in a range of rotational speed between 15 and 60 rpm. In summary, this configuration allows to quantitatively impose a rather low shear of the order of $\dot{\gamma} \sim 100\,s^{-1}$.

▷ **Apparatus.** The experimental system that we have in our laboratory at UC Santa Barbara is illustrated in figure 5(a). This system consists of a cylinder with a diameter that can be varied (the first tests will be done with a diameter of about 10 cm, but this could be adjusted to provide more control over the shear rate). We will choose small drum thicknesses, typically of the order of the centimeter, to be able to measure in real-time the evolution of the roughness of the free surface, which ideally will give us information on the characteristic size of the agglomerates flowing at the surface. The cylinder is rotated by two rollers and driving at a rotation speed of 0 to 60 rotations per minute.

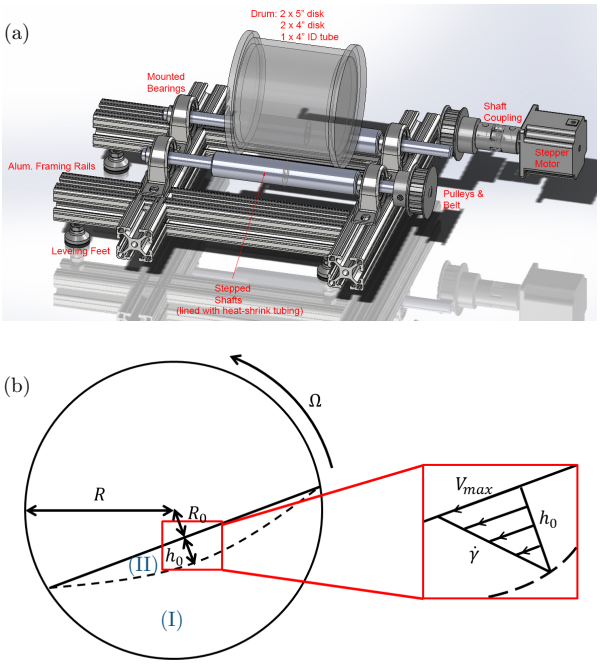

Figure 5: (a) Schematic of the rotating drum available in the PI's lab. (b) Schematic describing the properties of the flow in a rotating drum.

▷ **Principle of the measurements.** Similarly to the oscillating box described in the previous objective, we will prepare a sample of wet powders that will be placed in the rotating drum. The axis of the cylinders will be made of two holes so that the temperature and humidity will be controlled by placing the setup in the same environmental chamber. The experiments will start at $t = 0$, and we will visualize the flow within the rotating drum from the side. The roughness of the interface should provide us with information on the evolution of the agglomerates and, in particular, the cohesion between the grains. The rotating drum could easily be stopped during the experiments to pick up a small sample and measure the properties and size distributions of the agglomerate before resuming the experiments as we have done for the blending process in the past [8]. Methods similar to the one developed in the previous objective will be used.

Expected outcome of objective 2. The development of an experimental setup to characterize the drying of powders under medium shear and visualize the agglomerates during the process. The image analysis to obtain the time evolution of the particle size distribution will be similar to the methods developed in parallel to objective I.

Objective 3. Leveraging the tools: regime map of the resulting agglomerates formed

▷ **Validation of the methods.** The PI will use these two setups with model powders. The following ones have been identified as good candidates of hard inorganic powders: calcium aluminate, calcium carbonate, and silica glass sphere as they will not (or little) react with the liquid phase, *i.e.*, water within the framework of the project. Our goal is to choose materials that will not be too soluble to not precipitate when mixed with water. We will characterize the initial size distribution of each powder before using them in the experiments. Typically, we aim for powders of the size of order 10 µm and initially, the liquid phase that will be used is water. We will consider the role of the following parameters on the size distribution of the agglomerates to build a regime map of the outcome of the agglomeration following drying of wet powders under shear: (i) shear rate $\dot{\gamma}$, (ii) initial water content, (iii) dynamics of drying (controlling the relative humidity and the temperature), (iv) size distribution of the initial powders. Of particular interest, especially with the oscillating box, is that we will be able to track the dynamic evolution of the size distribution.

▷ **Interactions with IFPRI.** The core of the project is the development of these two innovative tools and their testing on some model powders. After the first characterization made with the model powders, the PI will seek candidate materials (samples) from interested companies within the IFPRI consortium. In particular, it could be interesting to also qualitatively consider the configuration of soft inorganic materials.

Expected outcome of objective 3. The last objective of this project will be to demonstrate the relevance of the two diagnostic tools with model and more realistic powders. The main result will be the size distribution of the agglomerates under different drying dynamics and shear.

4 Conclusion

Outcome. The proposed project will develop innovative tools to characterize the resulting size distribution of agglomerates resulting from the drying of wet powders under controlled shear. The oscillating amplitude and frequency will control the input energy in the case of the oscillating box, whereas it will be controlled through the size and rotation rate of the container for the rotating drum experiments. In both experiments, the temperature and the relative humidity will be controlled thanks to an environmental chamber.

Tentative timeline. Year 1 will be devoted to the development of the oscillating box, the diagnostic methods, and model experiments with silica beads and water. Year 2 will be devoted to running experiments with more complex powders in the oscillating box (from which the PI will seek the input of the IFPRI members), as well as the development of the rotating drum experiments and its testing with the same model powders. Finally, year 3 will be used to build the regime map (dynamics and final size distribution of the agglomerate) for varying powders, shear rate, and temperature/humidity conditions. The key results will be the resulting average agglomerate size and dispersion of the distribution around the mean value. Similar to his past works, the PI will also look for theoretical approaches that could capture, at least qualitatively, these evolutions and could thus be used to provide some guidelines for industrial processes involving the drying of wet powders.

References Cited

[1] G. V. Barbosa-Cánovas, E. Ortega-Rivas, P. Juliano, and H. Yan, *Food powders*. 2005.

[2] J. N. Michaels, "Toward rational design of powder processes," *Powder technology*, vol. 138, no. 1, pp. 1–6, 2003.

[3] A. Goldszal and J. Bousquet, "Wet agglomeration of powders: from physics toward process optimization," *Powder Technology*, vol. 117, no. 3, pp. 221–231, 2001.

[4] D. G. Bika, M. Gentzler, and J. N. Michaels, "Mechanical properties of agglomerates," *Powder technology*, vol. 117, no. 1-2, pp. 98–112, 2001.

[5] K. Dhanalakshmi, S. Ghosal, and S. Bhattacharya, "Agglomeration of food powder and applications," *Critical reviews in food science and nutrition*, vol. 51, no. 5, pp. 432–441, 2011.

[6] S. H. Schaafsma, P. Vonk, P. Segers, and N. W. Kossen, "Description of agglomerate growth," *Powder technology*, vol. 97, no. 3, pp. 183–190, 1998.

[7] G. Saingier, *Mécanismes et dynamiques d'interactions entre grains et liquide: du matériau granulaire sec au mélange saturé*. PhD thesis, Sorbonne université, 2018.

[8] P. Jop, G. Saingier, and A. Sauret, "Wet rolling stones: Growth of a granular aggregate under flow," in *EPJ Web of Conferences*, vol. 249, p. 09012, EDP Sciences, 2021.

[9] H. Hayashi, "Drying technologies of foods-their history and future," *Drying technology*, vol. 7, no. 2, pp. 315–369, 1989.

[10] J. Fu, G. K. Reynolds, M. J. Adams, M. J. Hounslow, and A. D. Salman, "An experimental study of the impact breakage of wet granules," *Chemical Engineering Science*, vol. 60, no. 14, pp. 4005–4018, 2005.

[11] J. D. Litster, K. Hapgood, J. N. Michaels, A. Sims, M. Roberts, S. Kameneni, and T. Hsu, "Liquid distribution in wet granulation: dimensionless spray flux," *Powder Technology*, vol. 114, no. 1-3, pp. 32–39, 2001.

[12] J. Fu, M. Adams, G. Reynolds, A. Salman, and M. Hounslow, "Impact deformation and rebound of wet granules," *Powder Technology*, vol. 140, no. 3, pp. 248–257, 2004.

[13] H. G. Kristensen, "Particle agglomeration in high shear mixers," *Powder Technology*, vol. 88, no. 3, pp. 197–202, 1996.

[14] B. J. Ennis, "Agglomeration and size enlargement session summary paper," *Powder technology*, vol. 88, no. 3, pp. 203–225, 1996.

[15] F. Boulogne, A. Sauret, B. Soh, E. Dressaire, and H. A. Stone, "Mechanical tuning of the evaporation rate of liquid on crossed fibers," *Langmuir*, vol. 31, no. 10, pp. 3094–3100, 2015.

[16] P. S. Raux, A. Troger, P. Jop, and A. Sauret, "Spreading and fragmentation of particle-laden liquid sheets," *Physical Review Fluids*, vol. 5, no. 4, p. 044004, 2020.

[17] V. Thiévenaz and A. Sauret, "Pinch-off of viscoelastic particulate suspensions," *Physical Review Fluids*, vol. 6, no. 6, p. L062301, 2021.

[18] G. Saingier, A. Sauret, and P. Jop, "Accretion dynamics on wet granular materials," *Physical review letters*, vol. 118, no. 20, p. 208001, 2017.

[19] A. Cervantes-Álvarez, Y. Escobar-Ortega, A. Sauret, and F. Pacheco-Vázquez, "Air entrainment and granular bubbles generated by a jet of grains entering water," *Journal of colloid and interface science*, vol. 574, pp. 285–292, 2020.

[20] D.-H. Jeong, A. Kvasnickova, J.-B. Boutin, D. Cébron, and A. Sauret, "Deposition of a particle-laden film on the inner wall of a tube," *Physical Review Fluids*, vol. 5, no. 11, p. 114004, 2020.

[21] J. M. N. T. Gray, "Granular flow in partially filled slowly rotating drums," *Journal of Fluid Mechanics*, vol. 441, pp. 1–29, 2001.

[22] F. Boschini, V. Delaval, K. Traina, N. Vandewalle, and G. Lumay, "Linking flowability and granulometry of lactose powders," *International journal of pharmaceutics*, vol. 494, no. 1, pp. 312–320, 2015.

[23] GDR MiDi, "On dense granular flows," *The European Physical Journal E*, vol. 14, pp. 341–365, 2004.

[24] J. Rajchenbach, "Granular flows," *Advances in physics*, vol. 49, no. 2, pp. 229–256, 2000.

IFPRI

International Fine Particle Research Institute

Research Project Brief

Spray-Drying of Pastes for Process Intensification

The International Fine Particle Research Institute (IFPRI) wishes to fund a research project on spraying of highly concentrated materials (pastes) as a means of improving process sustainability. Spray-drying of liquid products is a key technology that is widely used in many industries. Its environmental impact could be reduced through process intensification by increasing the concentration of the feed liquid to be dried, thereby reduce energy consumption and process footprint. This would require the ability to atomize highly viscous liquids (especially pastes) and achieve short drying times to produce a suitably dry product that does not stick to process surfaces without changing functionality of the dried product.

Key objectives of this project are:

- Identify and validate one or more atomization technologies that will enable spraying highly viscous liquids (up to 100 Pa.s) or dispersions with high solids fraction (pastes) and generate droplets smaller than 100 micron [see references below]
- Develop methods to measure drying kinetics of highly viscous liquid or paste droplets in controlled temperature and humidity conditions.
- Evaluate the impact of the composition and morphology of the atomized droplets on the drying kinetics and develop drying models for highly concentrated feeds.

The scope of this project is limited to viscous aqueous solutions and high solids fraction suspensions, with no limitation on the solute or dispersed particles. IFPRI members can provide recommendations for experimental systems and perhaps provide materials for study.

Some relevant papers on atomization approaches are:

1. Stähle, P., et al. (2017). "Comparison of an Effervescent Nozzle and a Proposed Air-Core-Liquid-Ring (ACLR) Nozzle for Atomization of Viscous Food Liquids at Low Air Consumption." Journal of Food Process Engineering 40(1)
2. García, J. A., et al. (2016). "Experimental characterization of the viscous liquid sprays generated by a Venturi-vortex atomizer." Chemical Engineering and Processing - Process Intensification 105: 117-124
3. Czisch, C. and U. Fritsching (2008). "Atomizer design for viscous-melt atomization." Materials Science & Engineering A 477(1-2): 21-25

Research proposal for IFPRI-Grant

Spray-Drying of Pastes with ACLR-Nozzle for Process Intensification

Creators:
P. D. Dr. Volker Gaukel, M. Sc. Sebastian Höhne
Karlsruhe Institute of Technology
Institute of Process Engineering in Life Science
Chair for Food Process Engineering
Kaiserstr. 12
76131 Karlsruhe
Germany

Recipient:
Jim Michaels
Vice President, Industry-Academia Liaison
International Fine Particle Research Institute (IFPRI)
2045 Wooddale Dr. Woodbury
Minneapolis 55125
USA

Date: 17th Dezember 2021

Description of research proposal

1 Topic of the research project

Spray-Drying of Pastes with ACLR-Nozzle for Process Intensification

2 Introduction and background

Spray-drying is a widely used process for the production of powdered products from liquid formulations. The spray-drying process can be divided into three main steps: Atomization, convective drying in a hot air stream, and powder separation [1]. A scheme is shown in Figure 1.

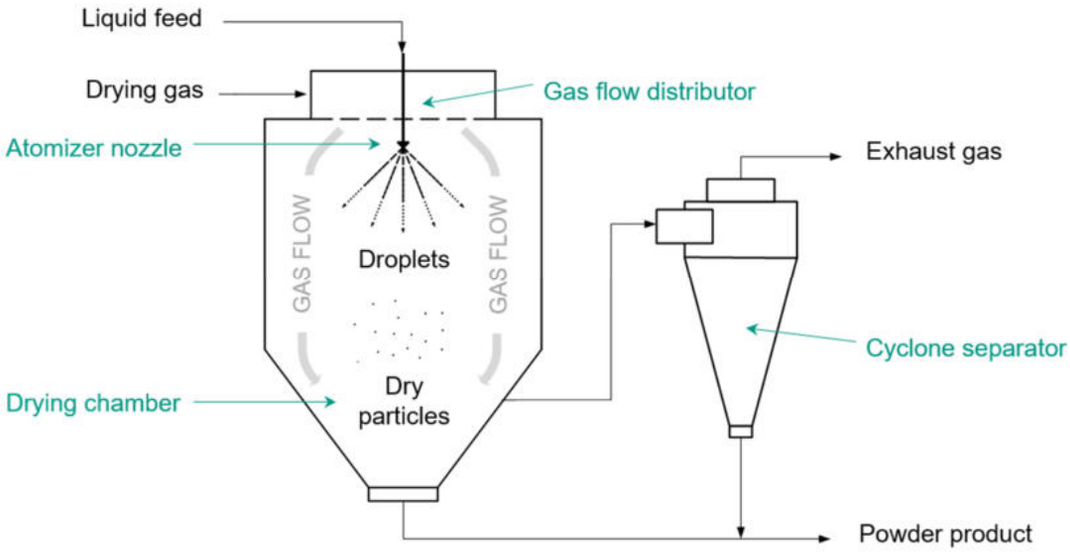

Figure 1: Schematic of the spray-drying process

The atomization of a bulk liquid into small droplets leads to a drastic enlargement of the surface-to-volume ratio, enhancing heat and mass flow in the subsequent convective drying step. The surface-to-volume ratio conditions product quality, since particles that are too small can burn, while particles that are too large do not dry sufficiently. The latter leads to increased stickiness of the particles, powder adhesion in the process equipment and storage problems [2]. Therefore, a narrow droplet size distribution is generally favorable. As with all drying processes, water removal is a very energy-consuming process, especially as internal-energy recovery is restricted in spray-drying [3]. Moreover, the powder throughput of a spray-dryer is limited by its specific water evaporation rate at given process conditions [2]. In industrial applications, the aim is therefore to feed the media into the drying process with the lowest possible water content (high dry matter content). This allows a higher product throughput with a constant water evaporation rate.

Using more energy-saving methods, such as membrane processes or multi-stage evaporation, for the upstream concentration, the total energy consumption and process footprint can be reduced. According to a model calculation on industrial spray drying by Fox et al. [4], an increase in feed dry matter content by 1% leads to a decrease in thermal energy consumption of the spray dryer by 3.8%. It also leads to a decrease in total energy consumption of 2.5%, when the energy for pre-concentration in an evaporator is taken into account. However, the dry mass content cannot be increased at will, since the viscosity of the liquid also increases with increasing solid concentration [5]. At high viscosities, the atomization step becomes more energy intensive, since the volume-specific atomization energy requirement for droplet breakup increases sharply as the internal resistance forces of the liquid increases. Larger droplets and/or wider spray droplet size distributions are then produced, up to the point where atomization is no longer possible.

For droplet formation, pressure-swirl (PS) nozzles are commonly used in spray-drying processes on industrial scale [1]. However, for PS nozzles the highest processable viscosity is considerably lower, compared to pneumatic nozzles [6].

Pneumatic atomizers are usually used for atomizing highly viscous liquids. The atomization energy is transferred via a gas stream [7]. In this type of atomizers, a distinction is also made between external-mixing and internal-mixing atomizers, depending on where the gas and liquid flows are combined [8]. An advantage of external mixing nozzles is that the gas and liquid flows can be set independently of each other. However, they tend to produce wide droplet distributions unless high rates of atomizing gas are used [9]. This makes the use of external-mixing pneumatic atomizers on an industrial scale not economically feasible.

In internal-mixing nozzles, an already formed two-phase flow exits through the nozzle channel. This allows for a more efficient transfer of energy from the gas to the liquid [9], as well as the ability to handle higher-viscosity liquids than with pressure swirl nozzles [10]. A drawback is that gas and liquid flow cannot be set entirely independently of each other [11].

With that in mind, the LVT-Institute developed a specific type of internal-mixing nozzle atomizer, the Air-Core-Liquid-Ring (ACLR) atomizer. A schematic of this nozzle can be seen on Figure 2 (left). The device is composed of two concentric tubes. The outer tube is where the liquid feed flows, while a capillary at the center carries the gas and injects it in the center of the mixing chamber. This forms an annular liquid flow, with a gas core. As this two-phase flow exits the nozzle through the outlet channel, the gas phase expands, and the liquid phase breaks up in a cone that then disperses into droplets. The studies so far published, have involved both experimental and numerical analysis of the atomizer, to better understand its performance and its potential (see Figure 2 (right)). The ACLR nozzle has been proven successful for the atomization of highly viscous liquids up to 690 mPa·s [11].

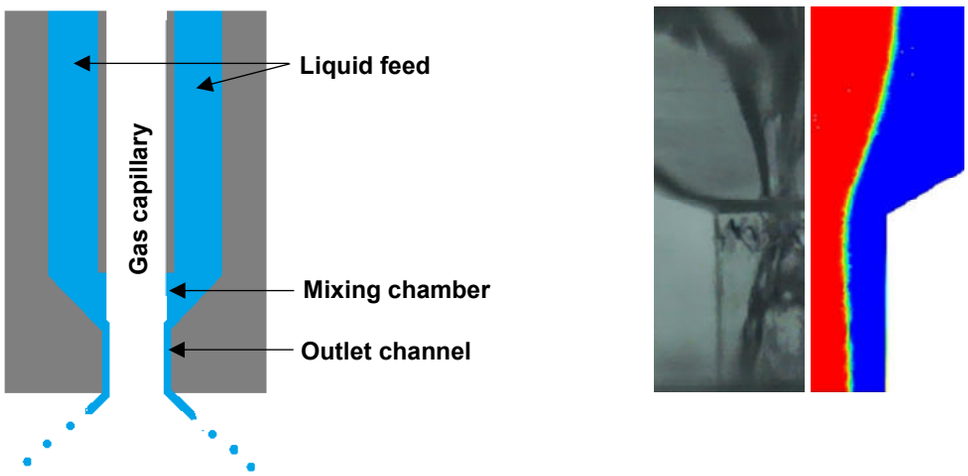

Figure 2: Scheme of the ACLR nozzle (left). Experimental high-speed image of the flow inside the nozzle and the computational simulations performed to represent the internal flow in the atomizer (right)

With the aid of high-speed images of the two-phase flow inside the atomizer, Stähle et al. [10] showed that, if a continuous liquid annular flow forms in the nozzle outlet channel, a stable spray is formed with small droplets. Wittner et al. showed the potential applicability of the ACLR for reducing total energy consumption in spray-dying processes, with theoretical energy savings of up to 29 % [12].

Despite these major benefits of the ACLR nozzle, further studies on the scale-up potential of ACLR atomizers are still needed before a widespread application of the technology in industrial processes is conceivable. As reported by Wittner et al. [11], moisture content and water activity in the final powder product should be decreased to meet industrial demands. Additionally, based on Wittner et al. [13], we assume that in order to properly understand the process-function of the nozzle, and how spray performance relates to operating conditions and feed composition, we need to comprehend the flow

behavior inside the ACLR nozzle. For this purpose in an ongoing project a CFD model is developed for the simulation if the internal flow of the ACLR-nozzle. Based on these investigations it is assumed that the spray performance of the ACLR-nozzle can be enhanced by geometrical improvements. This should lead to a further reduction of the spray droplet size widths and increase the maximum possible viscosity that can be atomized for spray drying applications. In addition a further nozzle scale-up can be based on these results. Comprehending this process-function is therefore not only important for the atomization itself, but also for the subsequent drying step.

This process-function establishes the relation between the entry feed composition and droplet morphology. But it is well known that the droplet composition and morphology together with the process variables have a high impact on the final powder product [14–16]. Powder properties such as powder flowability, particle size, as well as particle and bulk density relate directly to the morphological structure of the powder particles. Although morphology is material-specific, it is also dependent on, for example, initial feed solids content, atomization and drying temperature [15]. The work of Hecht and King [17] also showed, that morphological changes, such as vacuole formation, can influence mass transfer rates and therefore drying kinetics. Consequently, it is very import to investigate the dynamic interactions between particle composition, morphology development and drying kinetics.

One way to examine the drying kinetics and morphology development is to directly observe the structure of the drying spray-droplets. This also allows acquiring accurate insights into the structural changes during the drying process. Direct observation of the drying droplets is unrealistic in a commercial spray-dryer or a modular nozzle test rig, due to the number of droplets and the difficult accessibility of the equipment. Furthermore, the transition from a droplet to a particle during spray-drying occurs quasi-instantaneously, which makes it almost impossible to track the drying kinetics and the morphology development of the particle. Consequently, for mechanistic studies of the drying process, experimental setups that center around drying a single droplet have been more and more the focus of research [18].

In single droplet drying (SDD) experiments, an isolated droplet is dried under a controlled drying environment [19]. The drying temperature, air humidity and air mass flow is set to mimic the convective drying process during spray-drying. Several experimental setups exist for SDD and are usually divided into levitation methods and free flight drying methods. Free flight drying methods are rather impractical for the examination of drying kinetics, as a continuous tracking of the droplet during drying is not possible. A commonly employed contact levitation method is a SDD experiment with a droplet suspended on a thin filament [20–22]. This allows easy monitoring of droplet mass and temperature changes of the droplet [23]. A drawback of this method is the intrusiveness of the filament on heat transfer.

An alternative to contact levitation is the immobilization of the droplet by acoustic levitation. In acoustic levitation, a single droplet is suspended due to a counterbalancing acoustic force while drying. [24]. A major benefit of this setup is that the drying of a droplet can be investigated non-intrusively, while one drawbacks is the not well-understood influence of the ultrasound on the drying kinetics.

Another tool to investigate one-dimensional drying kinetics is thin film drying [25]. Previous work has shown that a film thickness of micrometer- to nanometer-scale is feasible [26]. Schutyser et al. [18] has suggested that thin film drying technology could be a valuable tool to compliment the results generated by single droplet drying experimental setup.

Single droplet drying has been used extensively in literature for studying the morphology development, both by contact levitation [20,22,27] as well as by non-contact levitation [14,23,28,29]. The SDD setups are usually equipped with a CCD-camera with microscope optics for a continuous observation of the droplet during drying. Crust formation and structural changes can thus be determined directly. Nuzzo et al. [23] found for milk powder that it was possible to predict the morphology of spray-dried particles largely by means of SDD experiments, despite significantly longer drying times. The effects in the SDD

tests were significantly more pronounced compared to the spray-drying tests. It is therefore expected that, despite the different drying systems, conclusions can be drawn between SDD and spray-drying tests with respect to the development of the particle morphology during drying.

The LVT-institute has many years of experience with single droplet experiments and equipment for the investigation of e.g. interfacial properties in single droplets. This mainly involves equipment with droplets suspended on filaments. In a just started research project financed by German Ministry BMWi, the LVT-Institute develops an experimental setup for SDD.

3 Project objectives

Spray-drying of liquid products is a key technology that is widely used in many industries. Its environmental impact could be reduced through process intensification by increasing the concentration of the feed liquid to be dried, thereby reduce energy consumption and process footprint. This requires the ability to atomize highly viscous liquids (especially pastes) and achieve short drying times to produce a suitably dry product that does not stick to process surfaces without changing functionality of the dried product. Key objectives of this project are:

- Validate the ACLR atomizer technology to enable spraying of highly viscous liquids for spray drying applications by improvement and upscale of the ACLR-nozzle.
- Evaluate the impact of the composition and morphology of the atomized droplets on the drying kinetics and develop drying models for highly concentrated feeds by single droplet drying.
- Investigation of the applicability of the ACLR nozzle for spray-drying of highly viscous liquids.

4 Methodology and work plan

The project is divided into three main working packages (WP). The ACLR nozzle is proposed as a suitable atomization technology for spraying of highly viscous liquids or pastes and generate droplets smaller than 100 micron. The central task of the first working package (WP) will be the validation of the ACLR nozzle to enable atomization of highly viscous liquids. CFD simulations will be used to optimize nozzle design. Process- structure-functions for the nozzle will then be established based on spray performance measurements. The gained insights can be used for further upscaling of the process. A period of 18 months is planned for this work package.

The objective of the second WP is to investigate the impact of the composition and process parameters on the drying kinetics and morphology development of highly viscous liquid or paste droplets in controlled conditions. For this purpose single droplet drying experiments will be carried out, in which droplets can be dried under precisely defined conditions. These studies will also be used to explore a possible relation between the morphology development and the drying kinetics. Taking into account the results of the first two WPs, a model for drying of highly concentrated feeds will be formulated as process-structure-function. Work on the second WP will start after viable formulations for the project are identified. It is currently estimated that the WP will be concluded after 18 months.

In the third WP, the applicability of the ACLR nozzle for industrial spray-drying processes of highly viscous liquids will be examined. For this purpose, spray-drying trials will be carried out. The results will be used to evaluate the validity of the in WP 2 formulated model. WP 3 will be the main workload during the project's third year. It is estimated, that work on the final WP will start after the first two WPs have been completed and the process-structure-function has been elucidated in WP 2.

A working diagram is shown in Table 1.

Table 1: Working diagram for the planned project duration

Project year	1				2				3			
Quarter	I	II	III	IV	I	II	III	IV	I	II	III	IV
WP 1: Atomization with the ACLR nozzle												
WP 2: Evaluation of the impact of composition and morphology on drying kinetics												
WP 3: Industrial applicability of the ACLR nozzle for spray-drying												

4.1 WP 1: Atomization with the ACLR nozzle

Numerical studies on the ACLR atomizer started with Wittner et al. [13], where an initial computational model to represent the multiphase flow inside the system was developed, using Ansys Fluent. This model is currently being refined, under a project financed by the DAAD, so that the nozzle design can be geometrically optimized and tailored for specific industrial applications.

In WP1 this model will be extended to the flow analysis of highly viscous liquid feeds. On the basis of the CFD results an optimized nozzle concept will be drawn and the suitability will be investigated in spray performance measurements. The focus of the research will be on the evaluation of process-structure-function for the nozzle. Therefore, the atomization capability of two different highly viscous liquids will be investigated. Process parameters are the nozzle design, the ratio of air-to-liquid flow rate (ALR) and the air pressure. Structure variables are the spray angle and the droplet size distribution, including its temporal stability. As model system, aqueous solutions of maltodextrin are proposed. Maltodextrin is commonly used as a thickener and stabilizing agent. The model system has to be defined and characterized at the beginning of the experimental study, to allow a systematic investigation of the relevant process parameters.

For validation of the CFD model, the flow pattern inside the nozzle will be analyzed. Based on these results a nozzle scale up concept will be proposed. Taking into account the numerical and experimental results, a comparative analysis can be done to investigate the feasibility of spraying highly viscous fluids and pastes to generate droplets smaller than 100 µm.

The experimental study can be carried out on the institute's facilities. For this purpose, a separate compressor (RSF-Top 7.5, Renner GmbH, Güglingen, Germany) is available for the operation of the ACLR atomizers in addition to the compressed air network. A pressure vessel and various eccentric screw pumps with volume flow between 5 and 100 L/h can be used for the liquid supply. Furthermore, a test rig is available, equipped with a temperature control for the feed liquid. Here the spray droplet sizes can be measured over time using a laser diffraction spectrometer (Malvern Spraytec, Malvern Panalytical Ltd, Malvern, United Kingdom) in a size range of 2-2000 µm. A high-speed imaging system (OS3-V3-S3, Integrated Design Tools Inc., Tallahassee, FL,USA) is available to analyze the spray angle and the flow pattern inside the atomizer. The rheological characterization of the model systems can be done with a double gap system (Physica MCR 101/103, Anton Paar, Graz, Austria).

4.2 WP 2: Evaluation of the impact of the composition and morphology on the drying kinetics and model development by single droplet drying

The development of a suitable methodology for single droplet drying experiments is already being pursued at the institute as part of the AiF project 21662 N "Spray-drying of emulsions for microencapsulation". For this project, an experimental setup is will be installed that allows continuous monitoring of the drying kinetics and particle morphology during the drying of emulsion droplets.

In WP 2, the experimental setup for emulsion droplets will be extended to droplets of highly viscous solutions. This is expected to be fairly straightforward. A potential challenge is mainly seen in the production of uniform droplets from formulations with varying solids concentrations, as the rheological

behavior differs between these formulations. Using of different droplet injection systems might be necessary. Nevertheless, as the development of the experimental setup is still in its early stages, advices and experiences of industry partners on single droplet drying could prove valuable. The experimental studies in WP 2 will focus on the influence of air temperature, air velocity and total solids content on the drying kinetics and morphology development during convective drying. Therefore, the same highly viscous liquids will be used as in WP 1. By monitoring droplet size, evaporation rate and temperature profiles of the droplet, the drying kinetics can be determined. For the morphology development, different structural changes are expected. Besides changes in particle size, other phenomena may occur during drying of a liquid droplet. These include the formation of an inhibitory skin, changes in the surface structure (smooth or wrinkled), and rupture of the particle. To observe these phenomena, various analytical methods are available at KIT. In addition to light microscopy and SEM (scanning electron microscopy) images, the particles can be examined in µCT (micro computed tomography). Solubility tests can provide information about the properties of the particle skin.

Based on the results of the experimental study a model for the drying of highly viscous liquids will be developed. The model will be formulated as a process-structure-function to elucidate the impact of feed composition and morphology development on the drying kinetics.

4.3 WP 3: Proof-of-concept of industrial applicability of the ACLR nozzle for spray-drying of highly viscous liquids

It is expected that from the results of WP1 and WP2 conclusions can be drawn on possible process windows for atomization (WP1) and drying (WP2) conditions for highly viscous liquids. In WP3 the applicability of these conditions on a spray drying process will be investigated. This will be executed in pilot scale on the institute's spray-dryer (Werco SD-20, Fa. Hans G. Werner, max. water evaporation capacity of 20 l/h, max. air inlet temperature 250 °C, max. air outlet temperature 100 °C). Solutions with the highest possible viscosity at acceptable spray droplet size are selected for this purpose. The spray-drying experiments can be conducted under variation of the air temperature at the inlet (160-220 °C) and outlet (65-95 °C), the air velocity and the spray droplet size. This way, the drying rate and the surface-to-volume ratio in the particle are varied. Measurements of the residual moisture content can be used to validate the drying kinetics determined in WP 2. After spray-drying, the structure of the produced powder will be characterized and compared to the results of WP 2. The same powder characterization methods can be used as in WP 2. The results allow a validation of the process-structure-function developed in WP 2, which will be modified if necessary.

Figure 3: The institute's pilot scale spray-dryer

5 Transfer of knowledge

Based on the results, solution concepts can be derived that contribute to a targeted and understanding-based process design for the production of powder products from highly viscous liquids. These solution concepts form the basis for an implementation by the industrial user with their own recipes and processes. The research results can be presented and discussed in accompanying meetings and appropriate international conferences and are summarized in annual reports. The results will be published in appropriate international journals.

6 References

[1] Mujumdar A. S., Ed., 2015. *Handbook of industrial drying,* 4th ed., CRC Press, Boca Raton.

[2] Masters K., 2002. *Spray Drying in Practice*, SprayDryConsult International ApS, Charlottenlund.

[3] Baker C. G. J., and McKenzie K. A., 2005,"Energy Consumption of Industrial Spray Dryers," Drying Technology, **23**(1-2), pp. 365–386.

[4] Fox M. B., Akkerman C., Straastma H., and Jong P. de, 2010,"Energy reduction by high dry matter concentration and drying," New Food, **6**(2), p. 60-63.

[5] Rao M. A., 2014. *Rheology of Fluid, Semisolid, and Solid Foods: Principles and Applications,* 3rd ed., Springer, Boston, MA.

[6] Stähle P., Schuchmann H. P., and Gaukel V., 2017,"Performance and Efficiency of Pressure-Swirl and Twin-Fluid Nozzles Spraying Food Liquids with Varying Viscosity," Journal of Food Process Engineering, **40**(1), p. 1–12.

[7] Ashgriz N., 2011. *Handbook of Atomization and Sprays: Theory and Applications*, Springer Science+Business Media LLC, Boston, MA.

[8] Wozniak G., 2003. *Zerstäubungstechnik: Prinzipien, Verfahren, Geräte*, Springer, Berlin, Heidelberg.

[9] Hammad F. A., Sun K., Jedelsky J., and Wang T., 2020,"The Effect of Geometrical, Operational, Mixing Methods, and Rheological Parameters on Discharge Coefficients of Internal-Mixing Twin-Fluid Atomizers," Processes, **8**(5), p. 563.

[10] Stähle P., Gaukel V., and Schuchmann H. P., 2017,"Comparison of an Effervescent Nozzle and a Proposed Air-Core-Liquid-Ring (ACLR) Nozzle for Atomization of Viscous Food Liquids at Low Air Consumption," Journal of Food Process Engineering, **40**(1), p. 1–9.

[11] Wittner M. O., Karbstein H. P., and Gaukel V., 2018,"Spray performance and steadiness of an effervescent atomizer and an air-core-liquid-ring atomizer for application in spray drying processes of highly concentrated feeds," Chemical Engineering and Processing: Process Intensification, **128**, pp. 96–102.

[12] Wittner M. O., Karbstein H. P., and Gaukel V., 2019,"Energy efficient spray drying by increased feed dry matter content: investigations on the applicability of Air-Core-Liquid-Ring atomization on pilot scale," Drying Technology, **38**(10), pp. 1323–1331.

[13] Wittner, Ballesteros, Link, Karbstein, and Gaukel, 2019,"Air-Core–Liquid-Ring (ACLR) Atomization Part II: Influence of Process Parameters on the Stability of Internal Liquid Film Thickness and Resulting Spray Droplet Sizes," Processes, **7**(616), pp. 1–18.

[14] Both E. M., Karlina A. M., Boom R. M., and Schutyser M., 2018,"Morphology development during sessile single droplet drying of mixed maltodextrin and whey protein solutions," Food Hydrocolloids, **75**, pp. 202–210.

[15] Walton D. E., and Mumford C. J., 1999,"Spray Dried Products—Characterization of Particle Morphology," Chemical Engineering Research and Design, **77**(1), pp. 21–38.

[16] Wu W. D., Liu W., Gengenbach T., Woo M. W., Selomulya C., Chen X. D., and Weeks M., 2014,"Towards spray drying of high solids dairy liquid: Effects of feed solid content on particle structure and functionality," Journal of Food Engineering, **123**, pp. 130–135.

[17] Hecht J. P., and King C. J., 2000,"Spray Drying: Influence of Developing Drop Morphology on Drying Rates and Retention of Volatile Substances. 1. Single-Drop Experiments," Ind. Eng. Chem. Res., **39**(6), pp. 1756–1765.

[18] Schutyser M. A. I., Both E. M., Siemons I., Vaessen E. M. J., and Zhang L., 2019,"Gaining insight on spray drying behavior of foods via single droplet drying analyses," Drying Technology, **37**(5), pp. 525–534.

[19] Fu N., Woo M. W., and Chen X. D., 2012,"Single Droplet Drying Technique to Study Drying Kinetics Measurement and Particle Functionality: A Review," Drying Technology, **30**(15), pp. 1771–1785.

[20] Shamaei S., Kharaghani A., Seiiedlou S. S., Aghbashlo M., Sondej F., and Tsotsas E., 2016,"Drying behavior and locking point of single droplets containing functional oil," Advanced Powder Technology, **27**(4), pp. 1750–1760.

[21] Wang Y., Che L., Selomulya C., and Chen X. D., 2014,"Droplet drying behaviour of docosahexaenoic acid (DHA)-containing emulsion," Chemical Engineering Science, **106**, pp. 181–189.

[22] Malafronte L., Ahrné L., Schuster E., Innings F., and Rasmuson A., 2015,"Exploring drying kinetics and morphology of commercial dairy powders," Journal of Food Engineering, **158**, pp. 58–65.

[23] Nuzzo M., Millqvist-Fureby A., Sloth J., and Bergenstahl B., 2015,"Surface Composition and Morphology of Particles Dried Individually and by Spray Drying," Drying Technology, **33**(6), pp. 757–767.

[24] Al Zaitone B., 2009,"Drying of Multiphase Single Droplets in Ultrasonic Levitator," Dissertation, Technische Universität Darmstadt, Darmstadt.

[25] Coumans W. J., 2000,"Models for drying kinetics based on drying curves of slabs," Chemical Engineering and Processing: Process Intensification, **39**(1), pp. 53–68.

[26] Börnhorst T., Scharfer P., and Schabel W., 2021,“Drying Kinetics from Micrometer- to Nanometer-Scale Polymer Films: A Study on Solvent Diffusion, Polymer Relaxation, and Substrate Interaction Effects,” Langmuir the ACS journal of surfaces and colloids, **37**(19), pp. 6022–6031.

[27] Both E. M., Siemons I., Boom R. M., and Schutyser M., 2019,“The role of viscosity in morphology development during single droplet drying,” Food Hydrocolloids, **94**(303), pp. 510–518.

[28] Tran T. T. H., Terrazas-Velarde K., Avila-Acevedo J. G., and Tsotsas E., 2014, Particle morphology as a mean for investigating single droplet drying of dairy products, *IDS 2014: Proceedings of the 19th International Drying Symposium August 24-27, 2014, Lyon, France*, Andrieu J., Peczalski R., and Vessot S., eds., EDP Sciences, Les Ulis.

[29] Abdullahi H., Burcham C. L., and Vetter T., 2020,“A mechanistic model to predict droplet drying history and particle shell formation in multicomponent systems,” Chemical Engineering Science, **224**(9), 115713.

IFPRI

International Fine Particle Research Institute

Research Project Brief

Numerical Modeling of Spray Droplet Formation

The International Fine Particle Research Institute (IFPRI) wishes to fund a research project on numerical modeling of droplet formation in atomization. Atomization is a critical process in many particle processes, and while the underlying physics of droplet formation is understood, quantitative simulation of atomizer performance is not yet possible. The objective of this project is to explore whether recent advances in simulation of complex fluid flows are sufficient to reproduce quantitatively the performance of commercial spray atomizers.

Specifically, the objective of this project is to develop an experimentally validated high-fidelity CFD model for spray atomization that captures both the near field behavior (sheet and filament formation and break up) and the ultimate far-field droplet size distribution. The model should be applicable to atomization of viscous liquids, aqueous and organic, with viscosity up to 1 Pa*s. Consideration of the behavior of non-Newtonian fluids (e.g., shear thinning) is a plus. The project should focus on pressure-driven atomizers (single or two fluid), however other atomizer types can be explored as a stretch goal.

High-Fidelity Modeling of Atomization from Nozzle Flow to Fully Developed Spray

Executive Summary

The objective of this research project is to demonstrate the ability of a recently-advanced high-fidelity modeling framework for spray formation to predict drop size and velocity distributions in high viscosity liquid atomization systems, such as found in spray drying applications. This framework, which has been developed by the PI's research group as part of an ongoing ONR MURI project on fuel spray control, hinges on several enabling components: (1) the large eddy simulation (LES) of the two-phase flow field, including the internal nozzle flow, in order to capture directly the large-scale flow dynamics critical to the liquid destabilization and break-up, (2) a fully conservative Eulerian interface tracking technique with the ability to capture subgrid scale liquid features such as thin films and thin ligaments, known to be of critical importance in the break-up of viscous fluids, and (3) a simple break-up model to convert these thin liquid features into spray droplets that can be tracked in a Lagrangian fashion.

In contrast to most existing atomization models, this framework has several key advantages: it is based on first principles instead of an assumed break-up phenomenology, it models an atomizer end-to-end, i.e., from its inlet to a fully dispersed spray, and it benefits from a much lower cost than brute-force direct numerical simulation (DNS). However, it has only been demonstrated on a two-fluid atomizer configuration with water and air so far. This project will explore the influence of higher viscosity and non-Newtonian behavior on the prediction of drop sizes. It is expected that thin liquid sheets and ligaments will dominate the atomization of higher viscosity fluids (e.g., in contrast to water), for which the ability to track subgrid scale interfacial features will prove invaluable. The work will begin by exploring the effect of increasing liquid viscosity on the predicted spray generated by an academic two-fluid atomizer for which extensive water-air data is available, but will seek reference data from IFPRI members and collaborators in order to validate the performance of the framework with high viscosity/non-Newtonian liquids.

1 Introduction

The reliable formation of a spray is a critical component of many engineering systems. In particular, producing powders often involves atomizing a liquid mixture into fine droplets, then drying them into solid particles. In this process known as spray drying, the quality of the powder hinges on the quality of the liquid atomization process, and as such, the droplet size distribution needs to be controlled. Yet, a well-controlled and predictable droplet size distribution is very challenging to achieve in practical applications, especially when considering that the liquids used in spray drying applications are often very viscous, potentially non-Newtonian slurries. Consequently, these systems are often designed and optimized through an expensive trial-and-error process instead of predictive modeling. **The main goal of this project is to bridge this gap by demonstrating that modern, high-fidelity CFD modeling of atomization can predict spray drop size and velocity distributions from first principles, thereby providing a critical modeling tool to engineers.**

Experimental studies of liquid atomization are needed to provide validation data for models and simulations. However, they present significant challenges: the liquid droplets effectively shield the liquid core and prevent optical access, making direct examination of the spray formation mechanisms difficult under realistic conditions. Velocity measurements in the gas phase cannot easily be obtained close to the liquid, so experiments are often limited to characterizing the size and velocity of droplets far downstream of the near-field spray formation region. Even when the atomizing flow is visible, light-scattering-based measurements require very careful analysis in order to extract quantitative data (e.g., see [1]). Recently, experimentalists have started using X-ray imaging techniques and other non-scattering methods in order to quantify liquid statistics in the near-field successfully [2]. For the first time, these new X-ray datasets are providing an opportunity to validate in details numerical simulations of atomization.

In a nutshell, all liquid atomizers follow the same principle: impart kinetic energy to the liquid-gas flow in such a way that as much of it as possible is converted into surface energy (i.e., more drops and smaller drops). The kinetic energy can be given to the liquid directly (using acoustic forcing for nebulizers, moving geometry for rotary disks, or pressurized tanks for pressure-driven atomizers), it may be given to the surrounding gas (using a pressurized gas in two-fluid atomizers), or a mixture of both (e.g., aerated injectors, jet-in-crossflow). Moreover, drop sizes can be selected by carefully choosing the topology of the liquid – in particular, the liquid is often flattened into a thin sheet (e.g., via prefilming or swirling flows). This wide range of atomization processes presents a fantastic challenge to modelers: they each display fundamentally different phenomenologies that, depending on operating conditions, can be dominated by turbulence, Kelvin–Helmholtz instabilities, Rayleigh–Taylor instabilities, flapping dynamics, ligament break-up, or bag bursting, to list just a few. Therefore, no single phenomenological reduced-order atomization model can be expected to capture accurately spray drop sizes over a range of injection strategies, flow conditions, and fluid properties. Nevertheless, the standard modeling strategy for atomization engineers today typically forgoes all details of the liquid injection process and break-up dynamics, instead representing the liquid stream as a series of large initial "blobs" that can be treated in a Lagrangian fashion and undergo break-up based on phenomenological processes such as surface instabilities [3–5], droplet shedding [6], and turbulence [7]. This approach is captured in the leftmost vignette in Fig. 1.

In contrast, first-principle higher-fidelity models based on the solution of the Navier-Stokes equations have the potential to capture all these phenomenologies appropriately, which is why they are the focus in this proposal. Of course, accurate simulations of multiphase turbulent systems in complex geometries are challenging to conduct, in part because of the wildly discontinuous densities and viscosities across the phases, as well as the singular surface tension force at the interface, and the wide range of length and time scales involved in these flows. Yet, numerical methods for complex atomizing multiphase flows have rapidly progressed in the recent years, and have reached a level of maturity that approaches that of single-phase flows. Given sufficient computational resources, it is possible to perform high-fidelity simulation of the early spray formation process, thereby providing direct access to droplet size and velocity in Eulerian frameworks such as level set and volume-of-fluid (VOF) methods. Note however that such simulations often require billions of degrees of freedom and thousands of computer cores over multiple weeks [8, 9], which limits their usefulness to purely academic studies in canonical configurations. This *full DNS strategy*, summarized in the rightmost vignette in Fig. 1, is not pursued in this project due to its inability to tackle atomization problems of industrial relevance.

Alternatively to DNS, **LES of two-phase atomizing flows is more promising for industrial applications**: instead of requiring all scales to be resolved, only the dynamically important

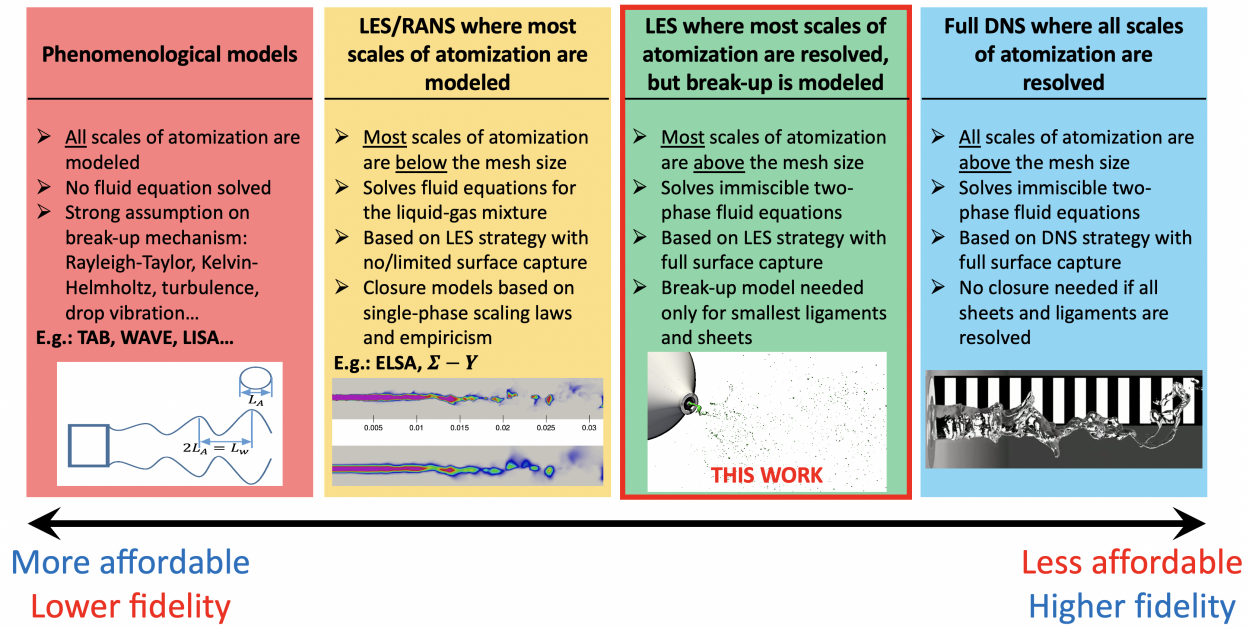

Figure 1: Overview of various modeling strategies for liquid atomization, ranging from ad-hoc, phenomenological models on the left which are cheap but non-predictive, to full DNS on the right which is accurate but overly expensive. The proposed work corresponds to the third box from the left, where only the final stage of ligament and sheet break-up is modeled.

large scales are resolved on the mesh, while the more universal small scales are modeled. One possible LES strategy is to choose a mesh size such that almost all interfacial dynamics happen at the subgrid scale, as summarized on the second vignette from the left in Fig. 1. Then, the liquid-gas interface does not need to be carefully tracked, but the entirety of the break-up process needs to be modeled: the $\Sigma - Y$ and ELSA models [10–12] are the most well-known examples of such a strategy. The subgrid scale closures needed are numerous, complex, and often based on empiricism and parameter fitting. In fact, recent results reported using this type of models still rely heavily on coefficient tuning and show that more work is needed to improve predictions (e.g., see [13]).

The third vignette from the left in Fig. 1 presents the alternative strategy pursued in this work. Still in the context of a two-phase flow LES, we propose to perform detailed interface tracking so that **most scales of interfacial deformation are captured on the mesh**. However, requiring that the mesh size is sufficiently small to resolve properly all topology-change events leads to an exorbitant cost, as mentioned earlier. This is especially true for high viscosity liquids for which very elongated ligaments and very thin sheets are know to abound. Therefore, we propose instead to model the break-up of thin liquid features at the subgrid scale by first tracking the geometry of these thin features as they fall below the mesh size, then using a simple closure to convert these thin features into Lagrangian droplets. This approach leads to several orders of magnitude of reduction in computational cost compared to full DNS, but only relies on models for the final, most universal step of break-up, thereby preserving high fidelity predictions.

2 Prior Research

Predictive high-fidelity modeling of atomization with application to spray control has been the focus of a ONR-funded Multidisciplinary University Research Initiative led by Prof. Desjardins at Cornell in the past five years. That project has led to significant advances in both numerical techniques and modeling framework for spray atomization. In particular, we demonstrated the first detailed validation of atomization simulations against X-ray data, and we proposed and demonstrated a novel modeling paradigm for spray formation simulations which explicitly addresses the mesh-dependent nature of break-up in interface capturing simulations.

2.1 High-Fidelity Multiphase Flow Simulations with Experimental Validation

The effort to perform high-fidelity modeling of spray formation has led to several advances of techniques for accurate multiphase flow simulations. In particular, a new multiphase-ready stabilized traction boundary condition was developed that allows for droplets to seamlessly leave the computational domain and also prevents interface wave reflection [14]. Additionally, a dynamic contact line model was developed that accounts for subgrid scale surface tension forces at the triple contact line [15]. This model allows the interface to meander along the edge of the nozzle's liquid needle, a phenomenon that was identified and quantified using X-rays, and found to influence the downstream dynamics. With these advances, we were able to carefully validate simulations of the early destabilization of a two-phase planar shear layer against linear stability analysis and experiments [14, 16], and simulations of a complete two-fluid annular airblast nozzle were validated against effective liquid path length (EPL) data obtained from X-ray measurements and against backlit imaging data (see Fig. 2).

2.2 Novel Modeling Framework for Mesh-Independent Break-up

Beyond improving the fidelity of the multiphase simulations of the very near-field region, we have focused on addressing head-on the issue of predictive break-up modeling. While level set and volume-of-fluid (VOF) methods provide visually pleasing interface topologies, it is important to understand that the droplet size distributions generated from classical interface capturing methods are *virtually always mesh-dependent*: this is due to the fact that the mesh size provides a minimal length scale for interface folding below which break-up is triggered. This is most obvious in the case of bag break-up, wherein a fast gas penetrates a liquid structure and inflates a thin liquid sheet into a large bag-like shape. From theory and experimental observations, the thin liquid sheet is expected to have a **sub-micron thickness** by the time the bag breaks. In contrast, in simulations, the bag always ruptures when the sheet reaches the mesh resolution. Simply put, it means that a true DNS of a flow with thin liquid bags would require a sub-micron mesh resolution, which is not affordable in most situations. To address this issue, we introduced a new approach that combines three elements: (i) the interface is reconstructed using R2P [17, 18], a new computational interface model that allows multiple interfaces per grid cells, thereby allowing for arbitrarily thin interfacial features to be tracked at the subgrid scale, (ii) regions that are likely to undergo break-up momentarily are identified and classified as Lagrangian objects, i.e., sheets and ligaments are identified as such using a specially-designed Connected Component Labeling (CCL) scheme [19, 20], and (iii) once a specified criterion has been reached, the sheet or ligament object is atomized through the use of a break-up model that creates droplets in a mass-conserving manner from physical arguments [21].

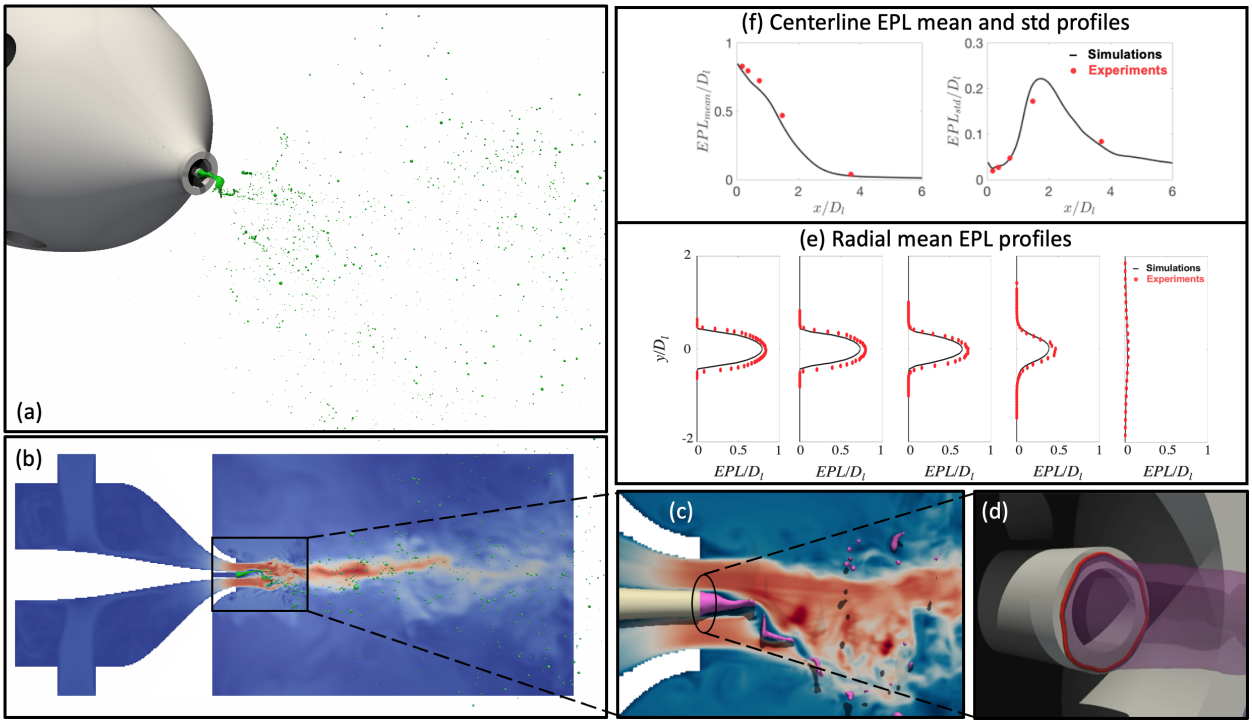

Figure 2: (a) Simulation of a complete annular airblast spray at a momentum flux ratio of 6, without swirl: the nozzle is visible on the top left in grey, and the liquid spray is shown in green. (b) Instantaneous velocity magnitude, showing the flow in the nozzle plenum, the near-field turbulence, and the turbulent spray dispersion downstream. (c) Zoom on the details of the liquid jet (shown in pink here) and the velocity field at the exit of the nozzle. (d) Zoom on the liquid needle, showing the dynamic anchoring of the liquid-gas interface. (e) and (f) show the comparison of the effective path length (i.e., line-of-sight integrated liquid length) obtained from X-ray measurements to the simulation data, along radial profiles and along the centerline.

This strategy is demonstrated in Fig. 3 with the classical problem of a droplet at a Weber number of approximately 20 undergoing bag break-up: a thin liquid sheet is formed, and bursts into $\mathcal{O}\left(10^4\right)$ droplets, while the rim forms a ligament that survives longer and undergoes a slower Rayleigh–Plateau break-up process. The classical VOF scheme, shown in green for a simulation with 13 cells across the droplet diameter, does not capture the formation of a bag and ultimately only generates a handful of large rim droplets. For such a VOF-based simulation to capture the correct drop size distribution via DNS, more than three orders of magnitude more grid cells would be needed. In contrast, the R2P+CCL+break-up model shown in pink at the same resolution of 13 cells per diameter generates a large bag which breaks into $\mathcal{O}\left(10^4\right)$ droplets as small as a few microns, in agreement with recent holographic measurements by Guildenbecher et al. [22]. Deployed in simulations of the canonical airblast nozzle studied mentioned above, this strategy enabled the end-to-end modeling of the atomization process shown in Fig. 2, a first of its kind. The drops generated by the break-up of the thin liquid structures are transferred to a Lagrangian representation, and their turbulent dispersion by the gas flow is computed downstream of the nozzle.

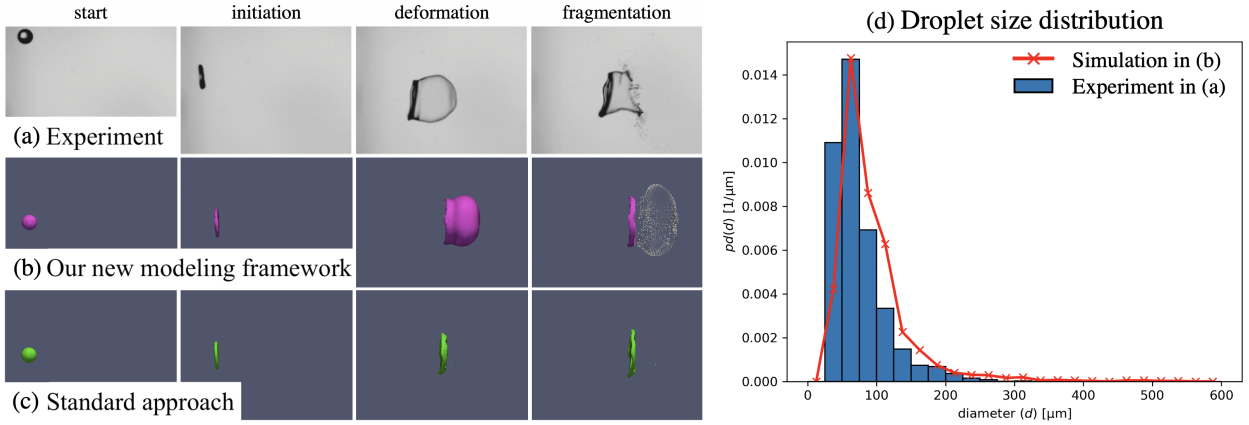

Figure 3: Bag break-up of a moderate Weber droplet: sequence of snapshots at four successive times from (a) experiments by Guildenbecher et al. [22], (b) a simulation using the new subgrid scale break-up model, and (c) a simulation using a standard volume of fluid strategy. The droplet size distributions generated by the bag break-up in (a) and (b) are compared in (d).

3 Proposed Work and Timeline

Several studies have elucidated the effect of increased viscosity on the performance of two-fluid airblast atomizers. For example, Mackrory [23] pointed out that ligaments that form during the primary break-up process are thinner and longer when the liquid is more viscous – and therefore more challenging to resolve numerically, which makes our approach that tracks these ligaments at the subgrid scale advantageous. Mackrory's study also reported a tendency of the more viscous liquids to pool at the nozzle lip, leading to large droplets being regularly released. Our ability to model accurately contact line physics will be important in capturing that effect. In general, the experimental consensus is that larger viscosities lead to larger droplets [24–27], although bimodal size distributions are not uncommon. These observations suggest that our spray modeling framework is already well-suited for predicting the atomization of high viscosity liquids without requiring significant changes, and as such we do not propose significant new development, instead focusing on assessing the performance of the framework, both in terms of computational cost and fidelity of predictions. Consequently, we propose the following work packages.

Work Package 1 – Exploring the Impact of Viscosity on Spray Formation

In WP1, we will investigate the impact of increasing liquid viscosity on the drop size and velocity distributions and on the atomization dynamics for the canonical two-fluid airblast atomizer that we developed as part of the ONR MURI project mentioned above. This atomizer, visible in Fig. 2 (a-c), captures the main features of externally mixed swirled two-fluid injectors, and has been extensively characterized using X-ray, backlit imaging, and PDPA for various swirl and momentum flux ratios using water and air, and as such it provides a validated starting point for our modeling effort. Increasing the viscosity presents no particular numerical challenge since our flow solver already treats the viscous terms fully implicitly, so we do not expect that we will have to drastically reduce the time step size to maintain stability, thereby keeping the cost of simulations low. We will compare the effect of increasing viscosity on the drop sizes to existing correlations, in particular the one proposed for high viscosity fluids by Aliseda et al. [27].

Timeline: Our ONR MURI airblast case will be studied with increasing liquid viscosity in year 1.

Work Package 2 – Detailed Validation of High Viscosity Liquid Spray Formation

In WP2, we will validate our detailed model predictions against experimental data. As a preliminary step during year 1, we will perform a review of the literature to identify the best reference data set for the purpose of validation. At the moment, we believe that the experimental work of Aliseda [27] might be optimal, especially given the close ongoing collaboration between the groups of Aliseda and Desjardins. We will also interact closely with IFPRI members and assess whether they can avail relevant pre-competitive data to augment our validation effort. Then, in year 2, we will study in details the experimental case (or potentially few cases) chosen in year 1 and compare our modeling predictions against spray measurements. We will draw conclusions regarding the computational performance of the method: in particular, we will characterize the impact of mesh resolution on the predictions, and the overall accuracy of our strategy.
Timeline: The best experimental dataset for validation will be identified in year 1, then the detailed comparison will be done in year 2.

Work Package 3 – Exploring the Atomization of Non-Newtonian Liquids

In WP3, we will first implement a simple non-Newtonian liquid model in our flow solver using a shear-dependent viscosity coefficient. While straightforward in an explicit flow solver, this will present some challenges in our time-implicit solver as the Jacobian of the viscous term will increase in complexity. We will test our implementation on well-known laminar flow solutions. We expect most of this work to be done within year 2, so we can then test the impact of non-Newtonian liquid dynamics on our model predictions in year 3. In particular, we expect that our current model closure for converting thin ligaments and sheets into droplets will need to be modified to reflect the non-Newtonian break-up dynamics of these simple topologies. The detailed study of the non-Newtonian Raleigh–Plateau instability for ligaments and of the Taylor–Culick instability for liquid sheets might be needed to elucidate how these fundamental break-up processes change for complex liquids.
Timeline: A simple non-Newtonian liquid with shear-dependent viscosity will be implemented in year 2, then will be used in atomization simulations in year 3 to better understand the capability of our approach for complex liquids. Subgrid scale modeling closures will be revisited for complex liquids.

4 Team Qualifications

Professor Desjardins is uniquely qualified to conduct this research. He has over fifteen years of experience working on high fidelity computational modeling of turbulent multiphase flows. He develops numerical methods and modeling strategies to investigate turbulent liquid-gas flows and particle-laden flows using large-scale computing resources. Specifically, he has focused on the prediction of turbulent liquid atomization, as well as the dynamics of dense disperse two-phase flows. He is the recipient of the National Science Foundation CAREER Award and the International Conference on Multiphase Flow Junior Award, and he is currently leading a $9 million ONR MURI project on spray control.

5 Budget

For the proposed work, $40,000 per year for three years is requested. This amount accounts for one semester per year for a Cornell graduate student, some time for Prof. Desjardins, travel once a year internationally to the IFPRI general meeting, and limited funds for minor equipment. A detailed budget is included, along with a budget justification.

References

[1] N. Machicoane, G. Ricard, R. Osuna-Orozco, P. Huck, and A. Aliseda. Influence of steady and oscillating swirl on the near-field spray characteristics in a two-fluid coaxial atomizer. *International Journal of Multiphase Flow*, 129:103318, 2020.

[2] N. Machicoane, J. K. Bothell, D. Li, T. B. Morgan, T. J. Heindel, A. L. Kastengren, and A. Aliseda. Synchrotron radiography characterization of the liquid core dynamics in a canonical two-fluid coaxial atomizer. *International Journal of Multiphase Flow*, 115:1–8, 2019.

[3] Rolf D. Reitz. Modeling atomization processes in high-pressure vaporizing sprays. *Atomisation Spray Technology*, 3(4):309–337, January 1987.

[4] P.J. O'Rourke and A. A. Amsden. The TAB Method for Numerical Calculation of Spray Droplet Breakup. *SAE* Paper 872089, 1987.

[5] Jennifer C. Beale and Rolf D. Reitz. Modeling spray atomization with the kelvin-helmholtz/rayleigh-taylor hybrid model. *Atomization and Sprays*, 9(6):623–650, 1999.

[6] Rolf D. Reitz. Modeling the primary breakup of high-speed jets. *Atomization and Sprays*, 14(1), 2004.

[7] K. Y. Huh. A phenomenological model of diesel spray atomization. *Proc. of The International Conf. on Multiphase Flows '91-Tsukuba*, 1991.

[8] Y. Ling, D. Fuster, S. Zaleski, and G. Tryggvason. Spray formation in a quasi-planar gas-liquid mixing layer at moderate density ratios: A numerical closeup. *Phys. Rev. Fluids*, 2:014005, 2017.

[9] J. Carmona, N. Odier, O. Desjardins, B. Cuenot, A. Misdariis, and A. Cayre. A comparative study of direct numerical simulation and experimental results on a prefilming airblast atomization configuration. *Atomization and Sprays*, 31:9–32, 2021.

[10] A. Vallet and R. Borghi. Modélisation Eulerienne de L'Atomisation d'un Jet Liquide. *C. R. Acad. Sci. Paris Sér. II b*, 327:11015–10208, 1999.

[11] R. Lebas, T. Menard, P. A. Beau, A. Berlemont, and F. X. Demoulin. Numerical simulation of primary break-up and atomization: DNS and modelling study. *International Journal of Multiphase Flow*, 35:247–260, 2009.

[12] J. Chesnel, J. Reveillon, T. Menard, and F. X. Demoulin. Large eddy simulation of liquid jet atomization. *Atomization and Sprays*, 21:711–736, 2011.

[13] B. Wang, M. J. Cleary, and A. R. Masri. Coupling explicit volume diffusion with $\Sigma - Y$ model for LES of airblast atomisation. In *ICLASS 2021, 15th Triennial International Conference on Liquid Atomization and Spray Systems*, Edinburgh, UK, August 29 - September 2, 2021, 2021.

[14] Cyril Bozonnet. Primary wave of an air-water mixing layer: a numerical study. *Doctoral Dissertation, Grenoble Alpes University*, 2021.

[15] Sheng Wang and Olivier Desjardins. 3D numerical study of large-scale two-phase flows with contact lines and application to drop detachment from a horizontal fiber. *International Journal of Multiphase Flows*, 101:35–46, 2018.

[16] C. Bozonnet, J.-P. Matas, G. Balarac, and O. Desjardins. Stability of an air-water mixing layer: focus on the confinement effect. *Journal of Fluid Mechanics*, accepted, 2022.

[17] Robert Chiodi. Advancement of numerical methods for simulating primary atomization. *Doctoral Dissertation, Cornell University*, 2020.

[18] Robert Chiodi and Olivier Desjardins. General, robust, and efficient polyhedron intersection in the interface reconstruction library. *Journal of Computational Physics*, 449:110787, 2022.

[19] Kelli Hendrickson, Gabriel D. Weymouth, and Dick K.P. Yue. Informed component label algorithm for robust identification of connected components with volume-of-fluid method. *Computers and Fluids Fluids*, 197:104373, jan 2020.

[20] Austin Han and Olivier Desjardins. Liquid structure classification towards topology change modeling. In *ICLASS 2021, 15th Triennial International Conference on Liquid Atomization and Spray Systems*, Edinburgh, UK, August 29 - September 2, 2021, 2021.

[21] Austin Han and Olivier Desjardins. Liquid structure classification towards breakup and coalescence modeling. In *ILASS-Americas 31st Annual Conference on Liquid Atomization and Spray Systems*, Madison, WI, May 16-19, 2021, 2021.

[22] Daniel R. Guildenbecher, Jian Gao, Jun Chen, and Paul E. Sojka. Characterization of drop aerodynamic fragmentation in the bag and sheet-thinning regimes by crossed-beam, two-view, digital in-line holography. *International Journal of Multiphase Flows*, 94:107–122, 2017.

[23] A. J. Mackrory. Characterization of black liquor sprays for application to entrained-flow processes. *Doctoral Dissertation, Brigham Young University*, 2006.

[24] G. Ferreira, J. A. García, F. Barreras, A. Lozano, and E. Lincheta. Design optimization of twin-fluid atomizers with an internal mixing chamber for heavy fuel oils. *Fuel Process. Technol.*, 90:270–278, 2009.

[25] Z. H. Li, Y. X. Wu, C. R. Cai, H. Zhang, Y. L. Gong, and K. Takeno. Mixing and atomization characteristics in an internal-mixing twin-fluid atomizer. *Fuel*, 97:306–314, 2012.

[26] Z. H. Li, Y. X. Wu, H. Yang, C. R. Cai, H. Zhang, K. Hashiguchi, K. Takeno, and J. Lu. Effect of liquid viscosity on atomization in an internal-mixing twin-fluid atomizer. *Fuel*, 103:486–494, 2013.

[27] A. Aliseda, E. J. Hopfinger, J. C. Lasheras, D. M. Kremer, A. Berchielli, and E. K. Connolly. Atomization of viscous and non-Newtonian liquids by a coaxial, high-speed gas jet. Experiments and droplet size modeling. *International Journal of Multiphase Flow*, 34(2):161–175, 2008.

PROPOSAL TO:

International Fine Particle Research Institute

PREPARED BY:

A/Prof. Meng Wai Woo

Unveiling the Potential of CFD for Nozzle Spray Prediction

25. October, 2021

EMAIL:
wai.woo@auckland.ac.nz

PHONE:
+642 1664 363

Unveiling the Potential of CFD for Nozzle Spray Prediction

EXECUTIVE SUMMARY

The state-of-the-art in using the Computational Fluids Dynamics (CFD) technique for spray prediction lies in the pursuit of a delicate balance between the computational requirements and the flexibility and accuracy of the prediction. We will investigate the potential of the VOF-DPM technique (volume of fluid-discrete particle modelling), which is a subset of CFD, to provide this delicate balance for routine engineering spray prediction. The scope of this investigation will cover single fluid hollow-cone and full-cone atomization, with fluid viscosity ranging between 1 to 260 mPa.s. This project is in alignment with existing spray characterization facility in the University of Auckland. We will experimentally characterize the filament formation and the primary and secondary droplet breakup behavior, complementing the VOF-DPM analysis. The main outcome from this project are strategies in using the VOF-DPM technique for hollow cone and full cone spray prediction.

BACKGROUND

Commercially available swirl nozzles is commonly developed and characterized with water. This poses significant uncertainties in nozzle selection and operation for spray dryer or spray granulator operators, as the sprayed solutions are typically very different from water (eg. high viscosity binders, concentrated solution in spray drying, organic solvent-based solutions in the pharmaceutical industry). Contract manufacturers, in particular, will find these uncertainties even more challenging as they regularly deal with new product or binder formulations.

Direct measurement and characterization of nozzles in the industry is not routinely feasible due to manufacturing compliances and the cost associated in setting up the measurement facility onsite. Manufacturers work around these uncertainties by relying on guessing work and experiences with specific nozzles and settings. There are also a vast number of empirical correlations available in the literature to help guide manufacturers in nozzle selection and operation [1]. Due to the rapid development in nozzle design and the typically limited conditions in which these correlations are developed, the accuracy of these correlations adds another layer of uncertainty to the problem.

For these reasons, there is a need for a flexible toolbox to guide manufacturers in nozzle selection and operation. The flexible toolbox should overcome the current limitations and should be able to provide a reliable indication on the droplet size distribution and spray angle accounting for different nozzle constructions, product formulations and operating conditions. This project will explore the use of the Computational Fluid Dynamics (CFD) simulation technique as a flexible atomization predictive toolbox.

STATE-OF-THE-ART IN CFD SPRAY PREDICTION

The atomization process from a pressure nozzle involves the initial formation of thin filaments. Primary breakup of the filaments forms the primary droplets, which undergoes further secondary breakup into finer droplets (also potential coalescence throughout the process). Figure 1 illustrates this process. Within the CFD simulation framework, the Volume-of-Fluid (VOF) technique (and its variant in meshing and surface detection algorithm), is the main method used to capture these various phenomenon composing the atomization process. Figure 2 summarizes the state-or-the-art in this area.

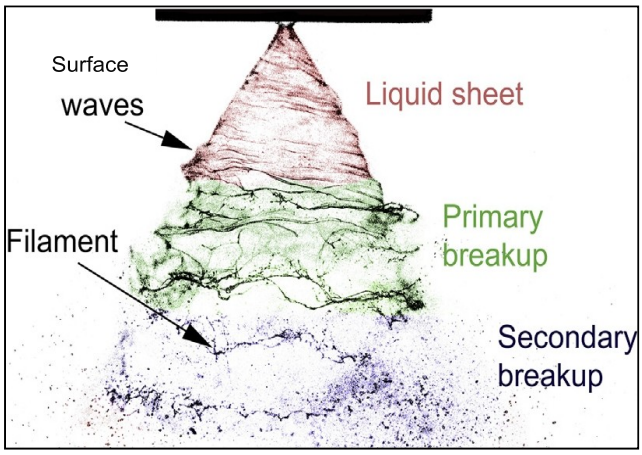

Figure 1. Breakdown of the atomization process [2]

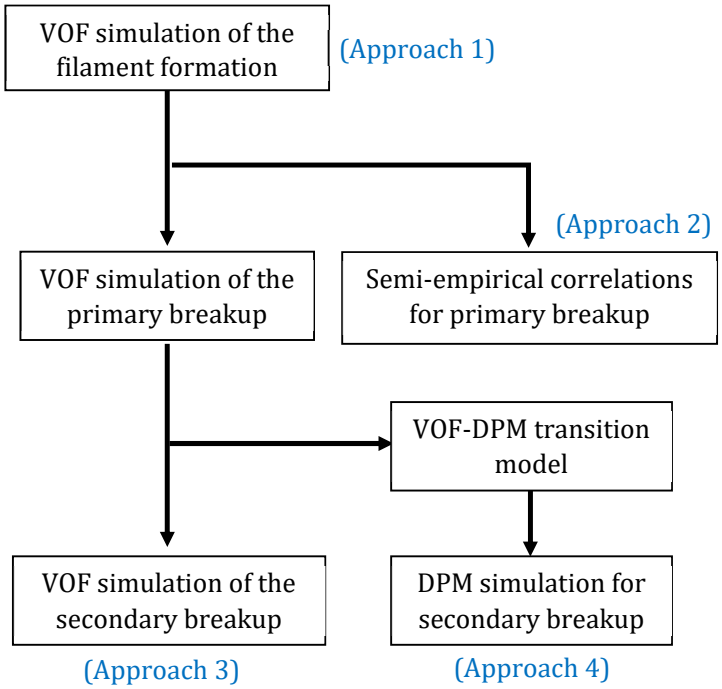

Figure 2. The state-of-the-art in CFD spray prediction

In essence, the VOF technique involves tracking the interface of the atomized fluid throughout the simulation domain. It is a very computationally expensive technique as excessively fine mesh is required to capture the characteristic length scale of the atomization process which stretches across several magnitudes: from centimeters (the nozzle size and the length scale of the whole spray), hundreds of microns (film formation), to tens of microns (primary and secondary droplets). The state-of-the-art in this area lies in the pursuit of a delicate balance between the computational requirements and the degree of flexibility and accuracy from the VOF simulation.

Most of the reported simulation work focuses on Approach 1 (Figure 2), as it provides a computationally inexpensive indication on the performance of the atomizer [3][4][5][6][7]. The application of just predicting the filament or cone formation is limited, because it does not provide a prediction of the final droplet size distribution. Some worker extended this approach by coupling the VOF predictions with empirical correlations linking the characteristics of the filament with the final droplet size distribution (Approach 2 in Figure 2) [8]. The empirical correlation developed so far, employed in the reported framework, was developed based only on an idealized primary breakup process [9][10][11]. While this approach may be low in computational cost, it is in essence empirical and there is significant random uncertainty in the accuracy of the prediction across a wide range of nozzle geometry and fluids [8].

At the other end of the spectrum, Approach 3 (Figure 2) utilizes the VOF technique to provide a full visualization of the atomization process, from the filament formation to the secondary breakup phenomenon [12][13][14][15][16]. The main drawback is that it requires very significant computational resources. Limiting the simulation to regions very close and adjacent to the nozzle may partly overcome this problem. However, this limits the predictive capability to capture the full effective characteristics of the spray. For this reason, this technique may not be useful for routine engineering application.

In the middle of the spectrum is Approach 4 (Figure 2), which involves the VOF-DPM technique [17][18][19]. This technique transforms the VOF predicted primary droplets and represents them as discrete points in the simulation (hence, DPM - Discrete Phase Modelling). This obviates the need for excessively high computational resources in modelling the secondary breakup of the primary droplets as imposed by Approach 3. This approach also does not have empirical limitations as imposed by Approach 2, because the VOF technique explicitly captures the primary breakup. Therefore, now, this technique provides the greatest potential for the application of CFD in atomization prediction for routine engineering applications; striking a balance between computational requirement and the level of details from the simulation. A survey of the literature on this approach revealed that there is currently limited systematic validation work for Approach 4. Most of the reported work focused on fuel injection atomization. There is currently no one single study systematically evaluating this approach across hollow and full cone swirl atomization, with fluids typically used in powder production or in the atomization of binders (for granulation). These two types of nozzles (hollow and full cone) will involve significantly different filament formation characteristics, hence, different distribution of the primary droplets and different propensity for secondary breakup or coalescence. It is uncertain how well the VOF-DPM technique captures these

scenarios. Most importantly, there is a need to ascertain suitable numerical strategies for the different spray conditions. This project will fill these gaps in knowledge.

On this basis, the following are the objectives of this project:

Objective 1: To evaluate the VOF-DPM technique for hollow cone single fluid swirl atomization prediction

Objective 2: To evaluate the VOF-DPM technique for full cone single fluid swirl atomization prediction

EXPECTED PROJECT OUTCOMES

We will gain a deeper understanding on how the various numerical parameters of the VOF-DPM technique affect the accuracy and the computational requirements of the atomization prediction. We will provide recommendations on strategies to achieve a balance between accuracy and computational requirements from an industry perspective. In most cases (particularly for contract manufacturers), the capability to realistically cover a range of possible operating conditions may bring more benefits than achieving very high accuracy within a limited range. We will develop strategies for both hollow cone and full cone atomization. We envisage two publications from this project, one publication from each objective.

PROJECT PLAN

Work Packages		Year 1				Year 2				Year 3			
		Q1	Q2	Q3	Q4	Q1	Q2	Q3	Q4	Q1	Q2	Q3	Q4
1	Retrofitting rig for film formation measurement.												
2	Nozzle CAD geometry development												
3	VOF-to-DPM modelling framework development												
4	Atomization experiments (hollow cone)												
5	VOF-to-DPM simulation (hollow cone)												
6	Objective 1 completion												
7	Atomization experiments (full cone)												
8	VOF-to-DPM simulation (full cone)												
9	Objective 2 completion												
10	Bi-quarterly project update												
11	PhD thesis completion												
12	Project final report												

Work Package 1: Retrofitting measurement rig for film formation measurement

We have an existing Spraytec laser diffraction facility, with a compressed air driven atomization system for up to 15 Bar pressure. This setup allows for vertical height adjustment of the nozzle, which will be important for measuring the primary and secondary breakup process, respectively. For this project, we will retrofit the system to allow high speed and high-resolution camera measurement of the film formation. Extending a reported method [3], we will use planar laser illumination to allow video capture of the shape of the filament formed. We will undertake 2D planar analysis of the filament formation process with ImageJ image processing, to obtain filament thickness, cone angle, penetration distance data. In the absence of an LDA system, we will determine the filament velocity by high-speed video recording and analysis using the Trackmate plugin in ImageJ.

Work Package 2: Nozzle CAD geometry development

From our experience, it will be difficult to obtain detailed nozzle CAD from nozzle manufacturers. We will 3D scan the nozzles used in the experiments (internal inserts and housing) to develop the CAD geometry for the simulations. We will be exploring two sets of hollow and full cone BETE nozzles. For the full cone single welded nozzles, we will 'dissect' the nozzles in the workshop to enable scanning of the internal geometry.

Work Package 3: VOF-to-DPM modelling framework development

We have access to the New Zealand NESI high performance-computing cluster. We will develop the modelling framework locally before integration with the NESI network. We will use the ANSYS Fluent CFD package.

Work Package 4 & 7: Atomization experiments

We will use glycerin, water and ethanol mixtures to generate fluid with a range of viscosity (1 – 260 mPa.s), density (970 - 1200 kg/m^3) and surface tension (41 – 72 mN/m) [20]. The advantage of the using mixtures with these components is that it is transparent and this will facilitate film measurements.

We will use the following set of nozzles and will undertake the experiments at various atomization pressures to cover a wide range of operating conditions. For each mixture, we will measure the filament characteristics as described earlier and will characterize the primary and secondary breakup phenomenon.

BETE Twist & Dry Low Flow Hollow Cone (TDL1-22, TDL4-22, TDL1-27, TDL4-27): This set of hollow cone nozzle will provide a combination of swirl velocity and orifice size for wide evaluation of the model.

BETE WL Low Flow Full Cone (WL1/4, WL1/2, WL3/4): This set of full cone nozzles will provide a set of orifice sizes for wide evaluation of the model.

Work Package 5 & 8: VOF-to DPM simulations

We will numerically simulate the extensive set of experimental runs. We will make comparison in terms of the prediction of the filament characteristics, droplet size

distribution from the primary breakup of the film and the droplet size distribution after the secondary breakup of the droplet. The bulk of the analysis will focus on analyzing how different meshing strategies, VOF surface tracking approaches and VOF-to-DPM numerical parameters affect the accuracy as well as the computational requirement of the model.

PERSONNEL

A/Prof. Meng Wai Woo has 15 years' experience in CFD simulations and have undertaken CFD projects with the spray drying, pharmaceutical and resource recovery industry. He will lead the project and will recruit a PhD student with strong CFD and CAD simulation background for the project. The student will be working on both objectives of the project.

PROJECT ALIGNMENT TO EXISTING FACILITIES

The project is in alignment with the following capabilities and facilities available to the team.

Spraytec: This will be the main equipment used for the sprayed droplet characterization. Meng has significant experience in using this equipment for high flow industrial scale spray characterization (current project with the NZ dairy industry).

Atomization rig: This compressed air driven rig developed for the current dairy based atomization characterization project will be used for the proposed work and will be able to handle up to 15 bar atomization pressure and can be retrofitted with different nozzles.

3D scanner for nozzle CAD development: We will have access to this facility as part of the University of Auckland Digital Research Hub.

ANSYS Workbench access: We have access to the ANSYS Workbench academic license package. The academic license is limited to simulations with 500k in the number of mesh. We will work within this boundary for the project. Achieving a suitable numerical strategy to work around this will provide a good incentive for industry adoption of the technique so that reasonable computation time and resources are feasible.

Access to NESI HPC Cluster: The University of Auckland is a partner of the NESI HPC cluster and we will have access to the cluster without any additional cost to the project.

BUDGET & JUSTIFICATION

Item	Year 1 ($NZD)	Year 2 ($NZD)	Year 3 ($NZD)
PhD Student:			
Stipend	28,500	28,500	28,500
Fees	9,540	9,540	9540
Measurement facility retrofitting:			
High speed camera purchase	10,000	-	-
Compressed air curtain for camera	1,000	-	-
Planar laser illumination setup	8,000	-	-
Workshop cost	1,000	-	-
Consumables and experimental needs:			
Solutions for experiments	1000	1000	1000
Nozzles	4000	-	-
TOTAL budget requested from IFPRI	**63,040**	**39,040**	**39,040**

PhD student stipend and fees: The amount requested is the standard three-year full scholarship provided to students in the University of Auckland.

Measurement facility retrofitting: The requested support goes towards retrofitting the existing facility for atomizer film or ligament formation measurement. The amount requested is for a Kron Technologies high-speed camera (Kronos 2.1 HD model) and includes the positioning adjustment tripod. The planar laser illumination setup includes the cost for the planar laser source. The compressed air curtain is to protect the camera from mists and splashes generated by the spray. We have significant experience managing this when undertaken measurements with high flow rate sprays.

Consumables and experimental needs: We will purchase two sets of nozzles suitable for low manageable spray rates in the laboratory and for covering the experimental range as described earlier. This cost includes purchasing additional (full cone nozzles) units for 'dissecting' to allow full 3D scanning of the nozzles internals. We will purchase glycerin and ethanol for the atomization experiments. Corresponding to the flowrates of nozzles described, we estimate that 25L of glycerin and 5L of ethanol will be sufficient each year for the experiments.

REFERENCES

[1] Masters, K. 1991. Spray drying handbook. 5th Edition, Wiley, New York.

[2] Jedelsky, J., Maly, M., del Corral, N.P., Wigley, G., Janackova, L., Jicha, M. 2018. Air-liquid interactions in a pressure-swirl nozzle. International Journal of Heat and Mass Transfer, 121, 788-804.

[3] Laurila, E., Koivisto, S., Kankkunen, A., Saari, K., Maakala, V., Jarvinen, M., Vuorinen, V. 2020. Computational and experimental investigation of a swirl nozzle for viscous fluids. International Journal of Multiphase Flow, 128, 103278.

[4] Laurila, E., Roenby, J., Maakala, V., Peltonen, P., Kahila, H., Vuorinen, V. 2019. Analysis of viscous fluid flow in a pressure-swirl atomizer using large-eddy simulation. International Journal of Multiphase Flow, 113, 371-388.

[5] Dash, S.K., Halder, M.R., Peric, M., Som, S.K. 2001. Formation of Air Core in Nozzles With Tangential Entry. Journal of Fluids Engineering, 123, 829-835.

[6] Shao, C.X., Luo, K., Yang, Y., Fan, J.R. 2017. Detailed numerical simulation of swirling atomization using a mass conservation level set method. International Journal of Multiphase Flow, 89, 57-68.

[7] Renze, P., Heinen, K., Schonherr, M. 2011. Experimental and Numerical Investigation of Pressure Swirl Atomizers. Chemical Engineering & Technology, 34, 1191-1198.

[8] Liao, Y., Sakman, A.T., Jeng, S.M., Jog, M.A., Benjamin, M.A. 1999. A comprehensive model to predict simplex atomizer performance. Journal of Engineering for Gas Turbines and Powder, 121, 285-294.

[9] Drombowski, N., Johns, W.R. 1963. The Aerodynamic Instability and Disintegration of Viscous Liquid Sheets. Chemical Engineering Science, 18, 203-214.

[10] Wang, X.F., Lefebvre, A.H. 1987. Mean drop sizes from pressure-swirl nozzles. Journal of Propulsion, 3, 11-18.

[11] Suyari, M., Lefebvre, A.H. 1986. Film thickness measurements in a simplex swirl atomizer. Journal of Propulsion, 2, 528-533.

[12] Galbiati, C., Tonini, S., Conti, P., Cossali, G.E. 2016. Numerical Simulations of Internal Flow in an Aircraft Engine Pressure Swirl Atomizer. Journal of Propulsion and Power, 32, 1433-1441.

[13] Fuster, D., Bague, A., Boeck, T., Le Moyne, L., Leboissetier, A., Popinet, S., Ray, P., Scardovelli, R., Zaleski, S. 2009. Simulation of the primary atomization with an octree adaptive mesh refinement and VOF method. International Journal of Multiphase Flow, 35, 550-565.

[14] Ding, J.W., Li, G.X., Yu, Y.S., Li, H.M. 2016. Numerical Investigation on Primary Atomization Mechanism of Hollow Cone Swirling Sprays. International Journal of Rotating Machinery, 1201497.

[15] Pairetti, C., Damian, S.M., Nigro, N., Popinet, S., Zaleski, S. 2020. Mesh resolution effects on VOF simulations of primary atomization. Atomization and Sprays, 30, 913-935.

[16] Zheng, G., Nie, W., Feng, S., Wu G. 2015. Numerical Simulation of the Atomization Process of a Like-doublet Impinging Rocket Injector. Procedia Engineering, 99, 930-938.

[17] Kumar, A.B., Kumar, V., Nakod, P., Rajan, A., Schutze, J. 2020. Multiscale modelling of a doublet injector using hybrid VOF-DPM method. Proceedings from the AIAA SciTech Forum, 6-10 January, Orlando, Florida.

[18] Herrmann, M. 2010. A parallel Eulerian interface tracking/Lagrangian point particle multi-scale coupling procedure. Journal of Computational Physics, 229, 745-759.

[19] Ul Haq, M., Latif, R., Shafi, I., Javaid, A. 2018. Modelling Primary Atomization and its effects on spray Characteristics under Heavy Duty Diesel Engine Condition. Proceedings from the 21st Australasian Fluids Mechanics Conference, Adelaide, Australia, 10-13 December.

[20] Mandato, S., Rondet, E., Delaplace, G., Barkouti, A., Galet, L., Accart, P., Ruiz, T., Cuq, B. 2012. Liquids' atomization with two different nozzles: Modeling of the effects of some processing and formulation conditions by dimensional analysis. Powder Technology 224, 323-330.

IFPRI

International Fine Particle Research Institute

Research Project Brief

Computational Modeling of Particle Suspensions

The International Fine Particle Research Institute (IFPRI) wishes to fund a research project on computational modeling of particle suspensions. IFPRI has a long history of supporting research in the rheology of Brownian and non-Brownian suspensions, however the last project that we funded focused on simulation of suspension behavior was John Brady's project on Stokesian dynamics which ended in 2004. With this project, we hope to fill this gap in IFPRI's "wet systems" portfolio.

New state-of-the-art simulations incorporate hydrodynamic interactions to generate large-scale (10^6 or more) particle simulations that quantitatively capture macroscopic properties, including sedimentation/stability, processability, dispersibility, flowability) and microstructural changes over time and in flows. With two excellent experimental projects currently in the wet systems portfolio (Jan Vermant, "Simulated Industrial Formulations"; Erin Koos, "Slurries and Pastes"), maximum benefit can be extracted from that work with computational support to give further insights to properties that cannot be disentangled experimentally.

Simulations with different particle shapes, sizes, chemical heterogeneities and at high loadings are now increasingly feasible, allowing the model to closely approach the complexity of real product formulations in the SIFs and Slurries and Paste projects.

The goal of this project is to bring insights to failure modes that can be experimentally observed but not understood (for example delayed collapse of particle networks) and provide detailed particle-level mechanistic details so that strategies to prevent or predict failure can be developed. Work can also guide formulation decisions, increase the applicability and relevance of the experimental projects by identifying key mechanisms that are difficult or impossible to access experimentally (e.g., role of friction, particle shape and dispersity). A long-term goal of this work is towards computer simulations that can be used to guide formulation design and explore large design spaces as the complexity of systems increases through the incorporation of multiple aspects of shape, roughness, polydispersity, heterogeneity, etc. Specific objectives include:

- Provide insight, and ultimately access, to current wet system modeling tools.
- Reflect the state of the art of modeling to predict flow phenomena in industrial systems to understand the gap and define the steps needed to improve the models.
- Develop and validate simulations against benchmark literature studies, such as shear rheology (e.g., viscosity, viscoelasticity, yielding), delayed consolidation, and microstructural transitions on shearing (e.g. as measured by scattering).

- Work with the experimental SIFs and Slurry and Pastes project groups to perform coordinated characterization of structure, rheology, and interactions.
- Advance simulations to combine with experiments for model suspension development.

IFPRI Research Project Brief

Atomization Under Industrially-Relevant Conditions

The International Fine Particle Research Institute (IFPRI) wishes to fund a project to investigate the atomization of fluids and slurries under conditions relevant to spray drying. The approach to spray drying varies broadly by industrial application, using several different spray nozzle types and a wide range of operating parameters (mass flow, velocity and pressure), spraying fluids with myriad rheological properties in different chamber conditions (temperature and pressure). Although, there is a large body of literature on spray characteristics, little is focused on comparing sprays at conditions relevant to spray drying industry. The purpose of this research is to map the breadth of spray characteristics for a broad range of industrially relevant fluid systems and operating conditions to enable the selection of a set of nozzles and conditions for a given application. The best choice of nozzle for an application depends in most cases strongly on specifics of the application. For example, it may be critical to limit oversize particles in some application or undersize particles in other. Just focusing on an average particle size, as most of the current correlations do, is rarely sufficient.

More specifically, the project should focus on the spatial variation of droplet size distribution for a variety of nozzle types under a range of operating parameters and fluid rheology. Results should be used to develop a "comparison map" of the different nozzles, identifying their operating range and limitations in terms of quality of atomization, i.e. droplet size distribution, spray pattern, and spray stability.

While the scope of the project should be defined by the PI, IFPRI members come from many industry sectors and therefore utilize a broad range of atomizers and fluids. For this reason, at least two nozzle types and 2-3 different scales should be investigated. Fluids should be selected to span the range fluid rheologies used in spray drying, including Newtonian and non-Newtonian solutions and suspensions over a range of solid fractions.

Characterization of Spray-Drying Nozzles at Industrially Relevant Conditions

Continuation Proposal
2021

Primary Investigator: **Nasser Ashgriz**
PhD Students: **Isaac Jackiw & Siyu (Jerry) Chen**
Institution: **University of Toronto, Canada**

IFPRI
International Fine Particle Research Institute

UNIVERSITY OF TORONTO | Department of Mechanical and Industrial Engineering

Abstract

This proposal is a continuation of the presently IFPRI funded research, aimed at developing physically realistic models for atomization processes in swirl and twin-fluid nozzles with a focus on fluids with suspensions. The objectives of the present research are (i) spray characterization of liquids with solid suspension, and (ii) development of atomization models for fluids with suspensions. We will study suspensions with different particle types and sizes, solutions with significant elongational viscosity, surface tension, and molecular weight. We will use both pressure-swirl and twin-fluid nozzles in this study.

The second objective will be achieved by a set of basic studies on the breakup of ligaments either injecting a jet in a cross flow or by suspending a liquid bridge in a cross flow. The breakup dynamics will be recorded using a highspeed video. The cross-flow temperature will be changed to study the effect of heating on the breakup of the ligaments. Effects of fluid rheological properties as well as particle size and concentration in different suspension will be investigated.

Present Proposal

Background

The prior studies on the atomization of liquid with suspensions have identified the followings:

- Large particles in a slurry may separate from the droplets.
  - Glaser (1989) tested a slurry with particle sizes of 20 μm and concentrations up to 71 weight percent using prefilming-swirl nozzle. He found that the large solid particles separated from the water droplets.
  - Isenschmid (1992) compared the twin-fluid atomization of various suspensions with particle sizes of 4 to 16 μm and concentrations of 0 to 30 weight percent but did not show a clear influence of solid particles on the droplet size.
  - Mulham et al. (2001) found some separation of large solid particles from the liquid, but not for fine solid particles.
- Effect of particle size on the SMD is still not clear.
  - Yan et al. (2014) performed experiments on lime particle slurries using a pressure-swirl nozzle that showed that SMD increased with increasing solid percentages of lime slurry. Also, spray angle slowly decreased with increasing solid percentages of lime slurry. A twin peaks flux distribution was observed, which increased nonlinearly with increasing injection pressure.
  - Mulham et al. (2006) found a unimodeal size distribution for slurry suspensions with $Dv_{50} > 50$ μm and a bimodal size distribution for $Dv_{50} > 50$ μm.
    - For $Dv_{50} < 50$ μm, drop diameter was about the same as the pure carrier liquid droplet diameter. The effect of increasing carrier liquid viscosity on the atomization of suspensions with large and fine solid particles is similar to the observed effect on the atomization of pure suspension liquids, i.e., the drop diameter becomes larger with increasing the carrier liquid viscosity.

- For Dv_{50} >50 µm, one peak corresponded to the solid particle diameter in the suspension, and the other peak represented pure liquid spray size. At low injection pressures, the peak of the liquid droplet diameter was controlled by the solid particle size. Suspension with relatively fine solid particles showed a smaller diameter peak than the suspension with relatively large solid particles. At high injection pressures, this diameter peak was controlled by the gas velocity. In this region further break-up of liquid or suspension drops was similar to the fragmentation process of a pure carrier liquid.

- Generally, the shear thinning behaviour of the suspension viscosity, which increases with increasing solid concentration and decreasing solid particle size, makes the influence of the viscosity on the suspension break-up within a twin-fluid atomizer less important with increasing velocity of the atomizing gas (Glaser, 1989; Parthasarathy, 1999; Mulhem, 2004).

The following issues are raised based on the current data on the atomization of fluids with suspensions.

1- How does a solid particle separate from the solution? It is not clear whether the liquid is sheared off the solid particle or the particle separates during the breakup of the mixture. We will try to answer these questions by near nozzle closeup imaging.
2- Is there a correlation between the particle separation from the solution with respect to its size, the suspension concentration, and other solution rheological properties?
3- Does the SMD of the spray increases with an increase in solid particle size? There are conflicting results on this, as some show no increase, whereas some show an increase in SMD with particle size.
4- At what conditions does the unimodal size distribution turns into a bimodal size distribution? One study shows that this happens for Dv_{50} >50 µm. However, this value corresponds to their specific experiment. There is neither a criterion nor a correlation for a critical suspension parameter, at which point the size distribution becomes bimodal.
5- What are the differences between the suspension fluid atomization in pressure-swirl and twin-fluid atomization? In pressure-swirl atomization, a solution is converted into a thin sheet, which is then atomized into droplets, whereas in a twin-fluid atomization, a high gas velocity tears the solutions into droplets and ligaments. The influence of particles in each of these processes can be different. For instance, particles in a sheet may expedite preformation and breakup, whereas particles may not break off the core liquid in shearing process of twin-fluid atomization.

The present proposal is designed to address these questions.

Objectives

Objective 1. Spray Characterization of Liquids with Solid Suspension

There have been several requests from IFPRI members to perform tests with slurry fluids, as well as considering the effects of other rheological properties on the atomization. We propose to investigate the effect of the following specific properties on the atomization: **slurries with different particle types and sizes** to determine how the atomization is affected; **fluids having significant elongational viscosity**, which influences the breakup of the ligaments during the secondary atomization; **surface tension**, which was not specifically studied in the previous work; and **molecular weight**, which was also not studied in the previous work. We will use both pressure-swirl and twin-fluid nozzles in this study.

Objective 2. Development of Atomization Models for Fluids with Suspensions

Because of the complicated nature of the atomization process, it is still not possible to have a pure theoretical model for the atomization. Therefore, our goal is to develop semi-empirical models (physics-based models with experimentally determined constants) to predict the droplet sizes generated by the two types of nozzles that we have been testing: pressure-swirl and twin-fluid nozzles. We will develop correlations for both SMD and for the spray size distribution. The following tasks are planned to achieve this objective.

2.1. Correlations for Droplet Size Distribution

The PDF of the size distribution provides much more information than just the SMD. For example, an increase in viscosity may result in the formation a large number of large droplets, as well as a large number of small droplets, such that the SMD remains the same. The PDF is also used as an input into the CFD models for sprays. Our current study on high viscosity fluids has shown that the size distribution in such sprays can be bimodal. Therefore, a bimodal distribution function that accurately fits the data is needed. We will use the experimental data to develop correlations for the distribution functions for fluids with suspensions, in addition to the commonly presented correlations for the SMD.

2.2. Secondary Breakup of Ligaments of fluids with suspensions

The atomization process comprises of the breakup of a liquid into small ligaments. For high viscosity and polymeric fluids, the ligaments are long and may breakup again. This is referred to as the secondary atomization. In order to develop semi-empirical models for the atomization of liquids with suspension, we need to have experimental data on the breakup of ligaments of such fluids. In the proposed study we will perform basic study of the breakup of ligaments of fluids with suspensions, by suspending or jetting a ligament in a gaseous cross flow.

2.3. Perforation Based Model for Pressure-Swirl Nozzles

Based on studying the near nozzle images, we have developed a new atomization model for the pressure-swirl nozzles. The new model is based on a combination of a Kelvin-Helmholtz wave (KH) and a sheet perforation. In order to extend this model to fluids with suspensions, we need to determine the breakup length of the swirling sheet of such fluids, characterize the diameter of

the ligaments formed, and determine the number and frequency of the perforations on the sheet. These are planned for the proposed period.

2.4. Atomization in Twin-Fluid Nozzles

Two key advantages to the atomization models that we developed for twin-fluid nozzles in our previous project term are the ability to relate the rate of the deformation to the breakup and to predict the formation of ligaments in the spray. This allows for the opportunity to directly include rheological effects such as extensional viscosity in our models and to support their development by using what we learn in our experiments on the breakup dynamics of the ligaments and the spray characterization. Our previously developed model for the atomization of twin-fluid nozzles is comprised of the following processes: KH waves form on the jet that exits a nozzle and cause small droplets to break off its surface; the liquid core in the jet (the liquid left behind after KH droplets break off) goes through flapping instability, forming larger droplets with length scale of the flapping wavelength, and the secondary atomization process breaks the large droplets to smaller droplets. The breakup model is related to the rate of deformation of the waves. The advantages of modelling the spray in this way is the isolation of the slow wave growth from the fast wave breakup and the prediction of ligaments in the breakup, which previous models do not consider. While the development of the KH and flapping instabilities will be somewhat affected by the rheological fluids, the greater effect is expected to be on their breakup, especially when the extensional viscosity is high. Using what we learn in task 2.2 about the breakup dynamics of the ligaments, we aim to extend our existing models to include these effects.

Procedure

1. Spray Characterization of Liquids with Solid Suspension

The objective of this part of the research is the development of a more quantitative understanding of the influence of solid suspensions on atomization and droplet size distribution. The non-Newtonian rheological properties of the suspension play an important role in their disintegration process. We will measure the droplet size distribution for a range of suspension fluids. We plan to use Kaolin particles in our study. However, we will also use some of the suspension fluids of interest to IFPRI members (to be identified). The following part gives an example of the procedure on how we are going to generate the droplet size distribution.

We have been using Mavlern Spraytec Dropsizer to characterize our sprays. The Malvern instrument measures the volume percentage of droplets in different size ranges. Although volume percentage is valuable information, the droplet size distribution is a better indicator of the atomization process. The following is a brief discussion of the procedure we have used for obtaining the size distribution (more detailed information on the nozzles tested and conditions are provided in Appendix A).

Figure 1 shows histograms generated by Malvern Dropsizer for water and glycerin-water solutions at three different operating pressures. For almost all the testing cases, the histograms have one peak with a long tail on the left corresponding to the smaller droplets of less than 10 μm. The results show that as the injection pressure increases, the volume percentage of large droplets decreases and that of smaller droplets increases (e.g., the peaks move to the left).

Next, the volume percentage is converted to the volume distribution by dividing the height of each bin by the corresponding bin width. Figure 2 shows the volume distributions corresponding to the volume percentage of figure 1. The volume distribution amplifies the changes in the effect of droplet size on volume. Therefore, Fig. 2 shows bimodal distributions for the unimodal distribution of Fig. 1. The small tail in Fig. 1, results in the first peak in volume distribution curves. In order to find a size distributions corresponding to a volume distribution, we first guess a size distribution, and then calculate the volume distribution based on that and compare it with the experimental results. The parameters of the size distribution are then changed to match the experimental data. This procedure is simple for unimodal distributions, but more complex for bimodal distributions. We seek a mixture number distribution $f_0(d)$ that is the summation of two different unimodal distributions $f_{0,1}(d)$ and $f_{0,2}(d)$ as

$$f_0(d) = k_n f_{0,1}(d) + (1 - k_n) f_{0,2}(d),$$

such that their corresponding volume distributions have the following relationship

$$f_3(d) = k_v f_{3,1}(d) + (1 - k_v) f_{3,2}(d),$$

where k_n is the number ratio of the droplets generated by each distribution and k_v is the volume ratio of the droplets generated by each distribution. Since volume distribution based on a size distribution can be written as

$$f_3(d) = \frac{d^3 f_0(d)}{\int_0^\infty d^3 f_0(d) dd},$$

it can be shown that

$$k_n = \frac{k_v S_2}{S_1 + k_v (S_2 - S_1)},$$

where $S_a = \int_0^\infty d^3 f_{0,a}(d) dd\,, a = 1,2$. In order to fit the data, a distribution function is needed. We will use a lognormal distribution, which has the following form

$$f_0(d) = \frac{1}{d\sigma\sqrt{2\pi}} \exp\left(-\frac{1}{2}\left(\frac{ln(d/\mu)}{\sigma}\right)^2\right),$$

whose corresponding volume distribution is

$$f_3(d) = \frac{d^3}{e^{3\mu + 4.5\sigma^2}} f_0(d)$$

Figure 3 shows several results for fitting a mixture of lognormal distribution to experimental data. The mixture of lognormal distribution can not only follow the position of two peaks and the troughs properly for bimodal distribution (case 1 and case 5 as noted in the appendix A), but also fit to the unimodal distribution well (case 11). The mixture model has the form

$$f_3(d) = k_v f_{3,1}(d; \mu_1, \sigma_1) + (1 - k_v) f_{3,2}(d; \mu_2, \sigma_2)$$

with 5 parameters. For most of the cases, $k_v > 0.95$, which means the main peak is responsible for more than 95% fluid atomized. However, for most of the cases $k_n < 0.2$, which means that the small droplets take up more than 80% of the total number of droplets and the number distribution will be largely dominated by the small droplets.

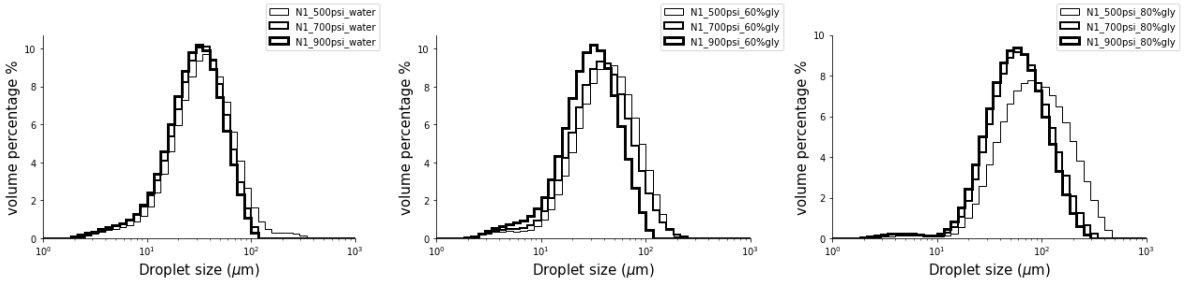

Figure 1: Volume percentage of each testing cases

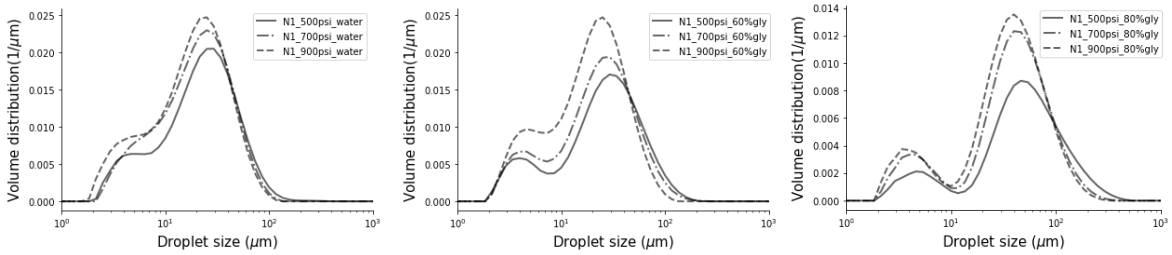

Figure 2: Volume distributions for all testing cases

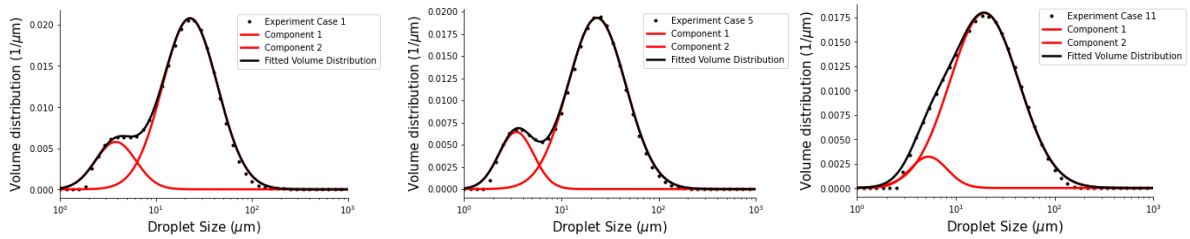

Figure 3. Fitting a mixture distribution of two lognormal distribution to experiment cases 1, 5 and 11, with nozzle diameters of 0.71mm, 0.71mm, and 1.07mm, and liquids of water, 60%gl-water, and water, respectively, and all at 700 psi injection pressure.

2. Development of Atomization Models for Fluids with Suspensions

2.1. Secondary Breakup of Droplets and Ligaments of Rheological Fluids

Our current near nozzle images of high viscosity liquid show the existence of long ligaments that may persist far downstream of the primary atomization region. This indicates a shortcoming in the traditional definitions of the atomization regions. Typically, the primary atomization results in the formation of droplets, while the secondary atomization is the breakup of those droplets. However, for viscous liquids, rather than only droplets being formed in the primary atomization region, ligaments are also produced that may undergo secondary breakup. Although the secondary breakup of droplets has been studied extensively in the literature, the secondary breakup of ligaments has not. Figure 4 shows an image downstream of the nozzle where large ligaments still exist.

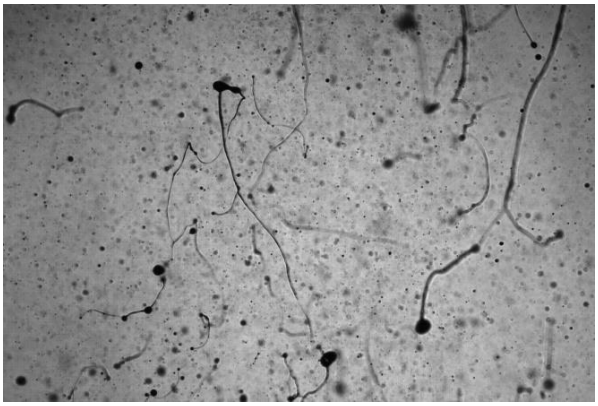

Figure 4: Image of a 0.5% CMC spray at 20-25mm downstream of the nozzle exit, showing the persistence of ligaments far downstream of the primary atomization region.

The question of the secondary breakup of the ligaments poses a few interesting problems, the most relevant of which is “do the ligaments break into small droplets or collapse into large droplets, and does this process occur over the timescales of spray drying?” If the timescale of the ligament secondary breakup is shorter than the drying process, then the resulting powder will have mainly spherical particles. However, if the ligaments do not break within the drying time, then the powder may have long, fibrous particles that decrease the quality of the powder. A better understanding of the secondary atomization of the ligaments will provide a basis for designing sprays to ensure that the ligaments do break within the drying time.

As we have found in our previous work, analyzing these ligaments based on commercial nozzle sprays is highly challenging. Due to the crowding of the images, ligament characterization and temporal tracking become difficult. Furthermore, there is no way to create controlled experiments of the ligament dynamics, as they are generated somewhat chaotically. By focusing on the fundamental aspect of the secondary breakup of single ligaments, we aim to provide models and understanding of the secondary breakup of ligaments that can be used as a basis for analyzing the complex ligament networks in commercial sprays more effectively.

We propose to study the fundamental behaviours of the secondary breakup of droplets and ligaments. The study of the breakup of droplets will be a direct continuation of our previous IFPRI term, which sought to understand and model the processes that lead to ligament formation and breakup. Some of the images that resulted from this study are shown in Fig. 5. The

secondary atomization model developed based on this study is already published Jackiw and Ashgriz (2021).

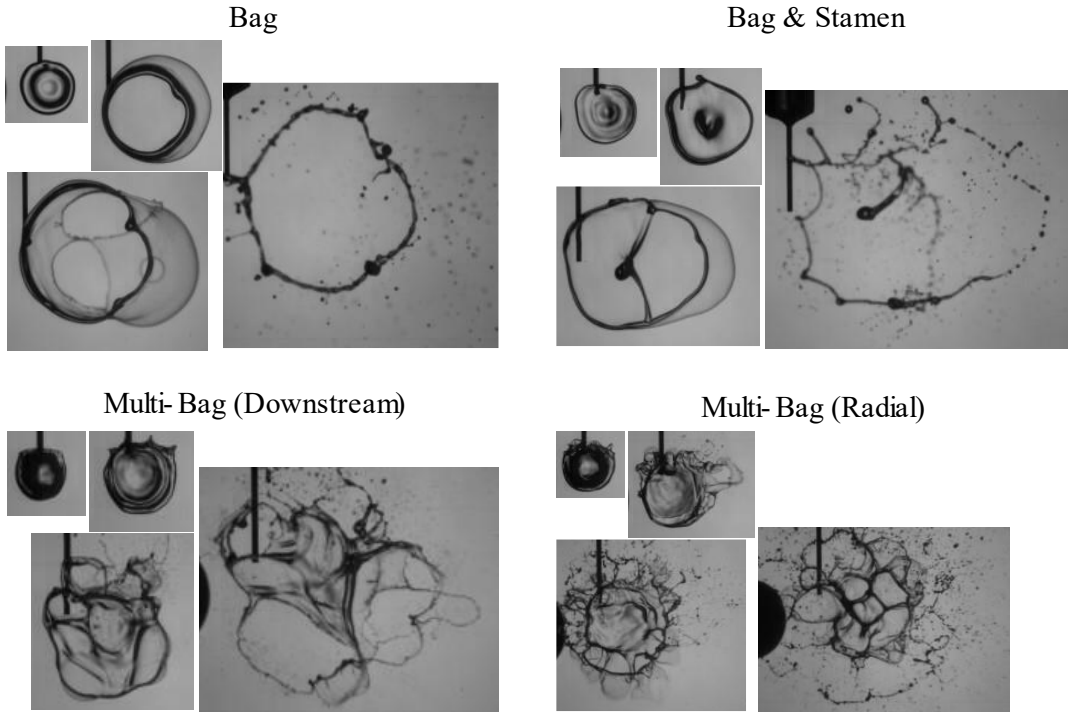

Figure 5: Images of droplet breakup for various morphologies showing the formation of ligaments.

To study the breakup of ligaments, we will generate small diameter ligaments of viscous, polymeric, and slurry fluids that we will expose to a variety of conditions such as a gaseous cross flow to study their breakup. Two methods that we can use to generate these ligaments are to study the breakup of a liquid jet in crossflow, which isolates the aerodynamic effects on the ligament breakup, or using the liquid bridge method, where we can add additional factors such as ligament stretching. These methods are illustrated in Figure 6. The dynamics of the ligaments will be captured using high-speed video so that the temporal behaviour of the ligaments can be resolved. Key factors to be determined in these experiments are the effects of the extensional viscosity on the breakup and the timescales of the ligament breakup in addition to the sizes generated. These factors are expected to be related by the critical conditions required for the ligament breakup or collapse, thus, we will aim to determine what the critical conditions are and what parameters affect or determine them.

In these experiments, we may also study the effects of elevated ambient temperatures. Since the primary atomization occurs rapidly for two-fluid nozzles, there is no significant heat transfer to the fluid during the primary atomization. However, since the ligaments in viscous sprays persist for a long time after they are formed, their dynamics may be affected by the elevated temperatures, either in the changing of the liquid properties due to heating or by the evaporation of the solvents in the liquid.

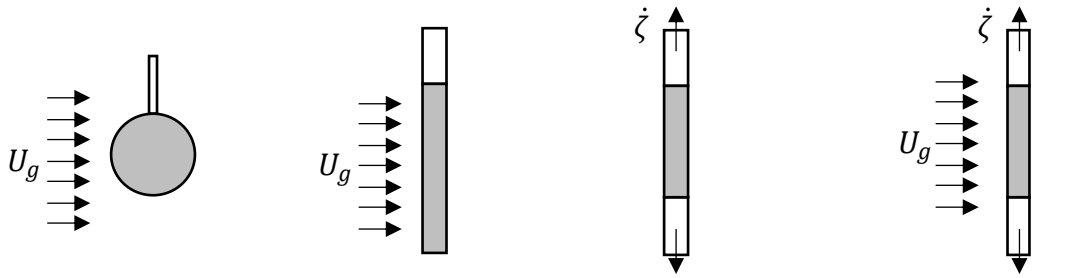

(a) Droplet in airflow (b) Jetted ligament in crossflow (c) Ligament bridge in extension (d) Ligament bridge in extension and airflow

Figure 6: Illustrations of experimental setups for study of droplet and ligament breakup

Similarly, the timescale for the primary breakup in pressure-swirl atomizer is short and there is no significant effect of heat transfer in this stage. A rough estimation can be made as the following. The velocity of liquid sheet for most cases studies is ~50 m/s. The primary breakup happens at around 15 mm downstream, therefore, the travel time is about 0.3ms. However, the heat transfer will influence the ligament breakup and the droplets generated. In addition, since the small diameter stream-wise ligaments usually form earlier and break up faster than the larger diameter span-wise ligaments in slurries and high viscosity cases, the effect of evaporation on the two types of ligaments is different. A rough estimation of the effect is given as the following. Consider an ambient temperature in the spray drying chamber of 100-200 °C. The spray size measurement is taken at 80 mm downstream, where the secondary breakup is almost completed. Therefore, the travel time from the primay breakup position to the the measurement point is about 1.3 ms. According to the D-square model for droplet evaporation, droplets less than 11.4 μm will fully evaporate at 80mm (using an evaporation constant of $\sim 0.1 \times 10^{-6} m^2/s$). Therefore, the droplets generated by streamwise ligaments may fully evaporate in the measurement position, whereas those generated by spanwise ligaments may not.

We have generated a large library of images of ligaments for sprays with different fluid properties and different nozzle operating conditions, such as ones shown in Fig. 7 for pressure-swirl nozzles. In these cases, there are two different length scales for the ligaments: larger diameter ligaments (red) in the spanwise direction, and small diameter ligaments (blue) in the streamwise direction. The large diameters are in the 100's microns, whereas, the small diameters are in 10's microns. Therefore, we will study breakup of ligaments in these size ranges.

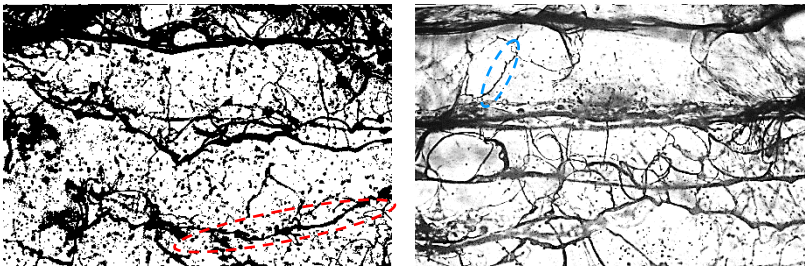

Figure 7. Large diameter spanwise ligaments (red) and small diameter streamwise ligaments (blue) in a pressure-swirl sprays.

2.2. Perforation Based Model for Pressure-Swirl Nozzles

Based on the near nozzle images, a new atomization model is proposed for the swirl nozzles. A perforation-based atomization model as depicted in Fig. 8 is proposed. The liquid sheet breaks up into droplets in the following steps:

1. As the high-speed swirling conical liquid sheet comes out of the orifice, surface wave is generated as it moves with respect to the ambient air due to the Kelvin-Helmholtz (KH) instability.
2. As the liquid sheet moves down stream, the amplitude of wave crests become larger, and these wave crests becomes the thick rims. Perforations appear on the liquid sheet surrounded by these thick rims.
3. As the conical sheet expands and the perforation grows, the conical sheet eventually forms a network of ligaments, with both stream-wise ligaments generated by the perforation and span-wise ligaments generated by thick rims.
4. When most of the stream-wise ligaments break into droplets, the liquid sheet disintegrates. The span-wise ligaments will last longer due to their larger diameters.

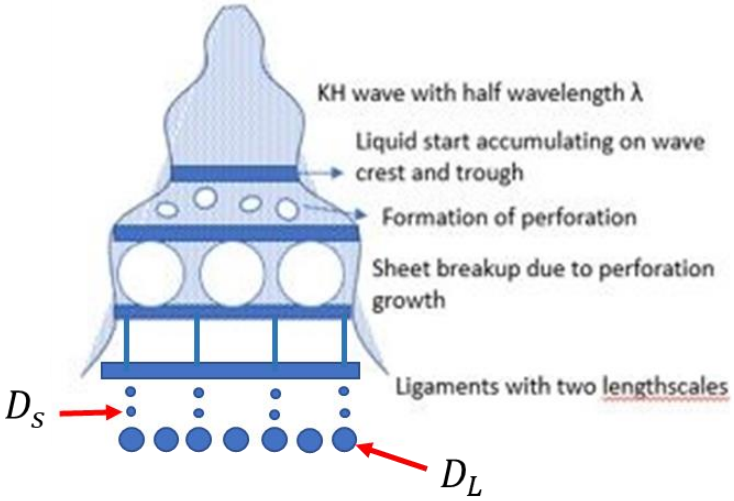

Figure 8. A schematic of the perforation-based atomization model

This breakup model provides two different length scales, which takes up different weight percentages: One based on the thickness of the thin sheet between the crests and troughs of the waves (D_S) with a total mass of m_S, and one based on the diameters of the crests and troughs (D_L) with a total mass of m_L and these can be given as

$$D_L = \sqrt{\frac{4m_c}{\pi^2 D_b}}, D_s = \sqrt{\frac{4(m - m_c)}{\pi n \lambda}}$$

where D_b is the breakup length, n is the number of perforations on the thin sheet and λ is the distance between the wave crests.

We will model the spray size distribution using two size distribution (PDF) each for one of the spray length scales. In order to complete this model, we need to determine correlations for the characteristic sizes of both the spanwise and the streamwise ligaments, in terms of the fluid

properties and the operating conditions. In order to develop a correlation that can be generalized to a wider range of fluids and operating conditions, the following tasks are planned

- Determine the frequency of perforations on the thin sheets with fluids with suspensions.
- Determine how much mass is accumulated at the wave crest
- Develop a theory for how long the sheet can stretch in Newtonian case
- Determine the breakup length of the fluids sheets with suspensions

Theses data will be combined with the ligament breakup model (Rayleigh-Plateau instability) for non-Newtonian fluids to generate a model for droplet size distribution. More detailed information on the testing cases and their results including droplet size distribution and near nozzle images are provided in Appendix A.

2.4. Atomization in Twin-Fluid Nozzle

Our currently developed model for the atomization of the twin-fluid nozzles comprises of the following processes:

- High-speed gas flow over the liquid breaks off small droplets from the surface of the liquid jet issuing from the nozzle based on Kelvin-Helmholtz (KH) instability. The droplet sizes are related to the wavelength of the fastest growing KH waves.
- The liquid core in the jet (the liquid left behind after KH droplet break offs) goes through flapping instability, forming larger droplets with length scale of the flapping wavelength.
- The secondary atomization process breaks the large droplets to smaller droplets. The following secondary atomization model is developed: The high-speed gas flow deforms the front of the droplet into a disk shape. The volume-fraction in the frontal disk determines the breakup morphology:
    - A model is developed that can predict the following morphologies: single bag and multibag breakup, as well as bag and stamen breakups. The breakup is related to the rate of deformation of the droplet.
    - Each disk shape droplet forms a bag with a relatively thick rim. The bag grows and eventually breaks forming small droplets, and the rim breaks forming larger droplets.
    - Rims are analogous to the ligaments seen in high-viscosity spray breakup.
- The final spray droplet size distribution is predicted based on the primary and the secondary atomization models.

The advantages of modelling the spray in this way is the isolation of the slow wave growth from the fast wave breakup and the prediction of ligaments in the breakup, which previous models do not consider. While the development of the KH and flapping instabilities will be somewhat affected by the rheological fluids, the greater effect is expected to be on their breakup, especially when the extensional viscosity is high. Using what we learn about the breakup dynamics of the ligaments, we aim to extend our existing models to include these effects. The data generated in objectives 1 and 2 will serve to validate and verify our models for the global spray breakup.

Further details on the developed twin-fluid nozzle is given in Appendix B.

References

Broumand, M., Shahzeb Khan, M., Yun, S., Hong, Z., Thomson, M.J., Development of an aqueous surrogate for the spray performance evaluation of viscous bioliquids, Experimental Thermal and Fluid Science 128 (2021) 110447.

Glaser, H. W., 1989 VDI Düsseldorf.

Isenschmid, T., 1992 Diss. ETH Nr. 9609.

Jackiw, I. M., and Ashgriz, N., "On Aerodynamic Droplet Breakup," J. Fluid Mech., **913**(A33), (2021).

Kim, H., Ko, T., Kim, S., Yoon, W., Spray characteristics of aluminized-gel fuels sprayed using pressure-swirl atomizer , Journal of Non-Newtonian Fluid Mechanics 249 (2017) 36–47.

Liu Z., and Reitz, R.D., "An analysis of the distortion and breakup mechanisms of high speed liquid drops," Int. J. Multiphas Flow 23, 631 (1997).

Mulhem, B. Fritsching, U. Schulte, G. and Bauckhage, "Characterisation of Twin-Fluid Atomisation for Suspensions," 2001 ILASS-2001 Zurich.

Mulhem, B., Schulte, G., Fritsching, U., Solid–liquid separation in suspension atomization, Chemical Engineering Science 61 (2006) 2582 – 2589.

Qian, L., Zhong, X., Zhu, C., Lin, J., An experimental investigation on the secondary breakup of carboxymethyl cellulose droplets, International Journal of Multiphase Flow 136 (2021) 103526

Ranger A.A., and Nicholls, J.A., "The aerodynamic shattering of liquid drops," AIAA J. 7, 285 (1969).

Schröder, J., Kraus, S., Rocha, B.B., Gaukel, V., Schuchmann, H.P., Characterization of gelatinized corn starch suspensions and resulting drop size distributions after effervescent atomization, Journal of Food Engineering 105 (2011) 656–662.

Theofanous, T.G., "Aerobreakup of Newtonian and viscoelastic liquids," Annu. Rev. Fluid Mech. 43, 661 (2011).

Yan, Y., Zhang, L., Pan, W., and Pu, G., Experimental Investigation of Atomizing Performance of Low Pressure Swirl Nozzle, Advances in Mechanical Engineering, Volume 2014, Article ID 782064, 10 pages.

Zhao, H., Liu, H-F, Xu, J-L, , "Secondary breakup of coal water slurry drops," Phys. Fluids, 23, 113101 (2011).

Zhao, H., Hou, Y-B., Liu, H-F., Tian, X-S., Xu, J-L., Li, W-F., Liu, Y., Wu, F-Y., Zhang, J., Lin, K-F., Influence of rheological properties on air-blast atomization of coal water Slurry, Journal of Non-Newtonian Fluid Mechanics 211 (2014) 1–15.

Appendix A - Pressure-Swirl Nozzle

A.1. Introduction

Most spray studies provide a mean size for the spray. One commonly presented mean size is the Sauter mean diameter, noted as SMD or d_{32}. The SMD is usually correlated with the operating conditions (injection pressure P, mass flow rate $\dot{m}$, etc.), fluid properties (liquid density ρ_l, viscosity μ, surface tension σ, etc.) and nozzle geometry parameters (orifice diameter d_{or}, etc.). For example, Tratnig and Brenn (2010) provided the following correlations for a swirl nozzle

$$\frac{d_{32}}{d_{SC}} = 3.074\left(\frac{\sqrt{P\rho_l}d_{SC}}{\mu}\right)^{-0.8505}\left(\frac{\mu}{\sqrt{\sigma d_{or}\rho_l}}\right)^{-0.7538}\left(\frac{h_{SC}}{d_{SC}}\right)^{-0.0574}\left(\frac{d_{or}}{d_{SC}}\right)^{-0.3496}\left(\frac{b_{SC}}{d_{SC}}\right)^{-0.0426}$$

where d_{SC} is the swirl chamber diameter, h_{SC} is the swirl chamber height and b_{SC} is the swirl chamber inlet width.

Wang and Lefebvre (1986) developed an empirical correlation with insight on the atomization process. They claimed that the atomization in a pressure swirl nozzle can be viewed as two stages. In the first stage, surface waves develop on the conical sheet due to instabilities. As the surface waves grow, they become large enough that some parts of the liquid break off from these surface waves and forms ligaments. The droplet size, SMD_1, generated at this stage is related to the Reynolds number, which indicates the strength of inertial force to breakup the sheet and Weber number, which governs the development of the surface wave. In the second stage, the rest of the sheet breaks up into ligaments as the surface wave grows when it moves downstream. The droplet size, SMD_2, generated at this stage is only related to the Weber number. The final SMD can then be predicted as a sum of these two $SMDs$. Fitting on their experimental data resulted in the following equation

$$SMD = SMD_1 + SMD_2 = 4.52\left(\frac{\sigma\mu^2}{\rho_g P^2}\right)^{0.25}(t_{or}cos\theta)^{0.25} + 0.39\left(\frac{\sigma\rho_l}{\rho_g P}\right)^{0.25}(t_{or}cos\theta)^{0.75}$$

where ρ_g is the density of the gaseous medium, t_{or} is the liquid sheet thickness at the exit of orifice, θ is the half spray cone angle. Xiao and Huang (2014) have noted that this correlation better fits their experimental data. Wang and Lefebvre's model is one of the earliest models indicating that there might be multiple breakup mechanisms in the atomization process of a pressure swirl nozzle.

Since the empirical correlation have limited insight on the actual atomization mechanism in the nozzle, they only make good prediction in a certain range of operating conditions and for the specific type of fluids used. A better understanding of the physical processes involved in these atomizers are needed to develop a model that is generalized enough to be applied to a wider range of operating conditions and fluids.

The current theoretical models describe the breakup of a liquid sheet in two steps: The breakup of liquid sheet into ligaments and the breakup of these ligaments into droplets. These models commonly use Kelvin-Helmholtz, Rayleigh-Plateau, and/or Rayleigh-Taylor instabilities as the cause of the liquid sheet breakup. The dominant wavelength λ_{max} (or wavenumber k_{max}) of the instability is then used to predict the size of the ligaments or droplets generated from the breakup. For example, Dombrowski and Johns (1963) developed the following relation for the diameter of the ligament, d_{lig}, formed by the breakup of a liquid sheet moving in the ambient gas with a velocity u:

$$d_{lig} = \sqrt{\frac{8a}{k_{max}}} = 2\left(\frac{4}{3f}\right)^{\frac{1}{3}}\left(\frac{C_t^2\sigma^2}{\rho_g\rho_l u^2}\right)^{\frac{1}{6}}\left(1 + 2.6\mu\sqrt[3]{\frac{C_t\rho_g^4 u^8}{6f\rho_l^2\sigma^5}}\right)^{\frac{1}{5}}$$

where a is the half of the initial thickness of the liquid sheet, and the sheet is attenuating as $2a = C_t t^{-1}$, where C_t is a constant and t is the time. And f is a constant that appears from the surface wave of $y = A_0 e^f \sin(kx + \varphi)$, and it is assumed to be $f = 12$. The parameter f determines the place where the sheet breaks up and its value is set based on analogy to the jet breakup determined by Weber (1931). The ligaments then experience the Rayleigh-Plateau instability to breakup into the droplets. For a cylindrical ligament with a diameter of d_{lig}, the dominant wavenumber is given by

$$k_{max}d_{lig} = \frac{1}{2}\left(1 + \frac{3\mu}{\sqrt{\rho_l\sigma d_{lig}}}\right)^{-1/2} = \frac{1}{2}(1 + 3Oh)^{-1/2}$$

As the wave grows until its amplitude reaches the ligament radius, one droplet will be generated per wavelength. The SMD of these droplets is then given using a mass balance as

$$SMD = 1.882 d_{lig}(1 + 3Oh)^{\frac{1}{6}}$$

Another popular theoretical model developed for swirl nozzle is the linearized instability sheet atomization (LISA) model developed by Senecal et. al (1999). The main difference between LISA model and the model developed by Dombrowski and Johns (1963) is the way the dominant wavenumber k_{max} on the liquid sheet is determined. Instead of a 1-D force balance analysis, they performed a 2-D linear instability analysis. The maximum growth rate, ω_{max}, of the instability and its corresponding wavenumber, k_{max}, are found and used to evaluate the breakup time τ and breakup length L_b as: $\tau = \frac{1}{\omega_{max}}\ln\left(\frac{A}{A_0}\right)$, and $L_b = u\tau = \frac{u}{\omega_{max}}$, where A is the amplitude of the surface wave and A_0 is the initial amplitude of the surface wave. Similarly, $\ln\left(\frac{A}{A_0}\right) = 12$. Schmidt.et al (1999) applied this to a pressure swirl nozzle and found the sheet half-thickness t_b at L_b as

$$t_b = \frac{2t_{or}(d_{or} - t_{or})/cos\theta}{2L_b sin\theta + d_{or} - t_{or}}$$

According to the short wave assumption, one ligament is formed per wavelength. The diameter of these ligaments is found using a mass balance by

$$d_{lig} = \sqrt{\frac{16t_b}{k_{max}}}$$

These ligaments then break up into droplets with the same equation described above. Both of these models use a linearized instability analysis. Others, such as Clark and Dombrowski (1972), and Jazayeri and Li (2000), have developed higher order nonlinear instability models for the liquid sheet, which become too complicated to solve for the k_{max} directly, and therefore, they are hardly used for size prediction.

These atomization models usually overpredict the droplet size of the spray especially under high viscosity and high injecting pressure (Tratnig and Brenn, 2010). One reason that these models fail to make good prediction is that they oversimply the atomization mechanism. They assume that the liquid sheet stays intact until the instability waves grow enough to break the sheet. However, this is not the case in actual atomization processes. Experimental studies on liquid

sheet and swirl nozzle atomization show that perforations form on the liquid sheet. Perforations generate both stream-wise and span-wise ligaments in an liquid sheet with air-blast atomization (Stapper et.al in 1992). Sindayihebura and Dumouchel (2001) found perforations on the liquid sheet generated by a pressure-swirl nozzle using water solution of a non-Newtonian polymer. Loustalan et al. (2003) observed perforations in a spray of fuel atomizing at high injecting pressure. Therefore, new atomization models that better describe the mechanism of breakup are needed to improve droplet size prediction.
In this work, we present a set of experimental data on sprays generated by swirl nozzles, and a new model for the sheet atomization to better present the atomization process in these nozzles.

A.2. Experiment Setup

The experiments were carried out in the testing setup depicted in Fig. A1. A Hydra-Cell D10 pump was used to pump fluids from the tank at pressures up to 1000 psi. The pump was controlled by both a variable frequency controller (VFD) and a pressure regulating valve to adjust the pressure at the outlet. A high accuracy pressure gauge with ±1% accuracy was used to measure the inject pressure at the nozzle inlet. The fluid sprayed was collected below the setup for reuse. A curtain with an opening whose diameter allowed just the spray pass through without any blockage was mounted beneath the measuring region to prevent the equipment from measuring any recirculated droplets.

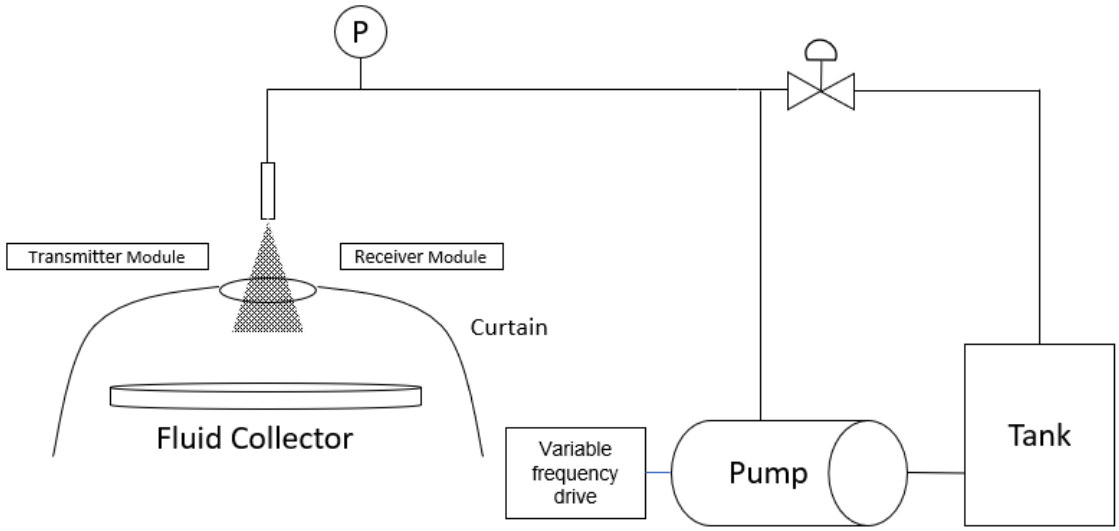

Figure A1: Schematic for Experiment Setup

The droplet sizes in the sprays were measured by the Malvern Spraytec Dropsizer, using a 300 mm lens. In this setup, the equipment could detect droplets from 0.1 μm to 900 μm. Malvern measures the volume distribution, which has to be converted to size distribution.

We used two different swirl nozzles with inserts, obtained from Spraying Systems. A smaller nozzle with an orifice diameter of 0.71 mm (N1), and a larger nozzle with an orifice diameter of 1.07 mm (N2). The testing fluids used were water, water-glycerin solutions and water-carboxymethyl cellulose (CMC) solutions with different concentrations. The surface tensions, viscosities and densities of water-glycerin solutions were obtained through a lookup table provided by Glycerin Producers' Association (1963) with linear interpolation at room

temperature (20 °C) as listed in Table A1. The properties of water-CMC solutions will be measured in the upcoming months. For each nozzle and each fluid, experiments were done at 3 different injection pressures of 500 psi, 700 psi, 900 psi. In order to measure the mass flow rate, the fluid was collected at the nozzle exit using a measuring cup for a certain time (more than 10 seconds) and weighted. This was repeated 3 times, and the average mass flow rate of the 3 runs was taken as the mass flow rate under the testing condition. Images are also taken at the nozzle exit to measure the spray angle. In total, eighteen different cases were tested. Measurements were taken at 8 cm downward from the nozzle exit. Each test case was repeated for at least 3 times to check the repeatability of the experiments. All the measurement result are listed in Table A2.

Table A1: Fluid properties of the testing fluids. The cells marked by * is to be measured in the future.

Fluid Type	Density (g/ml)	Viscosity (mPa.s)	Surface Tension (mN/m)
Water	0.997	1.005	71.68
60% glycerin/water	1.154	10.8	67.76
80% glycerin/water	1.209	60.1	65.49
0.25 % CMC/water	*	*	*
0.5 % CMC/water	*	*	*

Table A2: Measurement results for all testing cases. The cells marked by * are in progress.

Test Case	d_o (mm	Fluid Type	P (psi)	$\dot{m}$ (g/s)	Spray Angle	d_{32}(μm
1	0.71	Water	500	6.57	74.66	27.85
2	0.71	Water	700	7.70	78.72	22.75
3	0.71	Water	900	8.71	84.18	21.88
4	0.71	60% glycerin/water	500	9.90	54.68	29.68
5	0.71	60% glycerin/water	700	11.52	59.9	25.79
6	0.71	60% glycerin/water	900	13.02	61.92	22.28
7	0.71	80% glycerin/water	500	11.82	45.04	58.76
8	0.71	80% glycerin/water	700	13.02	49.95	45.44
9	0.71	80% glycerin/water	900	14.22	54.86	40.31
10	1.07	Water	500	18.74	73.02	30.97
11	1.07	Water	700	22.44	69.04	26.54
12	1.07	Water	900	24.94	70.14	24.18
13	1.07	60% glycerin/water	500	22.34	57.14	37.52
14	1.07	60% glycerin/water	700	26.39	61.58	32.83
15	1.07	60% glycerin/water	900	29.55	64.78	27.71
16	1.07	80% glycerin/water	500	24.50	53.19	50.18
17	1.07	80% glycerin/water	700	28.48	57.61	42.27
18	1.07	80% glycerin/water	900	31.94	62.11	37.38
19	0.71	0.25% CMC/water	500	*	*	77.71
20	0.71	0.25% CMC/water	700	*	*	53.71
21	0.71	0.25% CMC/water	900	*	*	42.92
22	0.71	0.5% CMC/water	500	*	*	174.0

23	0.71	0.5% CMC/water	700	*	*	109.2
24	0.71	0.5% CMC/water	900	*	*	83.33
25	1.07	0.25% CMC/water	500	*	*	55.66
26	1.07	0.25% CMC/water	700	*	*	45.47
27	1.07	0.5% CMC/water	500	*	*	76.45
28	1.07	0.5% CMC/water	700	*	*	61.08
29	1.07	0.5% CMC/water	880	*	*	54.14

A.3. Droplet Size Distributions

A.3.1 Raw Data from Malvern

The Mavlern Spraytec Dropsizer gives the droplet size measurement result in the form volume percentages of droplets in different bins, which are in the logarithmic scale. The histograms of all testing cases are shown on Fig. A2. For almost all the testing cases, the histograms have one peak with long tail on the left corresponding to the smaller droplets less than 10 μm. Increasing the orifice size will result in an increase in the span of the peak and a decrease in the maximum percentage of the peak. This indicates that the droplets generated have a wider range of sizes. For example, most peaks for the nozzle N1 are around 10%, while those for nozzle N2, which have a larger orifice diameter are around 8%. Atomizing high viscosity fluid with small orifice at low pressure have a similar effect, which is shown for the case of atomizing 80% glycerin/water solution with N1 nozzle at 500 psi. Furthermore, atomizing high viscosity polymeric fluid, such as 0.5% CMC solution, can result in a bimodal volume percentage histograms such as for N1 at all tested pressures and N2 at 500 psi. This indicates that the inertia force is not enough to counter the viscous force to break up the liquid properly into droplets. Increasing injection pressure can result in a change from bimodal volume percentage to unimodal volume percentage, for example for atomizing 0.5% CMC solution with N2 at 700 psi and 900 psi. The volume percentage of large droplets decreases and that of smaller droplets increases as the injection pressure increases. This is shown as the peak shifting to the left.

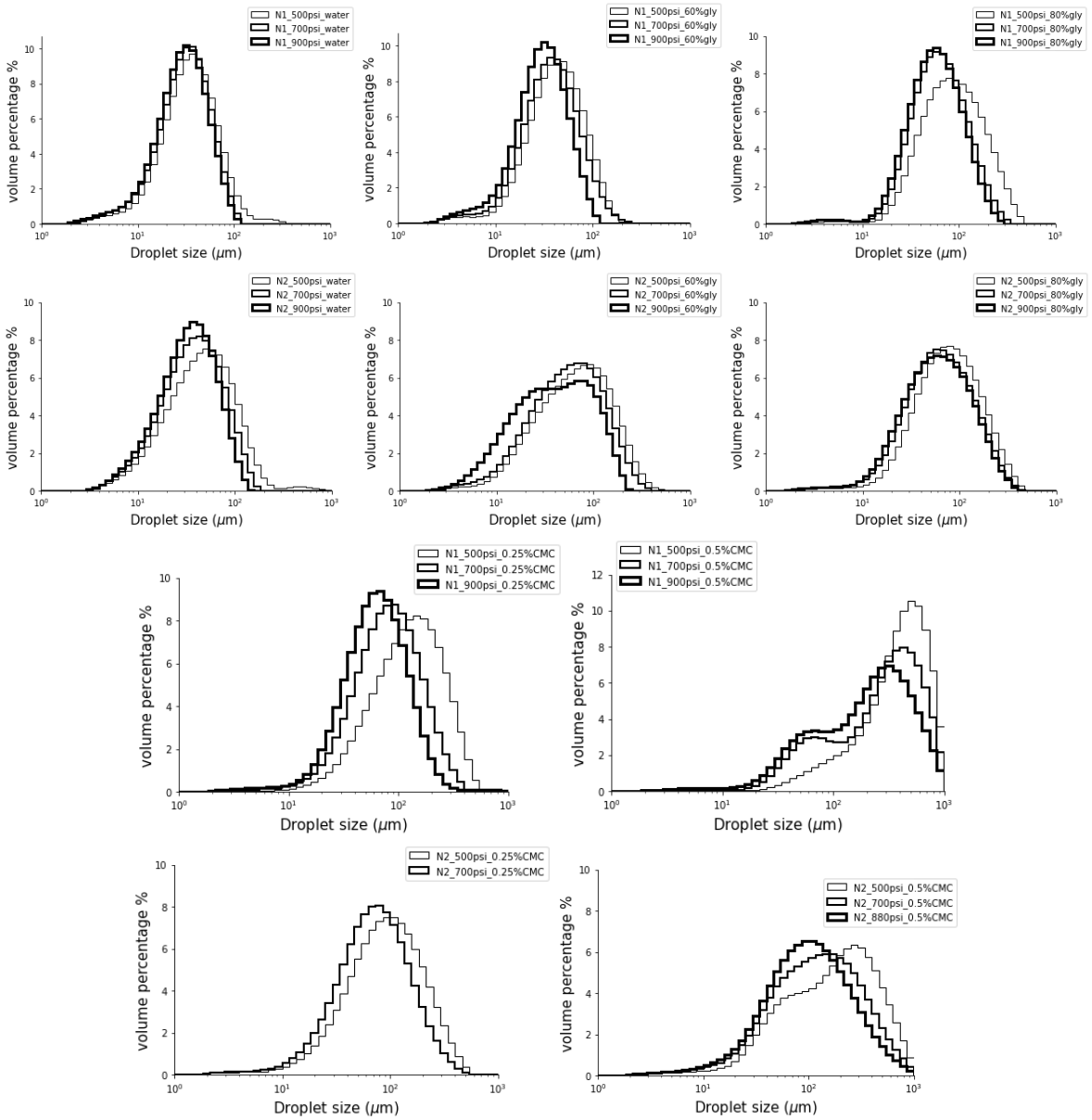

Figure A2: Volume percentage of each testing cases

A.3.2 Volume Distribution of Droplets

In order to get the volume distribution, the height of each bin is divided by the corresponding bin width and the results are shown in Fig. A3. As observed in Fig. A3, a unimodal volume histogram can become a bimodal volume distribution and a bimodal volume histogram can have three modes. It should be noted that the bin widths in the measurement result set by the Mavlern Spraytec Dropsizer are not equal. The bin width increases as the droplet size increases.

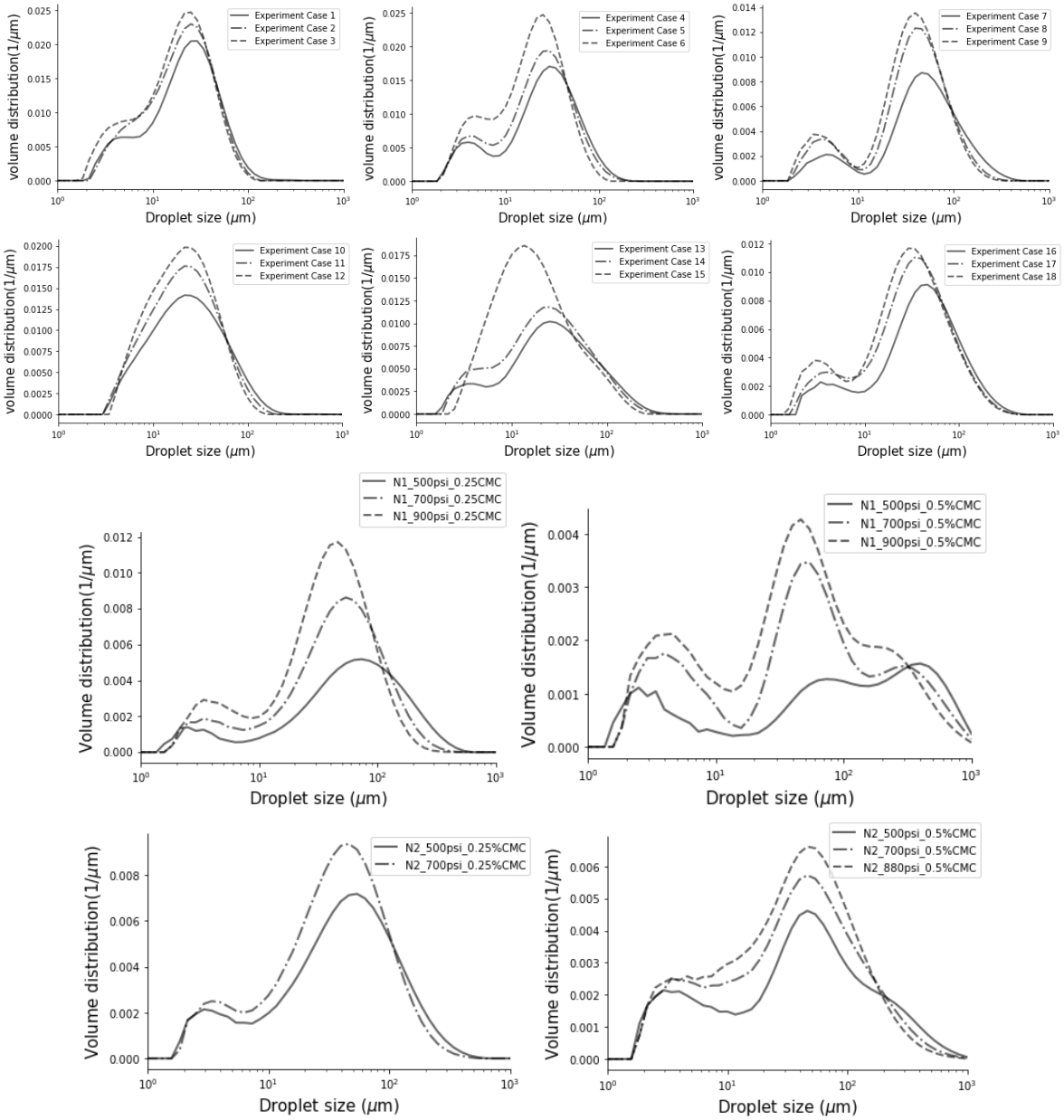

Figure A3. Volume distributions for all experiment cases

A.3.3 Cumulative Volume Distribution

The effect of operating conditions on the droplet size distributions is also presented in cumulative volume distribution in Fig. A4. The three horizontal dotted lines indicates the 90%, 50% and 10% of the total volume from top to bottom respectively. The x-coordinates of the intersections between these dotted lines and the accumulative volume distribution curve are the D_{v90}, D_{v50} and D_{v10}. As shown on the upper-left and upper-right plot, as the pressure increases, D_{v90}, D_{v50} and D_{v10} all decreases. The D_{v90} decreases most significantly among the three. This indicates that the number of large droplets decreases and the diameters of droplets vary in a smaller range. Increasing the orifice diameter of the nozzle does not have much effect on the D_{v10}, but largely increases D_{v90}. Similar effects can be observed in the lower-left plot as a result of increasing viscosity.

The cumulative volume distribution curves for both nozzles atomizing 80% glycerin/water solution at 700 psi are shown in the lower-right plot in Fig. A4. The D_{v10} of the spray generated by N2 nozzle is smaller than its counterparts, while the D_{v90} is larger. This indicates that the spray generated by N2 nozzle has a wider range of droplet sizes and there are more smaller droplets in the spray, which result in a smaller SMD than the spray generated by N1 nozzle.

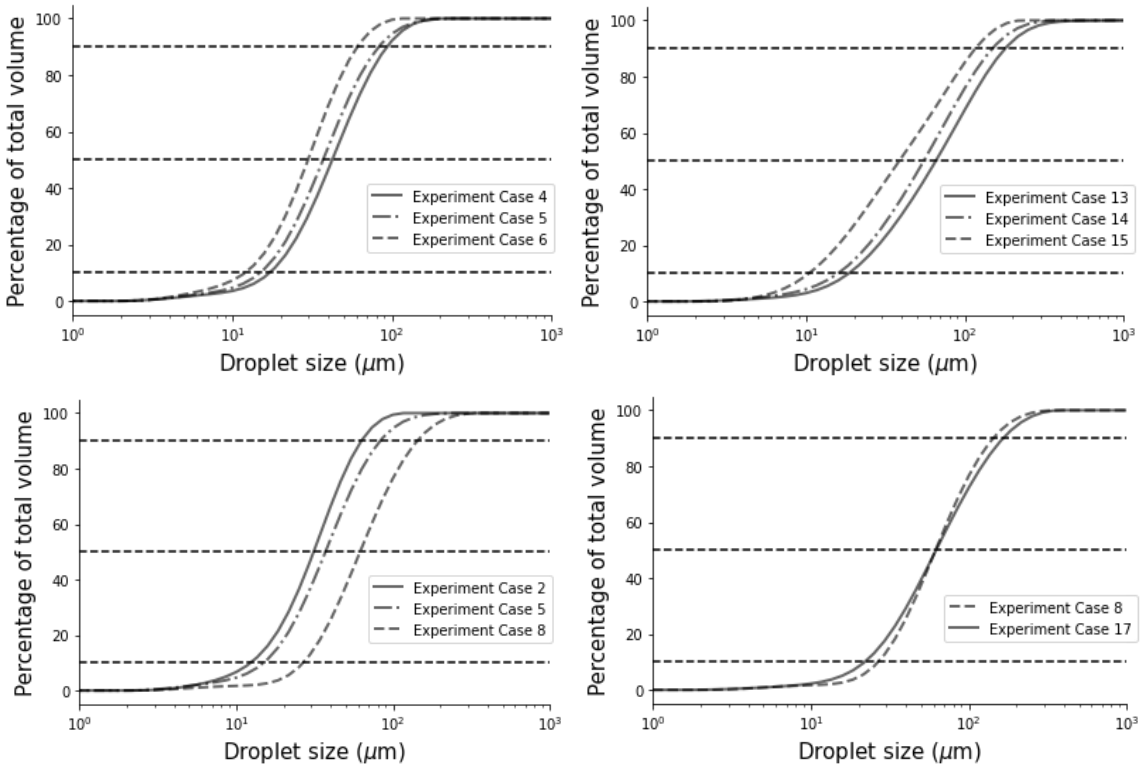

Figure A4. Comparison of accumulative volume distribution under different operating conditions

A3.4 Conversion of Volume Distribution to Size Distribution

In order to find the corresponding size distribution to a volume distribution, we will start with guessing a size distribution, and then calculate the volume distribution based on that and compare with the experimental results. The parameters of the size distribution are then changed to match the experimental data. This is complicated since we have a bimodal volume distribution.

We will seek a mixture number distribution $f_0(d)$ that is the summation of two different unimodal distributions $f_{0,1}(d)$ and $f_{0,2}(d)$ as

$$f_0(d) = k_n f_{0,1}(d) + (1 - k_n) f_{0,2}(d),$$

such that their corresponding volume distributions have the following relationship

$$f_3(d) = k_v f_{3,1}(d) + (1 - k_v) f_{3,2}(d),$$

where k_n is the number ratio of the droplets generated by each distribution and k_v is the volume ratio of the droplets. Since volume distribution based on a size distribution can be written as

$$f_3(d) = \frac{d^3 f_0(d)}{\int_0^\infty d^3 f_0(d) dd},$$

it can be shown that

$$k_n = \frac{k_v S_2}{S_1 + k_v(S_2 - S_1)}$$

where $S_a = \int_0^\infty d^3 f_{0,a}(d)dd\,, a = 1{,}2.$

As a result, as long as a bimodal distribution is fit to the volume distribution, their corresponding number distribution can be calculated. Although there are some methods developed for fitting a mixture model to the bimodal distribution, the author found that the performance of many of them largely rely on the initial value picked for these methods and it needs lots of effort to find the best initial guess to fit the bimodal distribution properly. Since the goal is to determine the parameters in the mixture model to fit the bimodal distribution properly rather than develop an algorithm with good mathematical base, the following method is used by the author. The main idea is to fit a distribution to the main peak first, and then adjust the ratio between two distributions to fit the residual, For a bimodal volume distribution function $f_3(d)$, we first guess the ratio k_v, then fit the main peak (the peak for larger droplets) by approximating the mean and variance for the main peak These values are used as an initial guess, and the parameters are optimized by minimizing the distance between the main peak and fitted distribution $f_1(d)$. The distance used in this work is the Earth Mover Distance (EMD) as:

$$EMD_1 = \int_{d_t}^{\infty} \left| f_3(d) - k_v f_{3,1}(d) \right| dd$$

where d_t is the diameter corresponding to the local minimum value in the bimodal distribution at the trough of volume distribution to separate the main peak and minor peak. Then the residual of the distribution is found: $r(d) = f_3(d) - k_v f_{3,1}(d)$, and parameters in $f_{3,2}(d)$ are optimized with similar method:

$$EMD_2 = \int_0^{\infty} \left| r(d) - (1-k) f_{3,2}(d) \right| dd$$

The above process is then repeated to minimize the total distance between the bimodal distribution and the mixture model, which optimizes the ratio k.

In order to fit the data, a distribution function is needed. One of the popular number distributions used in the literature is the Gamma distribution with 2 parameters α and β:

$$f_0(d;\alpha,\beta) = \frac{\beta^\alpha}{\Gamma(\alpha)} d^{\alpha-1} e^{-\beta d}$$

For example, Villermaux et. al. (2004) found that the number distribution of droplets generated from a ligament with size d_{lig} is a gamma distribution with 2 parameters as

$$f_0\left(d;\kappa,\nu,d_{lig}\right) = \frac{1}{\kappa d_{lig}} \frac{\nu^\nu}{\Gamma(\nu)} \left(\frac{d}{\kappa d_{lig}}\right)^{\nu-1} \exp\left(-\nu \frac{d}{\kappa d_{lig}}\right)$$

where κ and ν are determined empirically from experiment, in which the corresponding functions are $\alpha = \nu, \beta = \nu/\kappa d_{lig}$. The corresponding volume distribution based on the original size distribution parameters can be written as

$$f_3(d;\alpha,\beta) = \frac{\beta^{\alpha+3} d^{\alpha+2} e^{-\beta d}}{\Gamma(\alpha+3)} = \frac{\beta^{\alpha'}}{\Gamma(\alpha')} d^{\alpha'-1} e^{-\beta d},$$

which is also a Gamma function with $\alpha' = \alpha + 3$. However, as it shown on Fig. 10, a mixture distribution with two Gamma distribution does not fit well to experiment case 5. When fitting one Gamma component to the peak for larger droplets, although it fits the peak on right-hand side properly, its value is greater than the experimental data on the left-hand side, which makes it

impossible to find a mixture distribution by adding another Gamma component whose value is always positive. Another issue is, an α' value less than 3 will result in a negative α value when converting the volume distribution back to number distribution, which is unrealistic. Although Yongyingsakthavorn et. al (2008) successfully fit a mixture distribution with generalized Gamma distributions for an ultrasonic nozzle with smaller flow rate, a mixture distribution of Gamma distributions does not fit for the swirl nozzle at operating conditions tested in this work as shown in Fig. A5.

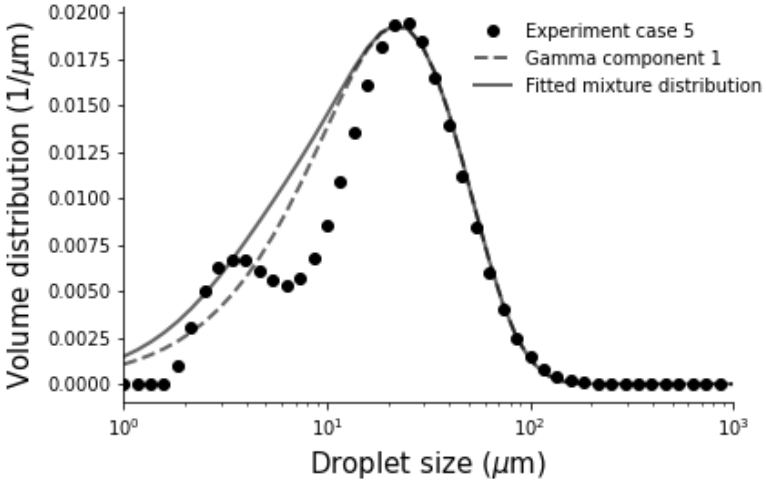

Figure A5. Fitting a mixture distribution of two Gamma distribution to experiment case 5. One of the components has a greater value than the experimental distribution in certain range.

Since Gamma distribution did not work well, we tried the lognormal distribution, which has the following form

$$f_0(d) = \frac{1}{d\sigma\sqrt{2\pi}} \exp\left(-\frac{1}{2}\left(\frac{ln(d/\mu)}{\sigma}\right)^2\right)$$

whose corresponding volume distribution is

$$f_3(d) = \frac{d^3}{e^{3\mu+4.5\sigma^2}} f_0(d)$$

Figure A6 shows several results for fitting a mixture of lognormal distribution to experimental data. The mixture of lognormal distribution can not only follow the position of two peaks and the troughs properly for bimodal distribution (case 1 and case 5), but also fit to the unimodal distribution well (case 11). The mixture model has the form

$$f_3(d) = k_v f_{3,1}(d; \mu_1, \sigma_1) + (1 - k_v) f_{3,2}(d; \mu_2, \sigma_2)$$

with 5 parameters. The parameters fitted for each case and the corresponding k_n are listed in Table A3.

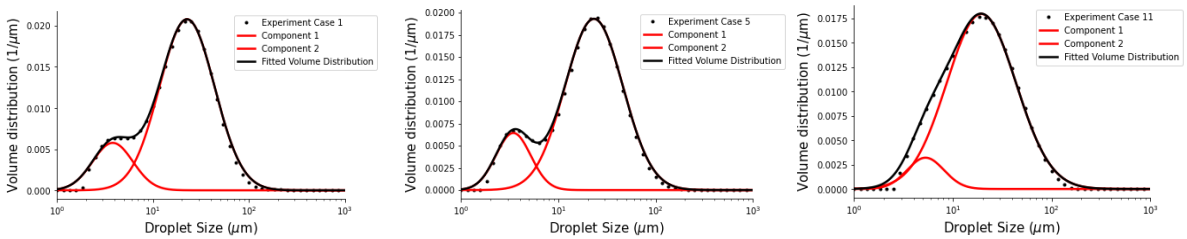

Figure A6. Fitting a mixture distribution of two lognormal distribution to experiment case 1, case 5 and case 11.

Table A3: Parameters in fitted mixture distribution of lognormal distributions

Case	k_v	k_n	σ_1	μ_1	σ_2	μ_2	d_{32} (μm)	Experimental Result (μm)
1	0.97	0.173	0.66	9.5	0.483	2.4	24.19	27.85
2	0.96	0.234	0.636	9.3	0.468	2.869	21.92	22.75
3	0.955	0.132	0.636	8.8	0.547	1.987	19.92	21.88
4	0.98	0.138	0.685	10.4	0.383	2.5	28.82	29.68
5	0.975	0.166	0.685	9.1	0.413	2.45	25.12	25.79
6	0.955	0.152	0.612	9.9	0.453	2.6	20.76	22.28
7	0.99	0.088	0.734	16.2	0.433	2.72	54.97	58.76
8	0.985	0.066	0.636	17.6	0.438	2.48	41.49	45.44
9	0.985	0.073	0.66	14.8	0.432	2.28	37.70	40.31
10	0.985	0.749	0.88	4.5	0.433	3.873	29.41	30.97
11	0.98	0.666	0.807	5.3	0.428	3.677	25.17	26.54
12	0.965	0.594	0.734	6.7	0.383	4.534	23.36	24.18
13	0.994	0.425	0.977	3.7	0.333	2.16	37.30	37.52
14	0.99	0.471	0.977	3.2	0.373	2.26	31.67	32.83
15	*	*	*	*	*	*	*	27.71
16	0.99	0.075	0.782	12	0.498	1.938	48.40	50.18
17	0.986	0.102	0.807	8.8	0.542	1.766	38.76	42.27
18	0.989	0.133	0.831	7.3	0.408	1.913	35.85	37.38

For most of the cases, $k_v > 0.95$, which means the distribution which has a larger μ is responsible for more than 95% fluid atomized. However, for most of the cases $k_n < 0.2$, which means that the small droplets take up more than 80% of the total number of droplets and the number distribution will be largely dominated by the small droplets. As a result, the corresponding number distributions may appear unimodal for a bimodal volume distribution. This can also explain why a single unimodal distribution cannot fit the number distribution of droplets in swirl nozzle properly (Tratnig and Brenn, 2010).

One reason for the huge number of small droplets is the uneven bin sizes in the result from the Dropsizer. Since the bins are in logarithmic scale, the bin width increases as the droplet size increases. Figure A7 shows the volume distribution converted from a volume distribution plot with the same height for all bins. It shows that the same percentage for smaller particles (those below 10 μm) resulted in a much larger value in volume distribution than that for larger particles. This indicates that the number of smaller particles, especially those less than 10 μm, is extremely prone to small errors.

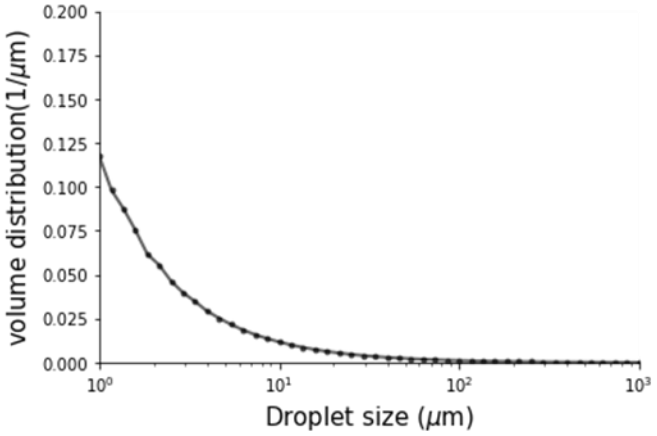

Figure A7. Volume distribution converted from a volume distribution plot with same height for all bins

A.4. Characteristic Droplet Sizes

The SMD of all the testing cases are plotted versus injecting pressure in Fig. A8, which shows that the SMD decreases as the injection pressure increases. The N1 nozzle, which has a smaller orifice diameter, generates finer droplets than the N2 nozzle for low viscosity fluids, such as water and 60% glycerin/water solution. However, when atomizing high viscosity fluids, such as 80% glycerin, N1 generates much larger droplets than N2.

The empirical correlation usually has the form of the power law. A dimensional analysis is carried out to study the relationship between the SMD and relevant parameters in the experiments for water and water-glycerin solutions. In order to calculate the non-dimensional groups such as Re and We, the velocity of the liquid sheet needs to be determined. Consider a fluid enters a pressure-swirl nozzle with a swirl insert at an injection pressure P. The liquid forms a swirling conical liquid sheet at the nozzle exit.

For a swirl nozzle, the mass flow rate of is written as $\dot{m} = (\rho U \cos\theta)\, \pi t_{or}(d_o - t_{or})$ where U is the total velocity of the sheet. However, since the size of the air core is hard to measure directly, the sheet thickness remains unknown, which makes it hard to calculate velocity U directly from the mass flow rate. The sheet velocity is determined using the pressure at the nozzle inlet P as $U = k\sqrt{2P/\rho}$, where k is the discharge coefficient. Although there are numerous methods to calculate the discharge coefficient in literature, they are all empirical and different from each other. As a result, the Re and We are modified to be as Re_p and We_p based on the inlet pressure, which is directly measured from the experiment. Since $P \sim \rho u^2$, $Re_p = \sqrt{P\rho}d_0/\mu$, $We_\rho = Pd_0/\sigma$. The correlation found for the non-dimensional SMD is

$$\frac{d_{32}}{d_o} = 42.52 Re_p^{-0.151} We_p^{-0.519} \tag{4}$$

The comparison between the experimental result and predicted SMD is shown in Fig. A9 on the left. The R^2 score for the correlation is 0.853, indicating a good result. However, the plot shows that there are 3 datapoints off the trends from the rest of the points. These datapoints are the experiments for the N1 nozzle, which has a small orifice diameter, atomizing 80% glycerin/water solution. If these datapoints are excluded, the new correlation found is

$$\frac{d_{32}}{d_o} = 7.37 Re_p^{-0.103} We_p^{-0.404} \quad (5)$$

The R^2 score improves to 0.894. This indicates that atomizing highly viscous fluid using nozzles with small orifice size may result in a different atomizing behaviour, generating larger droplets.

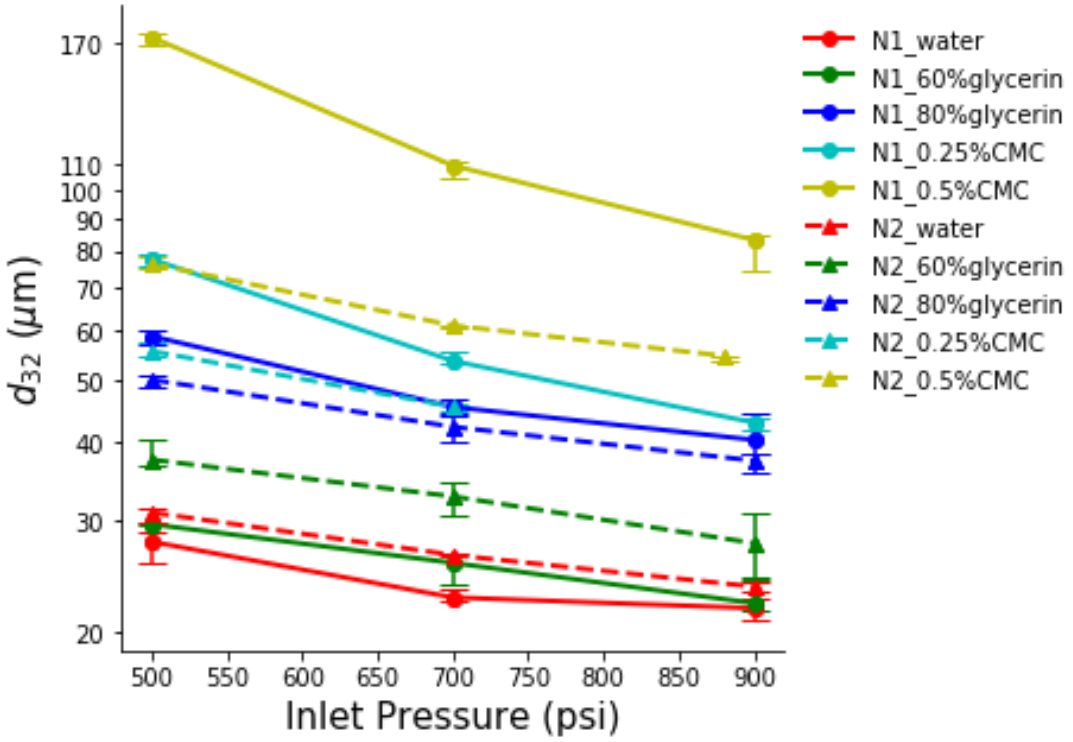

Figure A8. SMD versus Injection pressure for all testing cases.

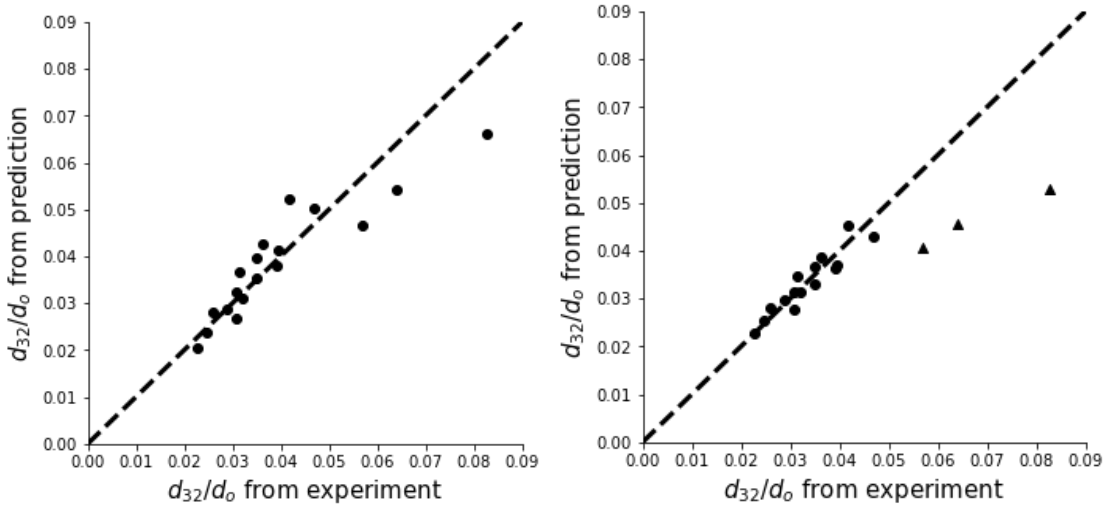

Figure A9. Comparison of non-dimensional SMD between experiment and prediction. Left: Correlation fit with all the data. R^2 = 0.853. Right: Correlation fit with data excluding ones from N1 nozzle, 80% glycerin (triangle points) R^2 = 0.894.

The comparison between the d_{32} calculated from LISA model and the d_{32} measured from the experiments for the current work is shown in Fig. A10. LISA model tends to overpredict the droplet diameters in most cases, which is also true for Tratnig and Brenn's data (2010). One main reason, also pointed out by Tratnig and Brenn (2010), LISA model overpredicts the breakup length in these cases. The breakup length predicted by LISA model for high viscosity fluid is 60~80 mm, while the near nozzles images show that the liquid sheet is already broken up into a web of ligaments within 20 mm for all the testing cases. A comparison between the breakup length measured and that predicted by LISA model is listed in Table A4. Such difference comes from the assumption that the liquid sheet stays intact until its thickness is attenuated less than twice the amplitude of the surface wave. In addition, according to LISA model, a shorter breakup length will result in a larger sheet thickness at the breakup, and thus, larger droplets. However, the experiments shows that not only the breakup length is smaller than predicted, but the d_{32} is smaller than that predicted by LISA model. As a result, it is important to study the breakup mechanism and see how it differs from what depicted by the LISA model.

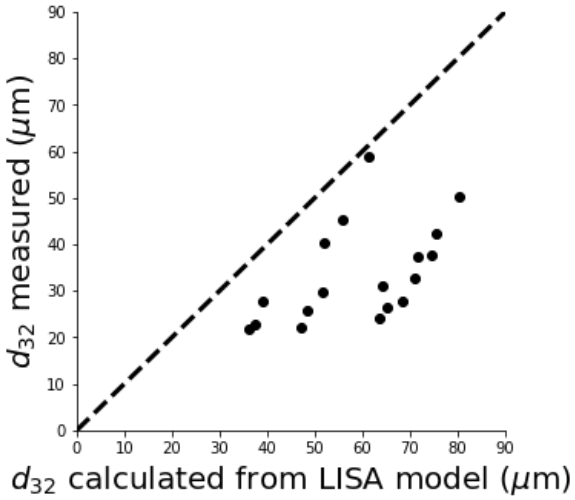

Figure A10. Comparison between d_{32} calculated from LISA model and experiment.

Table A4: Comparison of breakup length between experiment measurement and LISA model prediction.

Test Case	Breakup length predicted by LISA model (mm)	Breakup length measured (mm)	$d_{32}(\mu m)$
1	20.35	6.13	27.85
2	14.59	5.95	22.75
3	11.27	5.49	21.88
4	32.12	7.6	29.68
5	24.30	7.23	25.79
6	19.80	6.51	22.28
7	77.52	16.79	58.76
8	63.39	14.20	45.44
9	54.26	13.11	40.31
10	18.55	8.74	30.97

11	13.48	*	26.54
12	10.65	7.16	24.18
13	32.06	8.96	37.52
14	24.14	8.28	32.83
15	19.69	7.94	27.71
16	79.07	14.83	50.18
17	63.47	14.24	42.27
18	53.85	13.74	37.38

A.5. Atomization Mechanism in Pressure-Swirl Nozzle

Table A5 shows the images of the water spray atomizing with nozzle N1 at different pressures. The liquid sheet is not intact before the liquid sheet breaks up. The earliest observable perforation on the conical sheet is about 2 mm from the nozzle exit. These perforations occurred on the liquid sheet surrounded by the thicker rims, which is mostly span-wise. As a perforation grows, it will either be limited by the thick rims surrounding it or coalesce with its neighboring perforations and form stream-wise thick ligaments. As the sheet getting thinner and perforations growing, the liquid sheet will eventually become a web of ligaments. The stream-wise ligaments generated by the perforations usually have a smaller diameter compared to the rims and they tend to break faster in the atomization process. The sheet eventually breaks when most of the stream-wise ligaments break into droplets. The thick rims will then breakup into several shorter ligaments and then into droplets. Those shorter ligaments are still aligned in the span-wise direction as those rims.

Table A5: Near nozzle images for water spray atomizing with nozzle N1 at different pressures.

Z(Mm)	N1 - Water - 500PSI	N1 - Water - 700PSI	N1 - Water - 900PSI
0	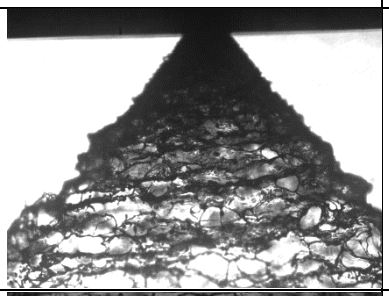	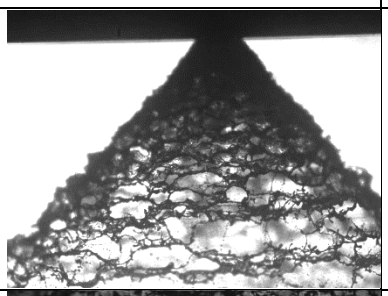	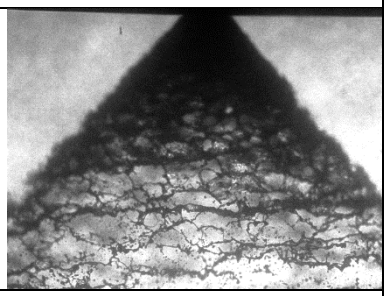
4.98	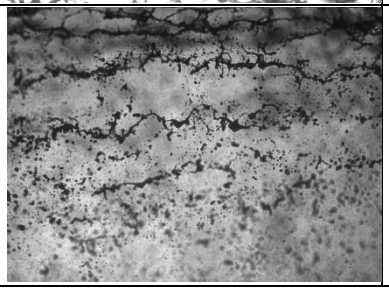	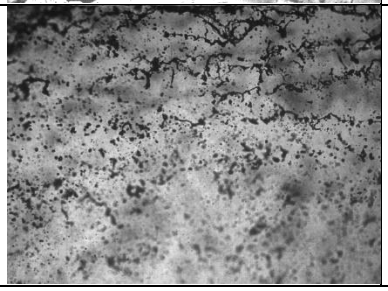	

Table A6 shows the images of spray with 60% glycerin/water solution for atomizing with nozzle N1 at different pressures. It can be observed from the edge of the cone that, the wavelength on the liquid sheet is larger compared to that of water spray. In addition, the amplitude at the wave crests is larger than that of water spray. It implies that the span-wise rims are thicker than that in the water spray, which is responsible for the larger droplet sizes. These thicker rims stay in the form of long ligaments while those stream-wise thin ligaments have already break up into multiple droplets.

Table A6: Near nozzle images for 60% glycerin/water spray atomizing with nozzle N1 at different pressures.

Z(mm)	N1 – 60% glycerin - 500PSI	N1 – 60% glycerin - 700PSI	N1 – 60% glycerin - 900PSI
0	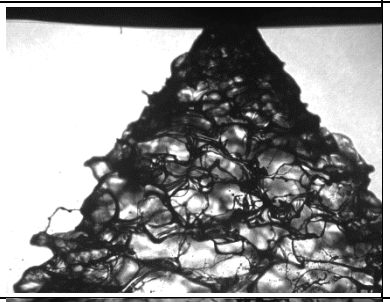	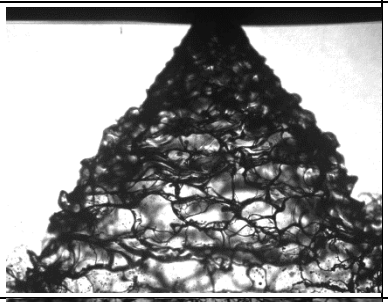	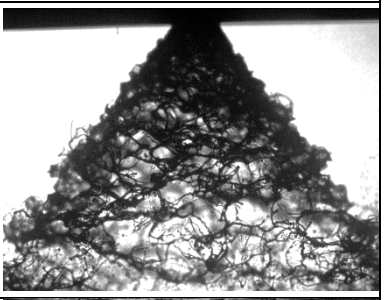
4.98	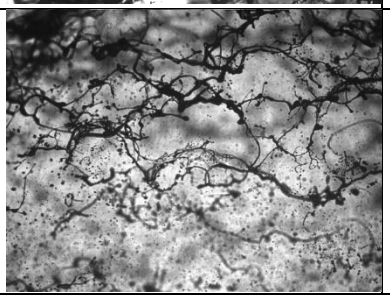	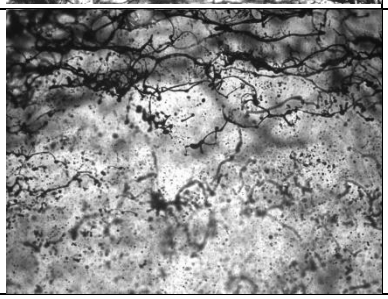	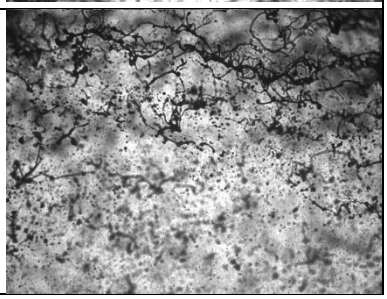

Table A7 shows the images of spray with 80% glycerin/water solution for atomizing with nozzle N1 at different pressures. The edge of the cone at the nozzle exit is smooth due to the high viscosity of the fluid. At 4.98 mm downstream, the amplitude of the wave crests starts to increase and the wave crests becomes thicker. In addition, the distance between the two consecutive wave crests increases. Take the spray atomizing at 700 psi as an example. It can be measure in the frame at 9.96 mm downstream that the distance between two wave crests is about 2 mm, which is much larger than the Kelvin-Helmholtz wavelength (481 μm). Compared to the lower viscosity cases, the thicker span-wise rims are more aligned in the horizontal direction.

Table A7: Near nozzle images for 80% glycerin/water spray atomizing with nozzle N1 at different pressures.

Z(mm)	N1 - 80% glycerin - 500PSI	N1 - 80% glycerin - 700PSI	N1- 80% glycerin - 900PSI
0	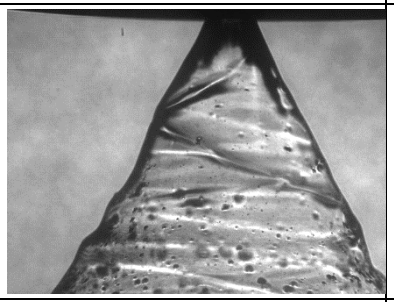	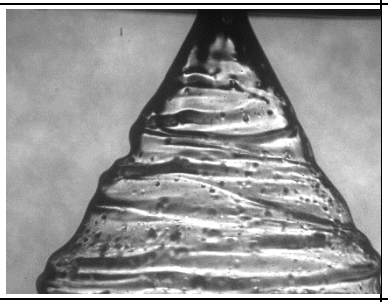	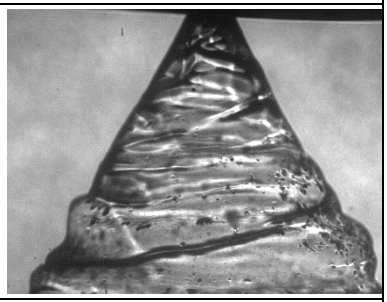
4.98	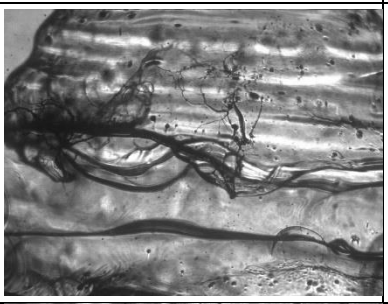		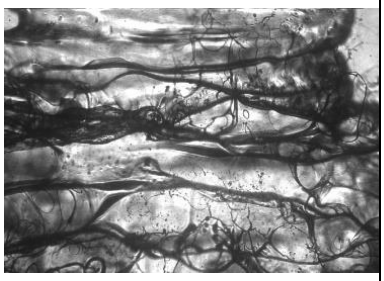
9.96	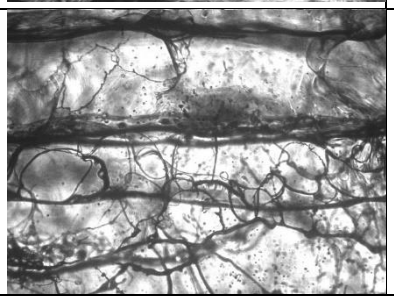	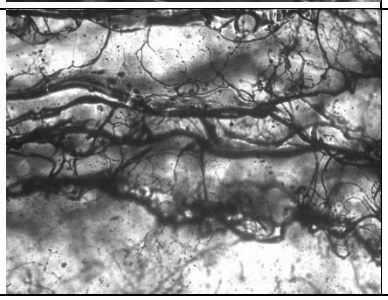	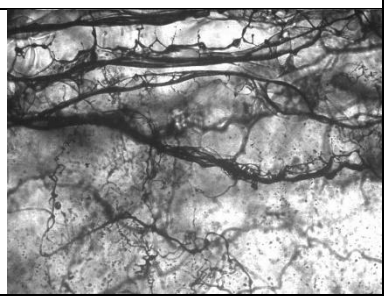

Table A8 shows the images of spray with 0.25% CMC/water solution for atomizing with nozzle N1 at different pressures. Compared to water and 60% glycerin solution, the conical sheet does not perforate until about 6 mm downstream. Compared to 80% glycerin, the sheet is wavier and the wavelength is smaller. The liquid sheet still breaks up due to perforations on the sheet. However, the streamwise ligaments do not break immediately as shown at 9.96 mm downstream for all the cases. There are almost no droplets generated at this position and the streamwise ligaments are stretched and entangled with the spanwise ligaments. It will take longer time for the web of ligaments breaks completely into the droplets.

Table A8: Near nozzle images for 0.25% CMC/water spray atomizing with nozzle N1 at different pressures.

Z(mm)	N1 - 0.25% CMC - 500PSI	N1 - 0.25% CMC - 700PSI	N1- 0.25% CMC - 900PSI
0	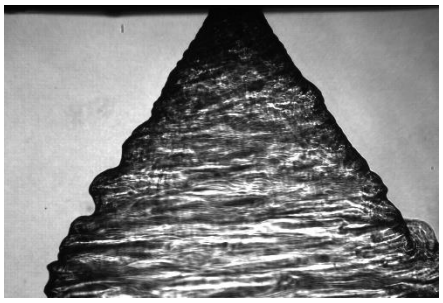	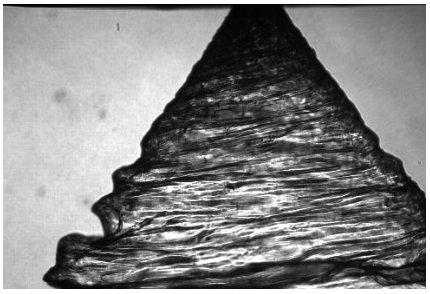	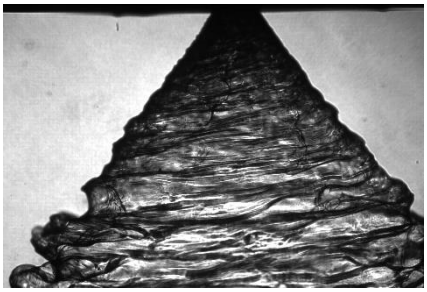
4.98	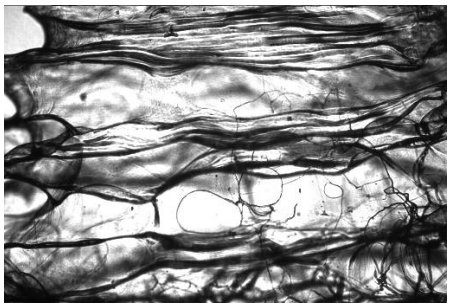		
9.96			

Table A9 shows the images of spray with 0.5% CMC/water solution for atomizing with nozzle N1 at different pressures. Compared to the above-mentioned cases, the injection pressure cannot provide enough inertia forces to counter the viscous force to form a stable air core at the center of the cone. The radius of the cone does not increase proportionally with the distance downstream. This will result in a breakup mechanism in a different regime which is not desired and will generates lots of large droplets (~1mm) as shown in Fig. A2.

Table A9: Near nozzle images for 0.5% CMC/water spray atomizing with nozzle N1 at different pressures.

Z(mm)	N1 - 0.5% CMC - 500PSI	N1 - 0.5% CMC - 700PSI	N1- 0.5% CMC - 900PSI
0	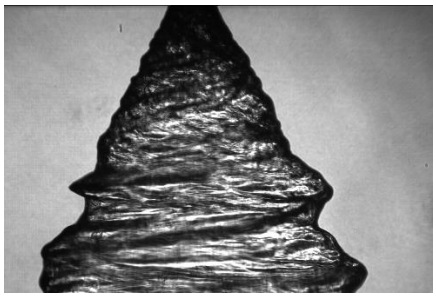	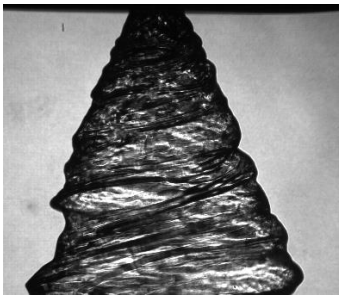	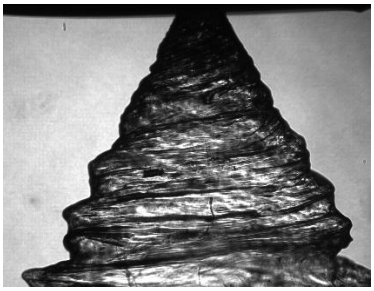
4.98	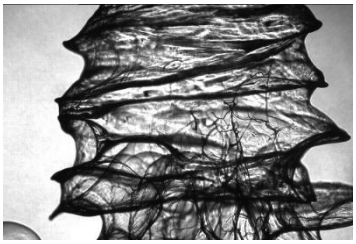		
9.96	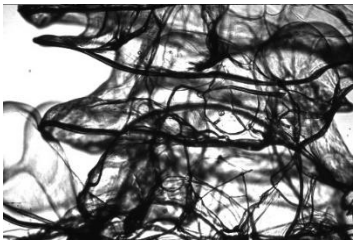		

A.6. Summary

Experiments were performed using two pressure-swirl nozzles with different orifice diameters. Eighteen different operating conditions were tested with high injection pressure (up to 900 psi) and high viscosity fluids (up to 60 mPa.s). The droplet sizes distribution and other statistics were measured using Malvern Spraytec Dropsizer at 80 mm downstream from the nozzle exit. In addition, images at the near nozzle region (within 20mm from the nozzle exit) were taken to study the breakup mechanism of the liquid sheet. The conical liquid sheet was found to break up due to the perforation growth on the thin region between the wave crests of the Kelvin-Helmholtz surface wave. This resulted in a much shorter breakup length compared to the prediction made in the popular LISA model, especially for the high viscosity cases. Two different breakup mechanisms were identified from the near nozzle images: the thick span-wise ligaments generated by the thick wave crests forms large droplets and the thin stream-wise ligaments generated by perforation on thin sheet between wave crests forms small droplets. The mixture distribution with lognormal distributions were found to fit the experimental data best and it made good predictions on the d_{32} of the sprays.

References

Bhatia, J., Domnick, J., Durst, F., & Tropea, C. ,1988. Phase ‐ Doppler ‐ Anemometry and the Log ‐ Hyperbolic Distribution applied to Liquid Sprays. *Particle & Particle Systems Characterization*, *5*(4), 153–164.

Clark, C. and Dombrowski, N., 1972. Aerodynamic instability and disintegration of inviscid liquid sheets. Proceedings of the Royal Society of London. A. Mathematical and Physical Sciences, 329(1579), pp.467-478.

Cousin, J., Yoon, S.J. and Dumouchel, C, 1996. Coupling of classical linear theory and maximum entropy formalism for prediction of drop-size distribution in sprays: application to pressure swirl atomizers. *Atom. Sprays*, *6*, pp. 601-622.

Dombrowski, N. and Johns, W., 1963. The aerodynamic instability and disintegration of viscous liquid sheets. Chemical Engineering Science, 18(7), p.470.

Dumouchel, C, 2006. A new formulation of the maximum entropy formalism to model liquid spray drop-size distribution. Part. Part. Syst. Charact, 23, pp. 468-479.

Dumouchel, C., Yongyingsakthavorn, P., & Cousin, J., 2009. Light multiple scattering correction of laser-diffraction spray drop-size distribution measurements. International Journal of Multiphase Flow, 35(3), pp. 277–287.

Glycerin Producers'Association, 2006. Physical properties of glycerine and its solutions. Glycerine Producers' Association, New York.

Jazayeri, S. and Li, X., 2000. Nonlinear instability of plane liquid sheets. Journal of Fluid Mechanics, 406, pp.281-308.

Kolmogorov A. N. ,1941. On the logarithmic normal distribution law of particles with dimensions of fragmentation. Dok. Acad. Nauk SSSR, 31, 99.

Li, X.; Tankin, R.S, 1987. Droplet size distribution: a derivation of a nukiyama-tanasawa type distribution function. Comb. Sci. Technol. 56, pp. 65-76.

Loustalan, P., Davy, M., and Williams, P., 2003. Experimental Investigation into the Liquid Sheet Break-Up of High-Pressure DISI Swirl Atomizers, SAE Technical Paper 2003-01-3102.

Nukiyama, S. and Tanasawa, Y.,1939. An Experiment on the Atomization of Liquid : 3rd Report, On the Distribution of the Size of Droplets. Trans. Soc. Mech. Eng. Jpn. 5, pp. 131-135.

Park, K., and Heister, S., 2010. Nonlinear modeling of drop size distributions produced by pressure-swirl atomizers. International Journal of Multiphase Flow, 36(1), 1–12.

Schmidt, D.P., Nouar, I., Senecal, P.K., Rutland, C.J., Martin, J.K., Reitz, R.D., 1999. Pressure-swirl atomization in the near field, SAE Technical Paper Series 1999-01-0496.

Sellens, R.W., 1987. Drop Size and Velocity Distributions in Sprays. A New Approach Based on the Maximum Entropy Formalism. Ph.D. Thesis, University of Waterloo, Ontario.

Sellens, R.W. and Brzustowski, T.A, 1985. A prediction of the drop-size distribution in a spray from first principles. Atom. Spray Tech., 1, pp. 89-102.

Sellens, R.W. and Brzustowski, T.A, 1986. A simplified prediction of droplet velocity distribution in a spray. Comb. Flame, 65, pp. 273-279.

Senecal, P., Schmidt, D., Nouar, I., Rutland, C., Reitz, R. and Corradini, M., 1999. Modeling high-speed viscous liquid sheet atomization. International Journal of Multiphase Flow, 25(6-7), pp.1073-1097.

Sindayihebura, D. and Dumouchel, C.,2001. 3. Pressure atomiser: Hole breakup of the sheet. Journal of Visualization, 4(1), 5–5.

Stapper, B., Sowa, W. and Samuelsen, G., 1992. An Experimental Study of the Effects of Liquid Properties on the Breakup of a Two-Dimensional Liquid Sheet. Journal of Engineering for Gas Turbines and Power, 114(1), pp.39-45.

Tratnig, A. and Brenn, G., 2010. Drop size spectra in sprays from pressure-swirl atomizers. International Journal of Multiphase Flow, 36(5), pp.349-363.

Van Der Geld, C.W.M. and Vermeer, H., 1994. Prediction of drop size distributions in sprays using the maximum entropy formalism: the effect of satellite formation. International Journal of Multiphase Flow 20, 363–381.

VILLERMAUX, E. 2007 Fragmentation. Annu. Rev. Fluid Mech. 39, 419–446.

Villermaux, E., Marmottant, P., Duplat, J., 2004. Ligament-mediated spray formation. Phys. Rev. Lett. Vol. 92, Issue 7,pp. 745011-745014.

Vijay, G., Moorthi, N. and Manivannan, A., 2015. INTERNAL AND EXTERNAL FLOW CHARACTERISTICS OF SWIRL ATOMIZERS: A REVIEW. Atomization and Sprays, 25(2), pp.153-188.

Wang, X. F., and Lefebvre, A. H., Atomization Performance of Pressure Swirl Nozzles, AIAA Paper, 1986.

Weber, C., Zum Zerfall eines Flüssigkeitsstrahles. Z. Angew. Math. Mech. 11, 136–154, 1931.

Yongyingsakthavorn, P.; Cousin, J.; Dumouchel, C.; Hélie, J. Piezo-Spray Drop-Size Measurements by Laser-Diffraction Technique in the Presence of Multiple Scattering Effects. In Proceedings of the ILASS-Europe 2008, Paper ID ILASS08-070, Como Lake, Italy, September 2008.

Appendix B - Twin-Fluid Nozzle

B.1. Benchmark data set: Two-fluid nozzles

To best support the analysis in Objective 2, we have focused on planar, external mixing two-fluid nozzles. That is, nozzles where the atomization occurs at the exit plane of the nozzle where it can be easily viewed and imaged. We have chosen the 1/4J external mixing family of nozzles from Spraying Systems Co., as their modular design allows for many nozzle geometries across a wide range of scales. Figure B1 shows the exploded view of this nozzle setup along with the relevant dimensions being controlled. These dimensions are the liquid orifice diameter, D_l, and the gas annulus inner and outer diameters, $D_{g,i}$ and $D_{g,o}$, that determine the gas annular thickness, b_g, which is commonly used in many analyses.

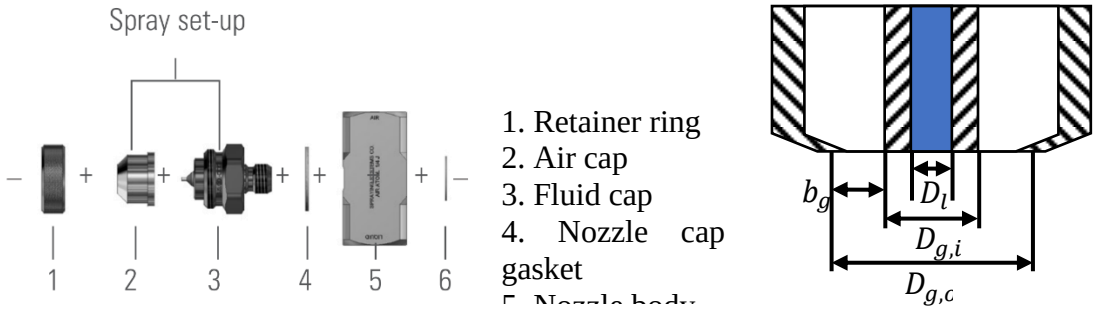

Figure B1: Exploded view and relevant dimensions of Spraying Systems Co. 1/4J external mixing two-fluid nozzle.

The two components that can be changed to alter the nozzle geometry are the fluid cap and air cap. Table B1 tabulates the fluid and air caps used in the present study with their related dimensions, as well as the standard setup configurations recommended by Spraying Systems Co. The 2050 and 2850 fluid caps are representative of typical lab-scale two-fluid atomizers ($D_l < 1$ mm), while the 60100 fluid cap is representative of production-scale two-fluid atomizers ($D_l > 1$ mm). While many nozzle permutations are available, we have focused specifically on the 2050-70 and 2850-70 setups for the lab-scale tests and the 60100-120 setup for the production scale. Comparing these setups allows us to isolate the effect of changing only D_l while keeping b_g constant. D_l is a stronger governing factor as it alters the interfacial area between the liquid and air streams, while b_g primarily serves to change the gas speed for a given flow rate, which is already being controlled directly via the flow rate.

Table B1: Spraying Systems Co. 1/4J external mixing two-fluid nozzle dimensions (in mm) and setups

Fluid Caps	D_l	$D_{g,i}$	Air Caps	$D_{g,o}$	Tested Standard Setups
2050	0.51	1.27	70	1.78	2050-70
2850	0.71	1.27	120	3.05	2850-70
60100	1.52	2.55			60100-120

The testing carried out in this project has captured both the droplet (or particle) size distribution (PSD), as well as near-nozzle images (NNI) and has consisted of three phases: 1. Water tests as

the baseline inviscid fluid, 2. Aqueous glycerin mixtures as a baseline for viscous fluids, and 3. Aqueous polymeric fluids, consisting of PEG 4000 (a viscous Newtonian polymer) and CMC (a shear-thinning non-Newtonian polymer). The tested mixture ratios and their viscosities are tabulated Table B2.

Table B2: Fluid viscosities

	Fluid	Wt.%	Viscosity [mPa.s]
Baseline inviscid	Water		1
Baseline viscous	Glycerin (aq.)	60	12
		85	148
		90	213
Newtonian Polymer	PEG 4000 (aq.)	20	6.2
		30	14.2
Non-Newtonian Polymer (shear-thinning)	CMC (aq.) [1]	0.25	>20-15
		0.5	>40-30

Note that the viscosities of the CMC mixtures are the expected viscosities based on ref. [1]; however, testing performed in the Rheology Laboratory and the University of Toronto using similar equipment have not provided results consistent with ref. [1]. The tested values suggest a Newtonian behaviour and a much lower viscosity. The measurements indicate a Newtonian behaviour with a considerably lower viscosity than expected; however, our spray testing indicates that the CMC mixtures behave as if they have a much higher viscosity, even than that reported by [1], similar to that of the 85% glycerin mixture. This can be seen in Figure B2, where the sprays of water, 60% glycerin, 85% glycerin, and 0.25% CMC mixtures are compared.

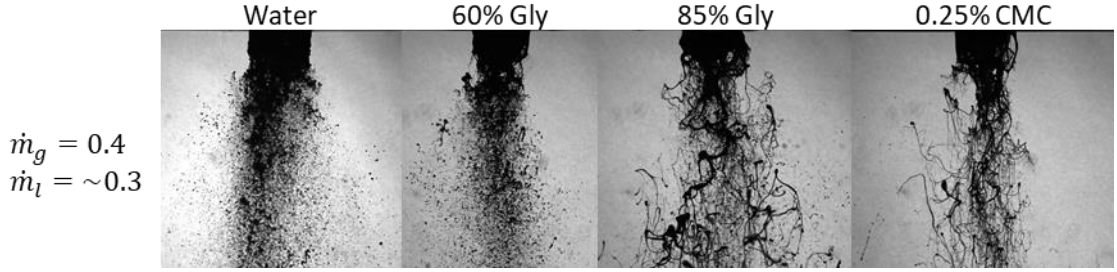

Figure B2: Comparison of water and glycerin mixtures to 0.25% CMC mixture

The more viscous the spray is, the more pronounced the ligaments become. If the CMC mixture really had a viscosity closer to that measured or reported in [1], then it would be expected to behave similarly to the 60% glycerin mixture; however, it clearly behaves more like the much more viscous 85% mixture. We suspect this is due to the CMC mixture exhibiting a much higher extensional viscosity, which would not be apparent in the measurement method implemented in [1] or in our own rheology measurements. We are still working to find an accessible measurement of the extensional viscosity to verify our theories.

Although previous studies have focused typically on mean spray statistics, such as the Sauter Mean Diameter (SMD), a significant drawback of these statistics is that they do not describe the distribution of the spray, particularly, it's modality. Real-world sprays, especially viscous ones, produce wide, multi-modal distributions. Although the SMD can provide a reasonable prediction of some trends, it does not tell the full story of the spray distribution.
NNI's of the glycerin mixture sprays at two selected conditions (one at low flow rates and one at high flow rates) using the pilot-scale (2850-70) and production scale (60100-120) nozzles are shown in Figure B3 and Figure B4, respectively.

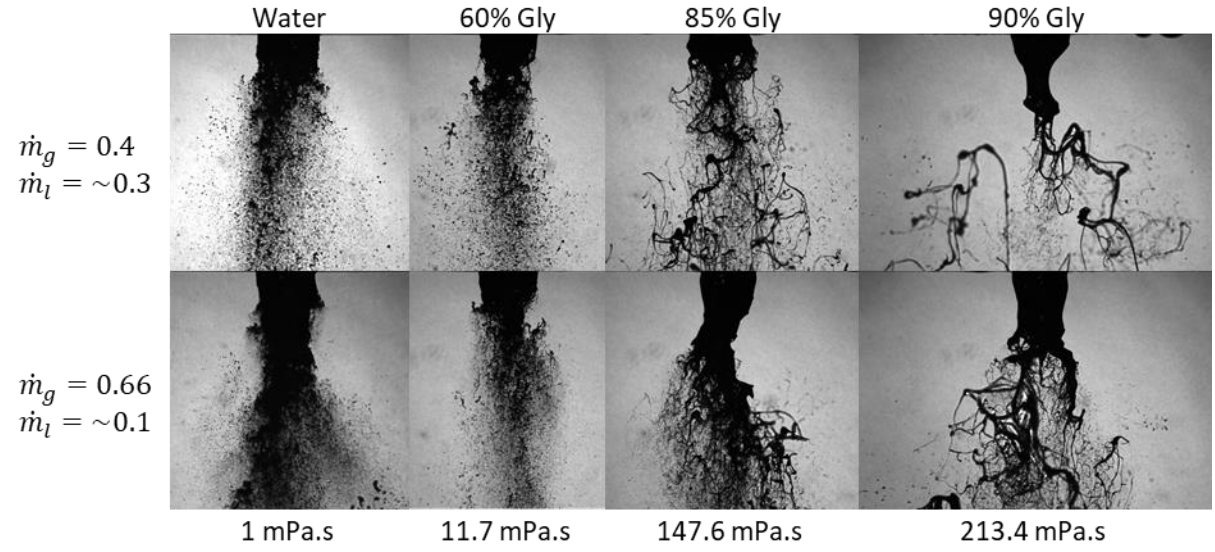

Figure B3: Images of pilot-scale spray for water and glycerin mixtures at low (top) and high (bottom) flow rates.

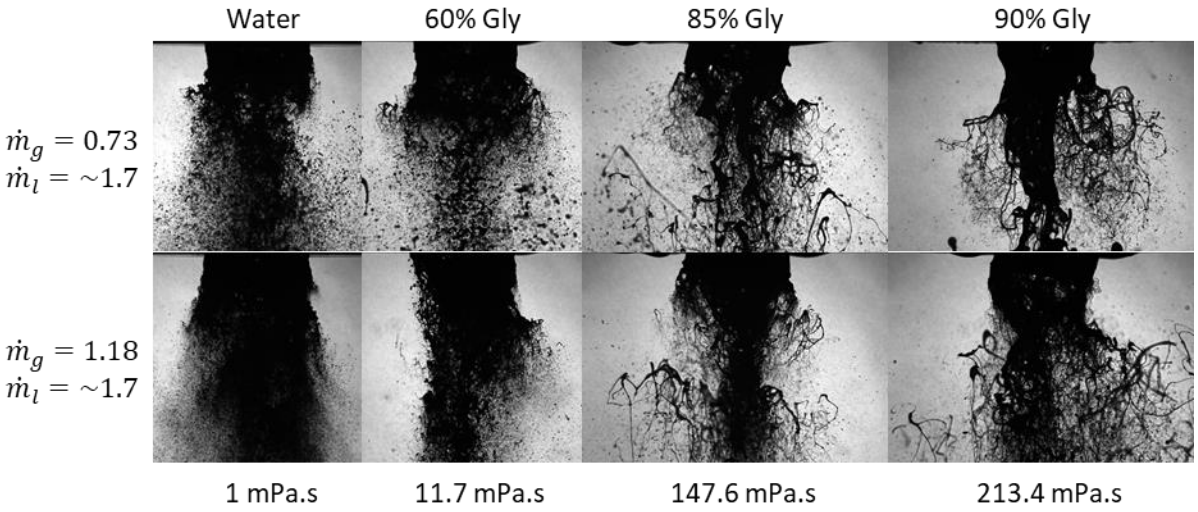

Figure B4: Images of production-scale spray for water and glycerin mixtures at low (top) and high (bottom) flow rates.

The measured PSDs for the water and glycerin mixtures at varying flow conditions using the pilot-scale (2850-70) and production scale (60100-120) nozzles are shown in Figure B5 and Figure B6, respectively.

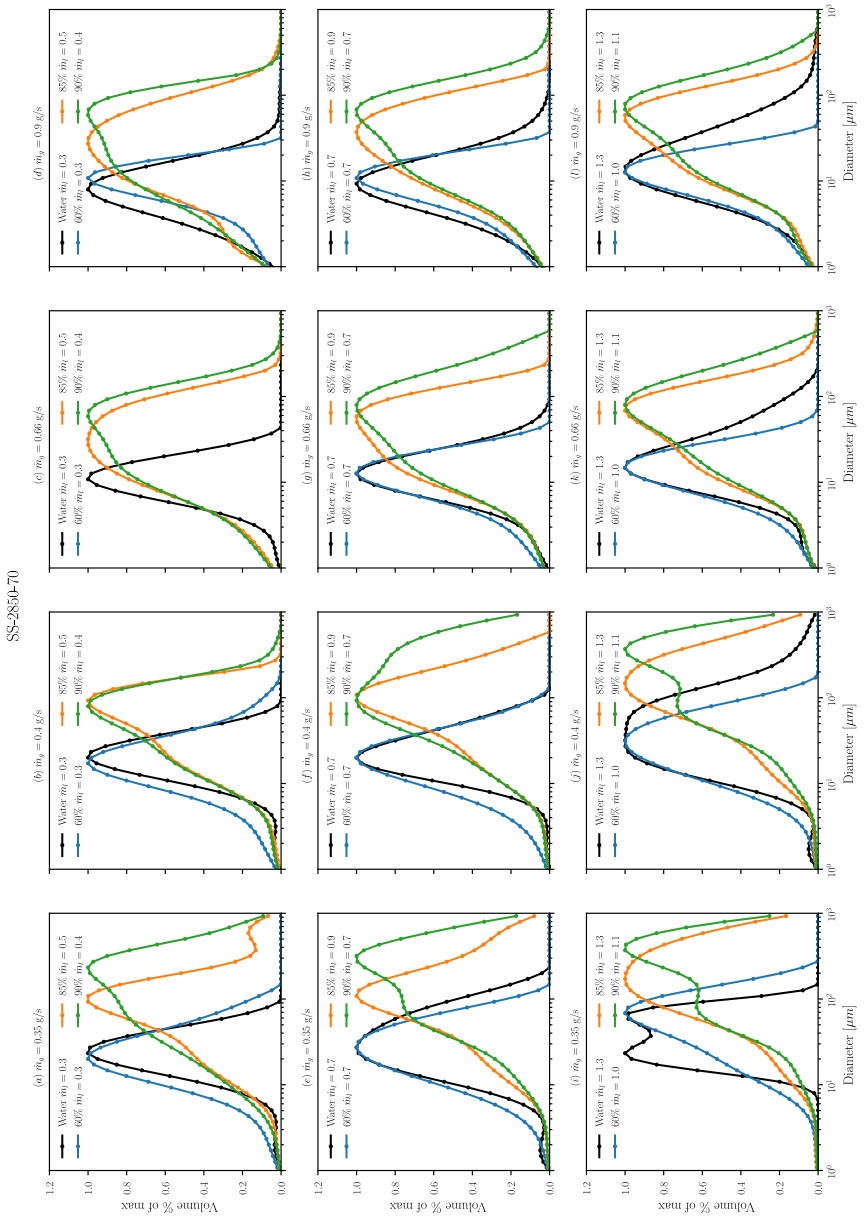

Figure B5: PSDs for water and glycerin mixtures at varying flow rates for pilot scale nozzle

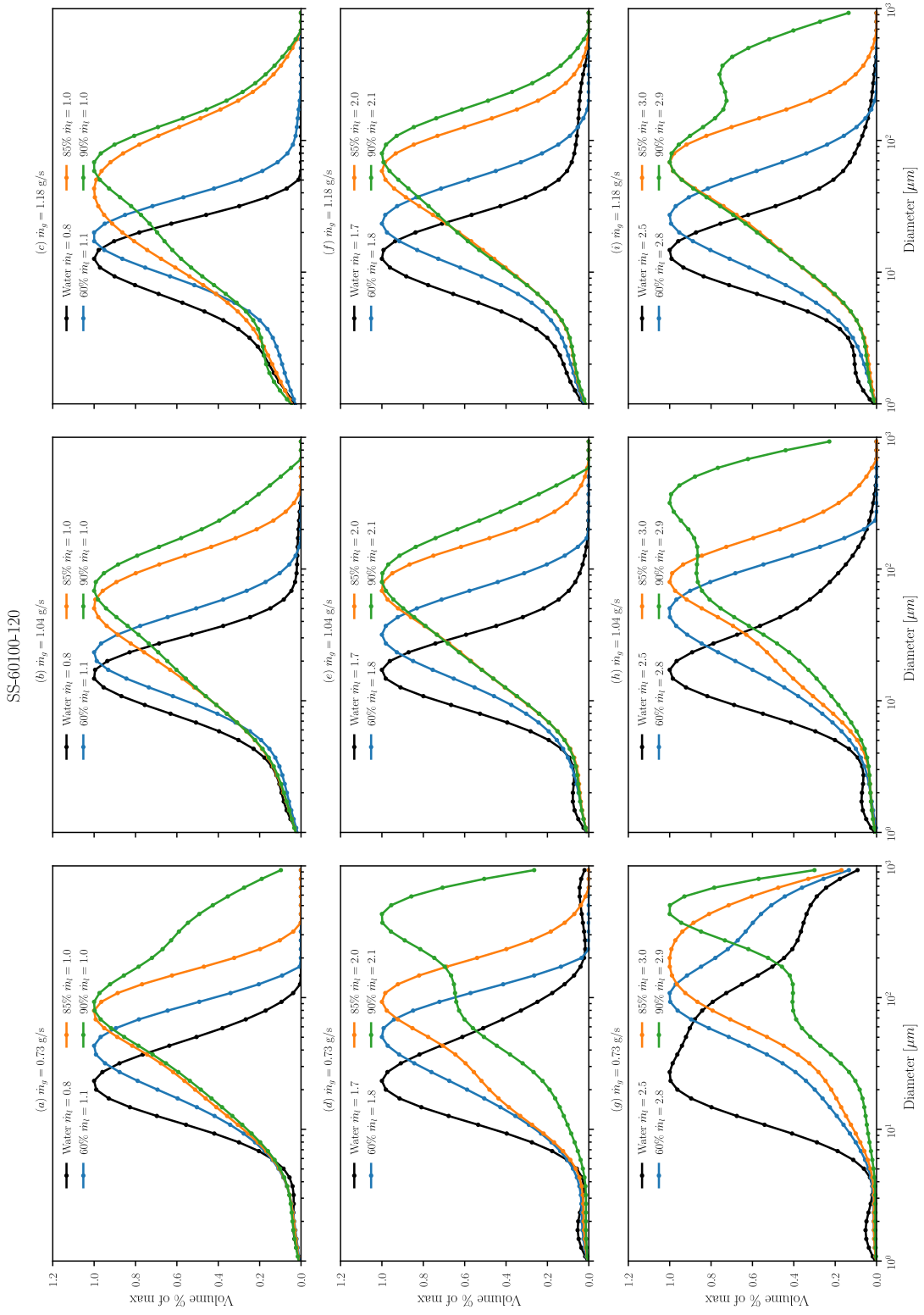

Figure B6: PSDs for water and glycerin mixtures at varying flow rates for production scale nozzle

B1.1 Measurement of ligament sizes

In addition to acquiring the PSD of the droplets from the spray, the NNI's were collected to provide a visualization of the atomization process, as well as to provide an opportunity to measure the ligaments that are prevalent in viscous sprays. While we had hoped to develop automated image processing algorithms to provide an extensive characterization of the ligaments, attempts to do so were not successful due to the complexity of the ligament networks. As a first step towards quantifying the ligament sizes, we have measured their thicknesses manually from images, randomly selecting ligaments and locations on them at which to take the measurements across 200 images. Such a measurement campaign is very time intensive, thus the same measurements for other liquids and nozzles are still in progress. The results of the ligament measurements for the water (inviscid) base case at varying gas and liquid flow rates for the 2850-70 nozzle are presented in figure below. Although these measurements are for an inviscid fluid at low gas flow rates, these conditions provide a dynamically similar spray to the more viscous case and provide a good basis for comparing our theoretical models for the formation of the ligaments independent of the viscous effects. Note that we have independently measured the ligaments generated immediately at the surface of the liquid jet, as well as those that result from the breakup of the bulk of the liquid jet. The ligaments generated at the surface of the jet are typically smaller than those generated in the breakup of the bulk of the jet.

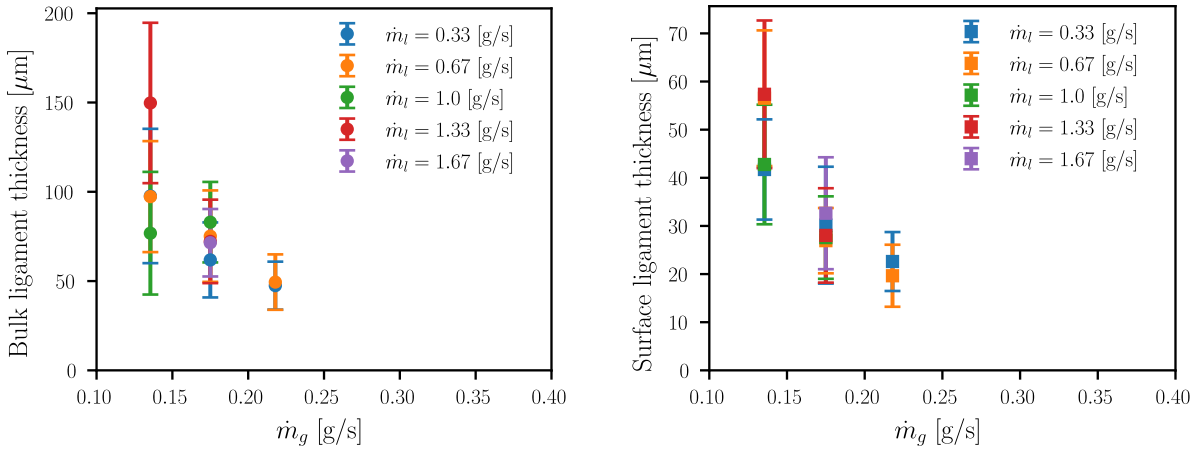

B.2. Correlations for nozzle scaling, size distribution

When developing correlations for sprays, it is important for the correlation to consider the phenomenology of the spray. One of the key factors for developing correlations for two-fluid atomization, therefore, is the morphology of the spray, which depends on the operating conditions of the nozzle. While various researchers classify these morphologies differently, the two morphologies of interest in the present work are membrane-type breakup and fiber-type breakup [2], which are shown in Figure B7.

Membrane-type breakup

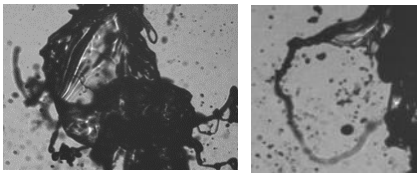

Fiber-type breakup

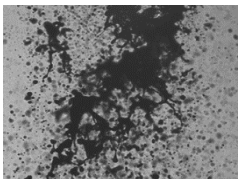

Figure B7: Example images of membrane- and fiber-type breakup

Previous studies have shown empirically that the breakup morphology can be categorized in terms of the Weber number (We) and the Ohnesorge number (Oh) [2,3]. We number describes the competition between the flow inertial and the surface tension forces, while Oh relates the viscous forces to the same. Fiber-type breakup occurs at higher We than membrane-type breakup, although as Oh increases, the We at which this transition occurs increases, as higher aerodynamic forces are required to overcome the damping viscous forces.

$$We = \frac{\rho_g U^2 d_0}{\sigma}, \qquad Oh = \frac{\mu_l}{\sqrt{\rho_l \sigma d_0}},$$

The existing analytical models for two-fluid atomization are focused on the fiber-type breakup morphology [4,5] as this morphology typically provides the smallest droplet sizes and a mono-modal droplet size distribution. However, for very viscous fluids, this morphology is not easily attainable as the gas velocities required are supersonic. Achieving these conditions requires specialized nozzle geometry and a very high consumption rate of the atomizing gas. No analytical models exist for the membrane-type breakup morphology, even for low viscosities. Importantly, the existing models do not predict the formation of the ligament networks characteristic of these types of breakup. This is further complicated by the need for the prediction of the size distribution, as the existing models are based only on one mechanism in the breakup, which in turn gives only a single size prediction that is typically related to the SMD. To model the distribution of the breakup, particularly for multi-modal distributions, multiple modes and mechanisms of breakup must be considered. This is evident in Figure B8 and Figure B9, where the sprays for varying glycerin mixtures (varying viscosity) are compared. The water and 60% glycerin cases exhibit similar morphologies (fiber-type breakup), which result in similarly shaped PSDs, while the 85% and 90% glycerin mixtures show a different morphology (membrane-type breakup), and exhibit much wider and multi-modal distributions.

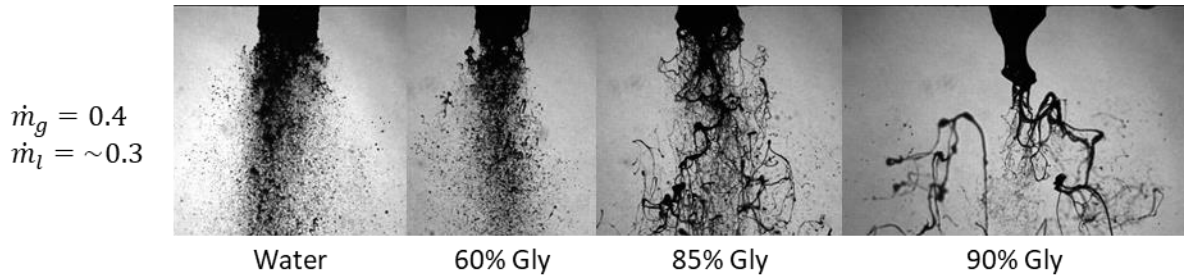

Figure B8: images of sprays at varying viscosities. Water and 60% glycerin solutions exhibit a similar morphology to each other, while the 85% and 90% glycerin mixtures exhibit a different morphology.

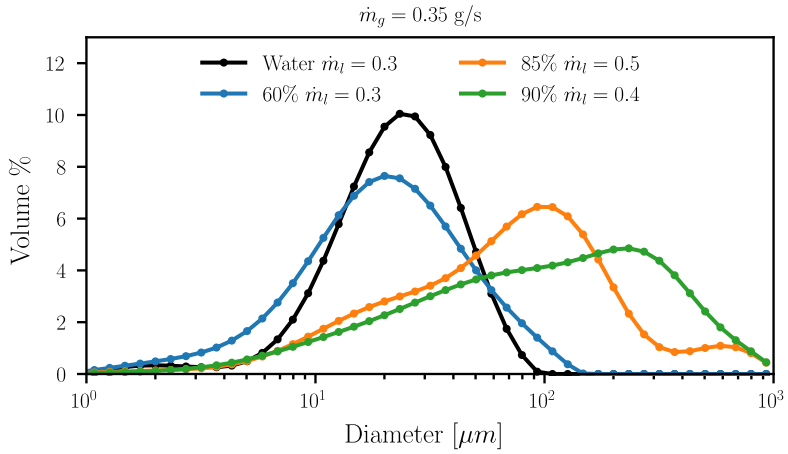

Figure B9: Size distributions for the cases in figure 3.

The two-fluid atomization process has been likened to the breakup of droplets in a high-speed airflow, which also exhibit various morphologies with We and Oh, such as bag or membrane-like morphologies at low We. Many of the existing analytical models for sprays use droplet breakup models to handle the breakup of the surface waves that form on the liquid jet [4,5], however droplet breakup modelling is also limited to the high We morphologies [6,7] which do not relate to the membrane-type morphology of interest in high viscosity atomization where ligament networks are formed. To formulate an analytical model for the breakup of a high-viscosity jet, it is therefore necessary to first model the breakup of inviscid drops and sprays in a way that models the formation of the ligament networks, and how the generated ligament networks break by a variety of mechanisms.

Therefore, the steps for the development of the two-fluid spray correlation are as follows:

1. Develop a model for inviscid droplet breakup, focusing on bag-type morphologies
    a. Formation of ligaments
    b. Breakup of ligaments into a distribution of sizes
2. Modify the droplet model for the geometries of inviscid two-fluid spray atomization
3. Modify the spray model to incorporate:
    a. High viscosity
    b. Elevated temperatures

B.2.1. Droplet breakup

B.2.1.1 Ligament formation

In our paper "On aerodynamic droplet breakup" [8], we presented a detailed study of the dynamics that lead to the ligament formation in droplet breakup. We showed how the initial expansion of the windward droplet face follows a linear relationship modelled by

$$\frac{\dot{d}}{d_0} = \frac{1.125}{\tau}\left(1 - \frac{32}{9We}\right).$$

This expansion of the windward droplet face results in the formation of a windward disk in front of an undeformed core. The windward disk goes on to form the rim and bag, while the undeformed core may go on to form a stamen or undergo its own breakup following the breakup of the windward disk. The expansion rate of the windward disk, in addition to a balance with the surrounding air flow, results in it forming a rim of thickness

$$\frac{d_i}{d_0} = \frac{4}{\frac{\rho_l \dot{d}^2 d_0}{4\sigma} + 10.4} - 0.05.$$

The windward disk, consisting of the peripheral rim (1) and the thinned sheet (2), and the undeformed core (3) are shown in Figure B10.

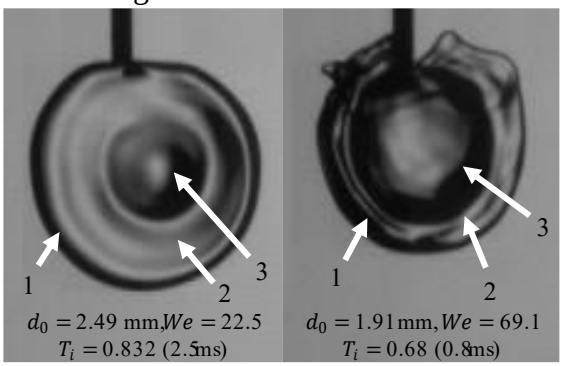

Figure B10: Images of the structures formed in the initial deformation stage for bag and stamen (left) and multibag (right) breakup, showing the rim (1), thinned sheet (2), and core (3).

The rim goes on to form the dominant ligament in the breakup, while the thinned sheet becomes the bag(s). If the core undergoes its own breakup, as in multi-bag or sheet-thinning breakup, it may also form ligaments. Based on the prediction of the rim thickness, the volumes of the windward disk and undeformed core can also be predicted, which are related to the morphology of the droplet breakup. As the bag grows inside of the rim, the bag forces the rim to expand. As the rim expands, it thins to conserve its volume, where the final thickness of the rim will govern the sizes that it breaks into. The bag growth was modelled considering a force balance on the bag tip and was related to the expansion of the rim from the time it was formed to the time it breaks. The nature of the relationship was assumed to be related to the morphology; however, since the work modelled the morphologies as discrete steps instead of continuous transitions, it is simpler to consider an average rim thinning ratio of $d_i/d_f \approx 1/0.64$. Assuming that the rim breaks by the Rayleigh-Plateau capillary instability mechanism, an assumption commonly used in the literature, the rim child droplet size will be given by

$$\frac{d_c}{d_0} = 1.89\frac{d_f}{d_0} = 1.89\left(\frac{d_f}{d_i}\right)\left(\frac{d_i}{d_0}\right).$$

The result is compared to the experimental measurements of the mean rim droplet sizes in Figure B11.

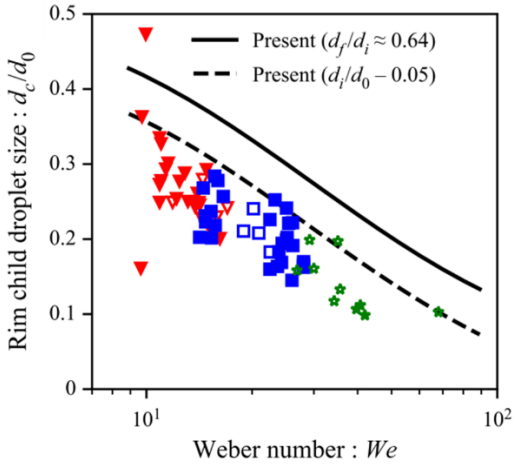

Figure B11: child droplet size vs We in droplet breakup

The results show reasonable agreement to the experiments; however, the prediction is somewhat high. This is due to the assumption that the Rayleigh-Plateau mechanism governs the rim's breakup, as shown in Figure B12. The primary focus of this paper was to model the formation of the rim ligament, which was done successfully. The other mechanisms at play in the breakup of the droplet are discussed in the following section. Note that the factor -0.05 in the equation for d_i/d_0 is an empirical correction for the air-flow separation in the wake of the deformed droplet.

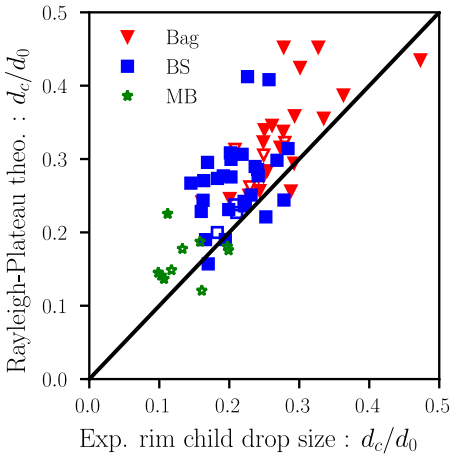

Figure B12: Comparison of the theoretical Rayleigh-Plateau breakup prediction of the rim to the experimental measurements.

B.2.1.2. Ligament breakup and size distribution

In our upcoming work, currently being prepared for submission to the Journal of Fluid Mechanics, we have extended the model for the formation of the rim ligament to include a plethora of breakup mechanisms, each of which contribute to the breakup, with the aim of

predicting for the first time the resulting size distribution of the spray. The main questions addressed in this work are 1. What are the main mechanisms of breakup for the various structures in the droplet, 2. What is the source of variation in these mechanisms that leads to a distribution of sizes, and 3. How can models of these mechanisms be combined to provide a prediction of the overall droplet size distribution.

There are three main geometries that form in droplet breakup that are considered: 1. The nodes that form on the rim of the drop, 2. The bag, and 3. The rim that remains after the nodes have formed.

The nodes that form on the rim are shown in Figure B13. In a previous work [9], the nodes were assumed to form by the Rayleigh-Taylor acceleration instability, and a prediction was made for the number of nodes formed but not the size of the nodes.

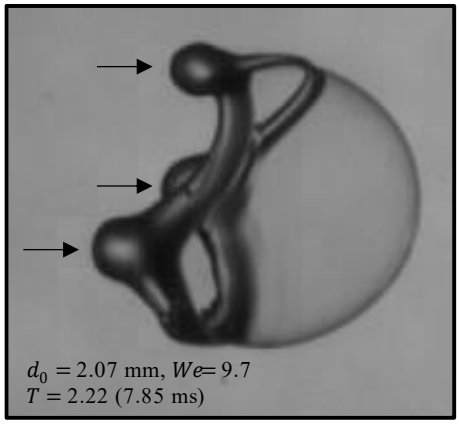

Figure B13: Image of nodes forming on the rim of a droplet undergoing breakup.

In our work, we compared this theory to the Rayleigh-Plateau capillary instability. In these analyses, the previous prediction of d_i/d_0 is used to estimate the rim dimensions at the time the instability takes hold. The two instability theories were found to give comparable results in terms of the predictions for both the number of nodes formed, as well as the resulting size of the droplets. The variation in the node sizes that can form was attributed to local effects that cause more or less of a segment of the rim to flow into the node, rather than remain in the rim. This factor was defined as the node-disk volume fraction, n, defined as the volume fraction of the windward disk that ultimately ends up in the node, and ranges from $n = 0.2 - 1$ with a mean value of $n = 0.4$. The prediction of the node sizes using the Rayleigh-Taylor and Rayleigh-Plateau theories are compared to the experimentally measured node child drop sizes in Figure B14.

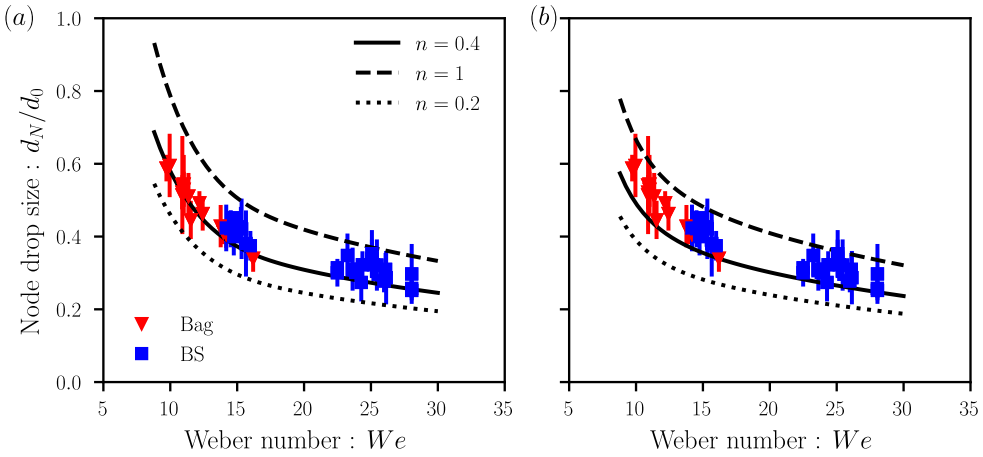

Figure B14: Rayleigh-Taylor (a) and Rayleigh-Plateau (b) predictions for the node child drop size.

The breakup of the bag is difficult to study as its dynamics span over a wide range of scales. The whole bag may form a bubble on the scale of mm, while the bag may have a thickness on the scale of μm, with its breakup taking place in ms, all while the entire drop moves over a few cm. This multi-scale characteristic makes the process difficult to image in a way that all relevant measurements can be made; in particular, the droplets resulting from the breakup of the bag. For this reason, the breakup is described mainly qualitatively, with some modelling used to estimate the characteristic sizes in its breakup. Images of the bursting bag are shown in Figure B15.

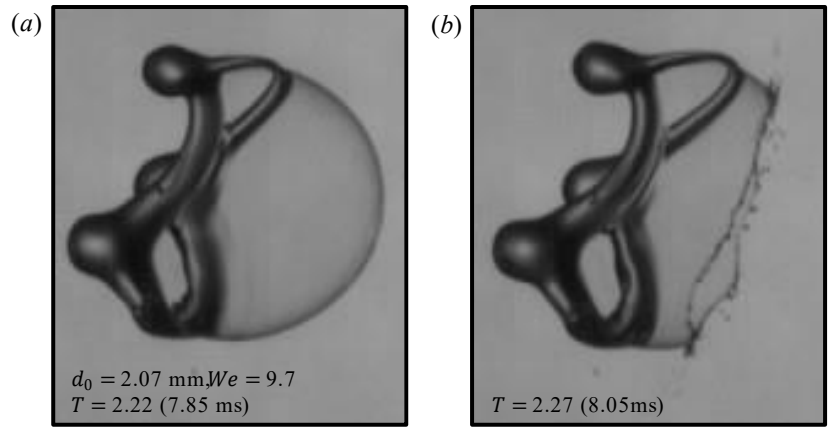

Figure B15: images of the bursting bag

The model of [10], developed for the bursting of static surface bubbles, was found to match the dynamics of the bag very well in terms of its recession speed and the instability at the rim that forms at the perforation of the bag. Using this model, the minimum bag thickness was estimated to be $h_{min} = 2.3 \pm 1.2\ \mu$m. The other relevant sizes in the breakup are the rim thickness, estimated by the model of [10], and its breakup due to capillarity.

As mentioned previously, the breakup of the remaining rim has been assumed to be due to the Rayleigh-Plateau instability; however, this assumption leads to an over-prediction in the average size of the rim drops. By carefully analyzing the breakup phenomenology, we discovered that an additional mechanism in the breakup of the rim is the collision of the receding rim of the bag, as shown in Figure B16.

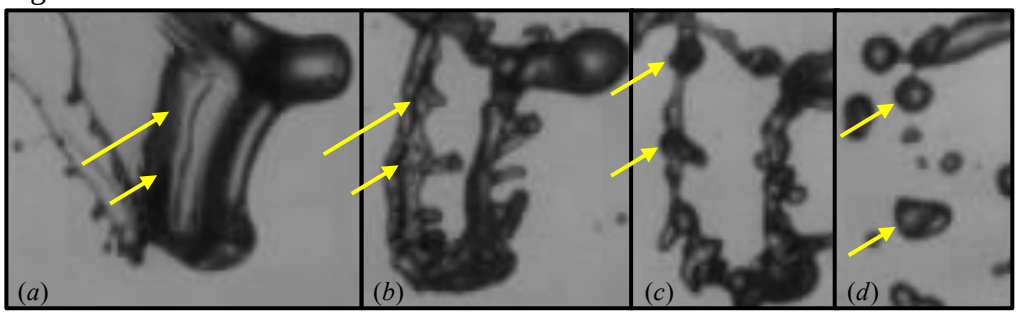

Figure B16: Images of the collision of the receding rim with the main rim of the drop

Since the receding rim is heavily corrugated owing to its own instability, as described previously, it imparts an unequal impulse on the rim, effectively forcing it to break at the same wavelength as the receding rim instability. Variation in this mechanism arises from different collision angles with the rim, which cause the effective imparted wavelength to be longer. At very high collision angles, the force of the collision is insufficient to dominate over the capillary Rayleigh-Plateau mechanism, and so Rayleigh-Plateau breakup can also occur in the breakup of the rim. Figure B17 shows how this variety of mechanisms leads to wide range of breakup sizes, where the Rayleigh-Plateau prediction gives the upper limit of the breakup sizes, the collision mechanism approximately follows the mean sizes, and the satellites resulting from the collision mechanism estimate the lower limit of the breakup sizes of the rim.

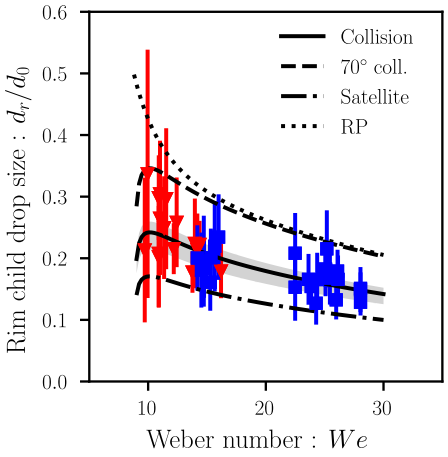

Figure B17: Rim child drop sizes from a variety of mechanisms

The distribution of sizes resulting from breakup is assumed to come from a combination of all of these mechanisms as well as the subtle variations within each mechanism. These mechanisms are are grouped in terms of the primary modes of the breakup (i.e. the geometries within the deformed droplet) such that the overall distribution is the result of the sum of the modes, which

can lead to a multi-modal distribution. While the volume weighting of each mode is determined by models for the volume estimation of each geometry, the relative number weighting of the mechanisms within each mode are assumed to vary as a two-parameter gamma distribution function where the parameters are estimated based on the mean and standard deviation of the predicted sizes for each mechanism within the mode.

In Bag breakup, there are three modes resulting from the rim nodes, the remaining rim, and the bag. The ranges of sizes given by the mechanisms for each of these modes is shown in Figure B18 (a). The resulting combined distribution using the analytical weightings is given in Figure B18 (b). While the location and width of the peaks are reasonably matched by the predicted distribution, the height of the peaks is not so well predicted. This is likely because the particular case being compared is near the transition to the Bag and Stamen morphology, where the breakup may exhibit the `twin-bag' transitional morphology in which a fold appears across the bag dividing it in two owing to the slightly larger mass at the center of the bag due to the small, undeformed core. While this fold primarily affects the bag, it may also have an influence on the rim; in particular, the formation of additional nodes on the rim where it is met by the fold of the bags. The presence of this fold then changes the assumed dynamics of the rim, and thus may reduce the remaining rim's volume more than presently predicted. Figure B18 (c) shows the result using fitted weights, with much better agreement. A better understanding of the transitional behaviour between the morphologies will lead to a better prediction at these conditions.

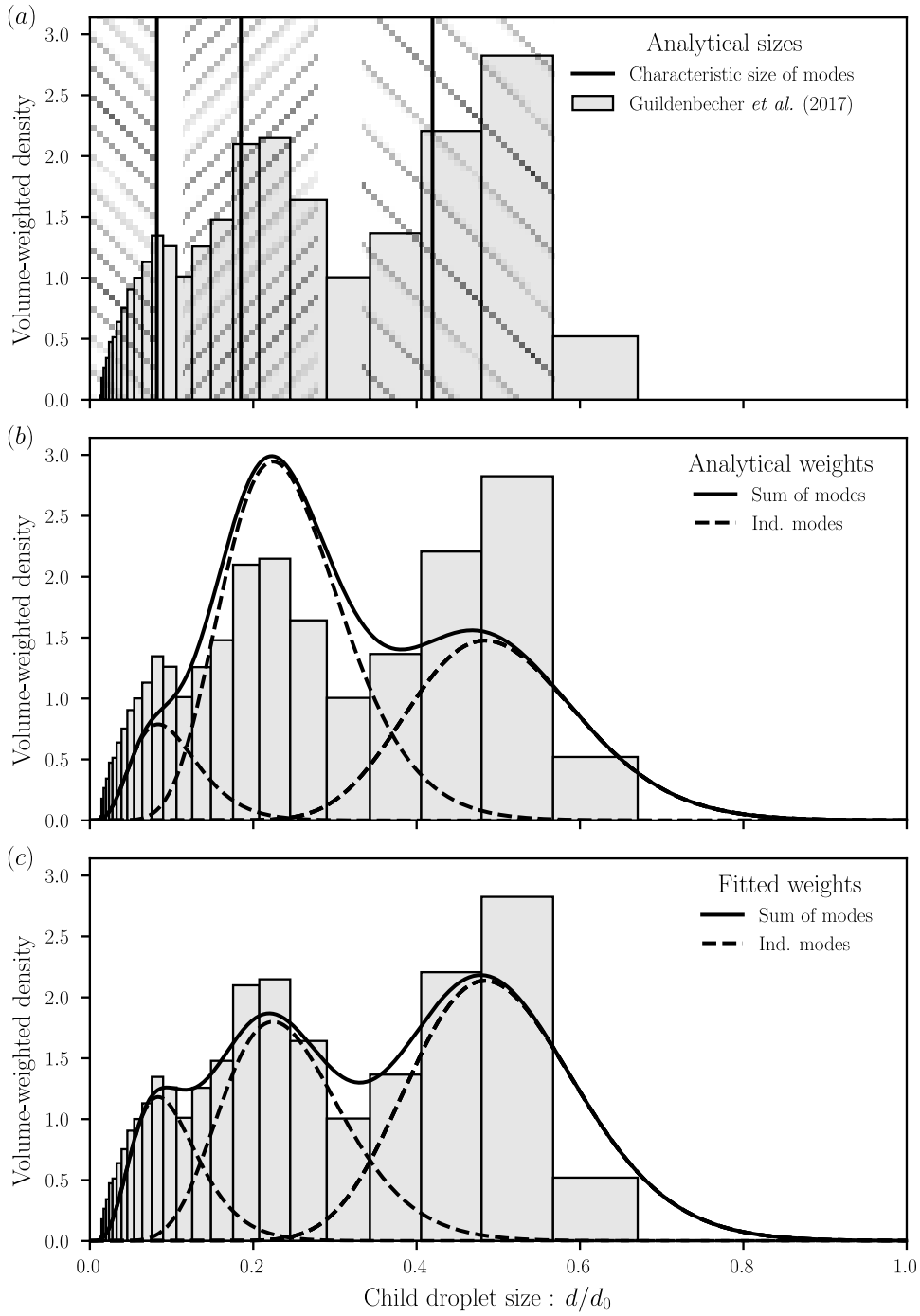

Figure B18: Comparison of distribution prediction to experiments [11] for bag breakup

In multibag breakup, there is the addition of the breakup of the undeformed core, which itself breaks into an additional three modes. Figure B19 (a) shows the resulting distribution considering all six modes of the breakup. Notably, the contributing volume of the bag appears to be over-predicted. This is likely due to the folds between the azimuthal bags being neglected.

The folds between the azimuthal bags leave behind ligaments after the rupture of the bags, which result in sizes similar to the breakup of the rim. As a result, some of the mass of the bag breaks into sizes similar to those of the rim breakup. Since this effect is neglected, the smallest sizes due to the breakup of the bag are over-predicted, while the sizes near the characteristic size of the rim breakup are under-predicted. A better understanding of the dynamics of the bag that lead to the formation of the azimuthal ligaments is needed to improve the present prediction.

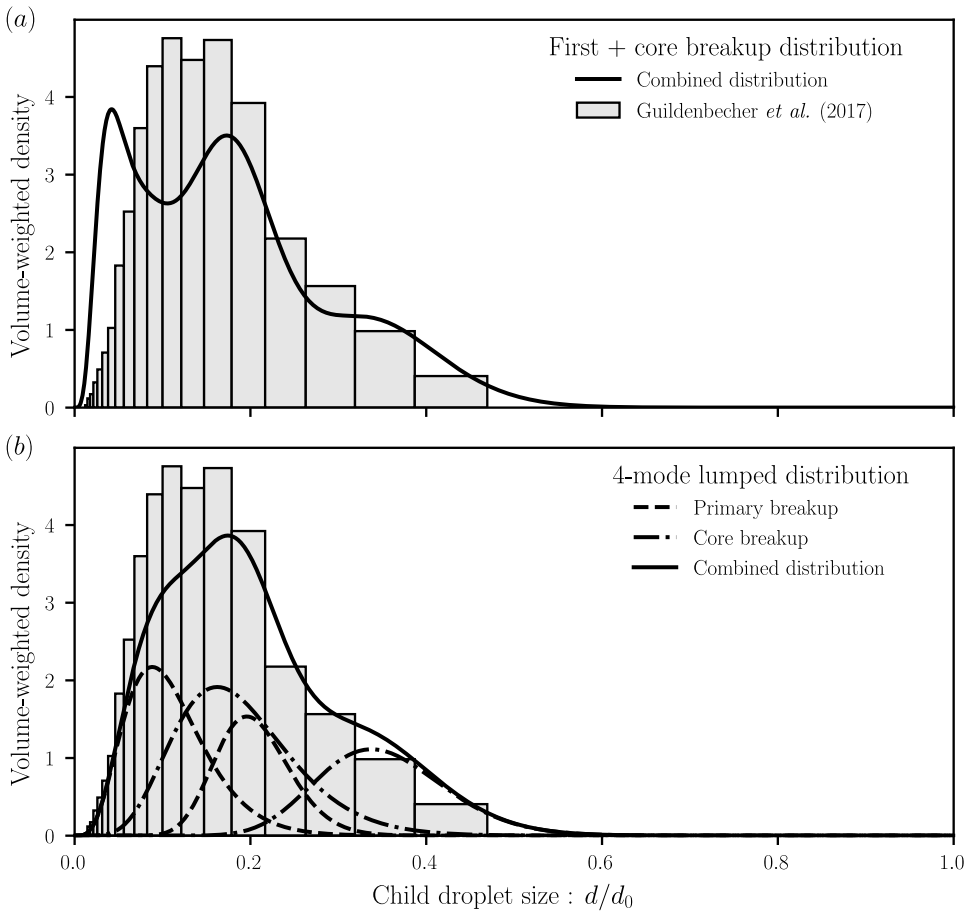

Figure B19: Comparison of distribution prediction to experiments [11] for multi-bag breakup

In multi-bag breakup, several of the modes overlap such that they appear to be monomodal. When this occurs, the weighted mean and standard deviation of the mechanisms contributing to each mode can be used to determine a lumped distribution that captures the overlapping modes as one. This is shown in Figure B19 (b), where the bag and rim modes for both the first and core breakups are lumped together. Since the volume weighting between the bag and rim is what caused the earlier deviation when the modes were treated separately, lumping the modes together somewhat negates this effect.

Figure B20 gives a flowchart of the calculation of the multi-modal distribution.

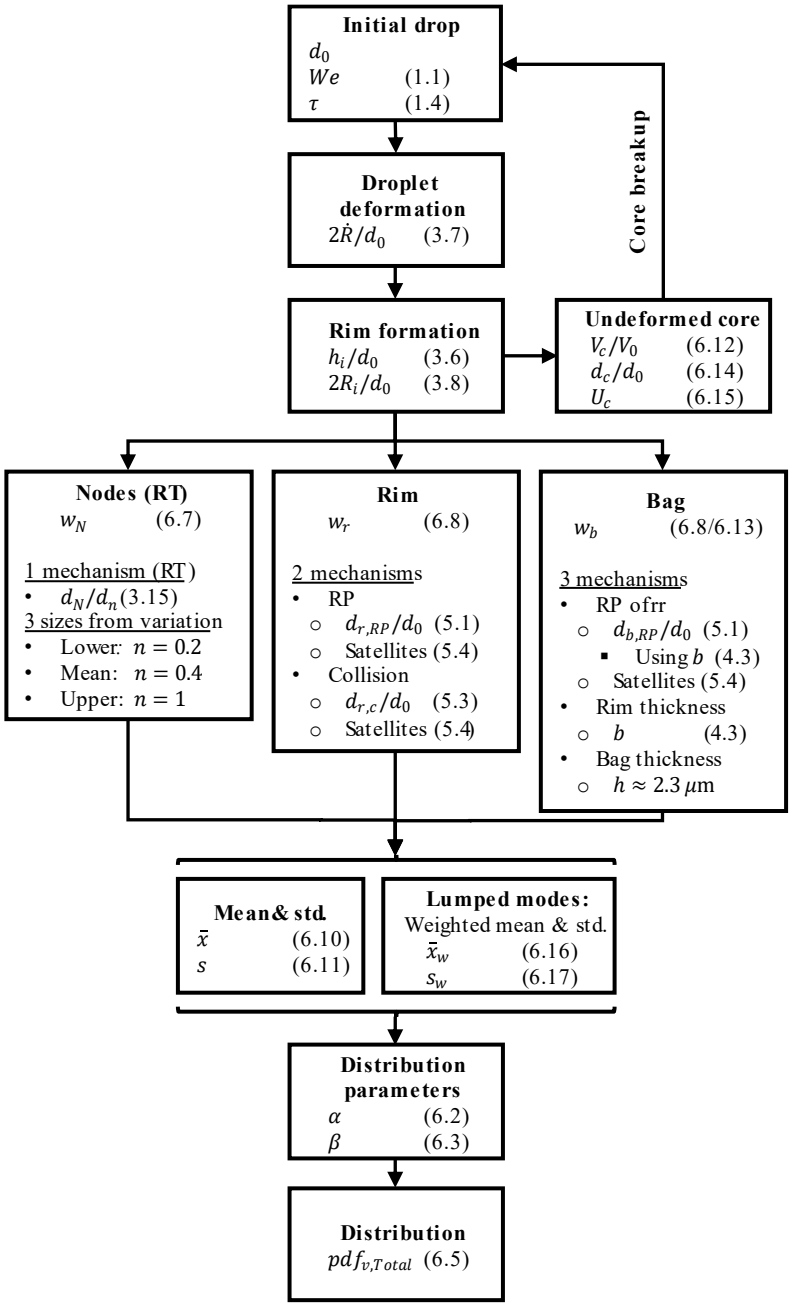

Figure B20: Flowchart of distribution calculation

B.2.2. Extension to two-fluid spray geometry

To extend the droplet breakup models to two-fluid sprays, we first identify the similar geometries that occur in the breakup. Previous works have primarily considered only the varicose surface waves on the liquid jet; however, in practical sprays, the surface waves grow until they start to couple, forming sinuous bulk waves in the liquid jet. Both geometries are susceptible to breakup, as shown in Figure B21.

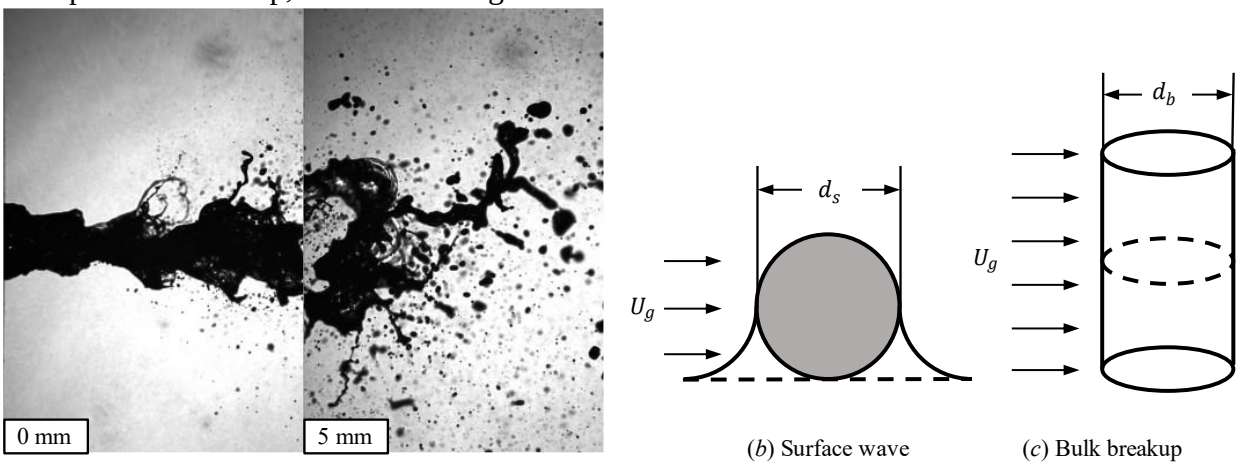

(*a*) Image of spray (*b*) Surface wave breakup geometry (*c*) Bulk breakup geometry

Figure B21: image of spray showing surface and core breakup, and illustrations of the surface wave and core breakup geometries.

The breakup of these geometries is modelled, as a first approximation, by the same model developed for the atomization of a liquid droplet. For the core breakup, the diameter of the liquid jet as it waves into the air flow is assumed to be the diameter of the equivalent droplet. The droplet breakup model for the prediction of the ligament size and characteristic breakup size is compared to the experimental measurements in Figure B22.

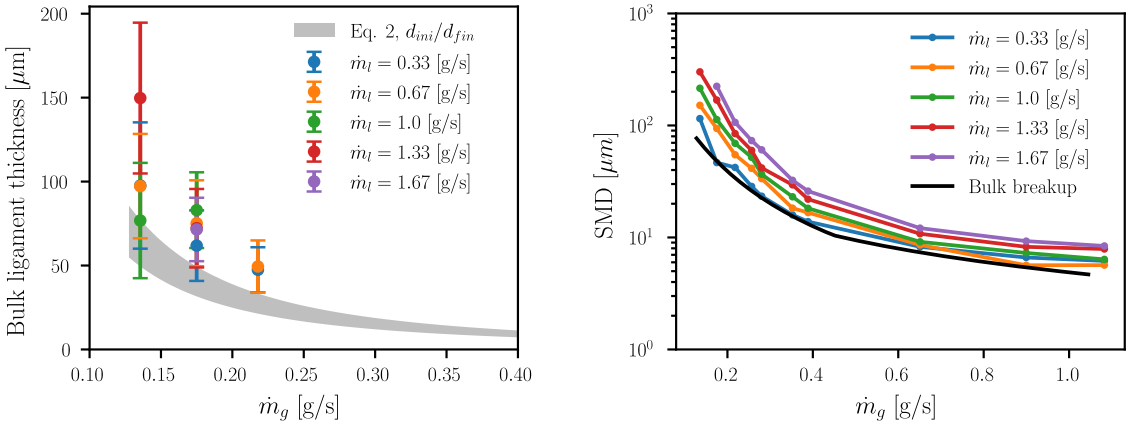

Figure B22: (left) comparison of bulk ligament thickness to theory. (Right) comparison of droplet breakup model for bulk breakup to SMD for varying flow conditions.

The trends and magnitudes in both are found to compare well; however, the effect of increasing liquid flow rate is not predicted by the model. To understand these effects, the PSD must be considered, as in Figure B23. Figure B23 shows how the modality of the distribution affects the

SMD. Since the current prediction only considers the one breakup mechanism, it does not capture the larger mode that grows as the liquid flow rate increases. The bulk breakup prediction, however, does give a good prediction of the lower mode in the PSD.

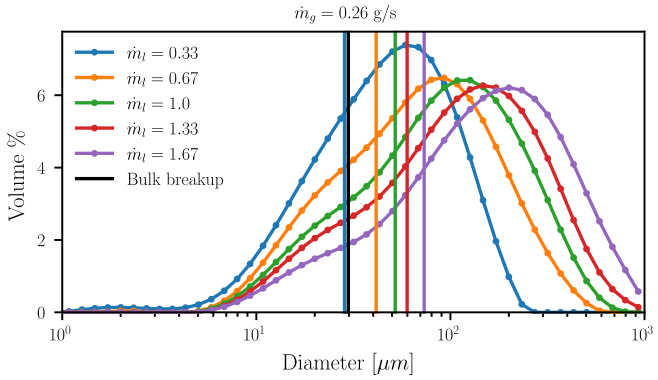

Figure B23: PSD and SMD comparison for varying liquid flow rate.

The larger sizes are believed to come from an intermittency in the breakup of the liquid core, due to the way it waves in and out of the airflow, as shown in Figure B24. This essentially relates to an incomplete breakup of the liquid jet due to insufficient aerodynamic forces, which occurs commonly in highly viscous sprays. This is expected to be modelled similarly to the breakup of the undeformed core in droplet breakup.

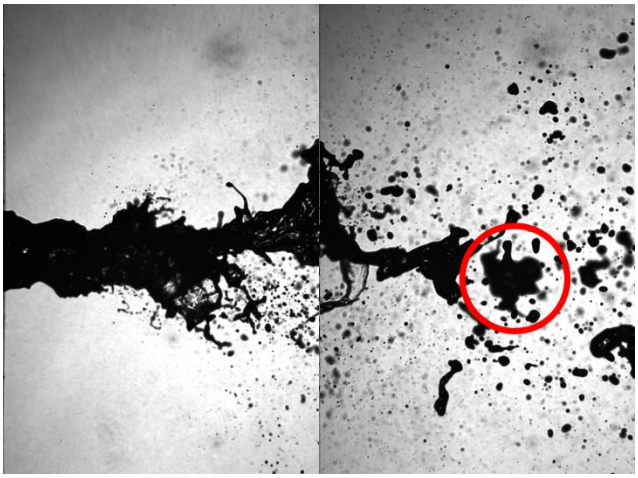

Figure B24: Images showing the intermittent core breakup

The breakup of the surface waves occurs when the surface waves grow to a critical size, given by the critical condition for droplet breakup of $We = \rho_g U^2 d_s/\sigma \approx 8.8$. The measured surface ligament sizes are compared to the theory in Figure B25. The measurements are found to be higher than the prediction. This is due to viscous effects, as the surface waves are sufficiently

small at this scale that viscosity plays a role in their breakup, despite the fluid being relatively inviscid.

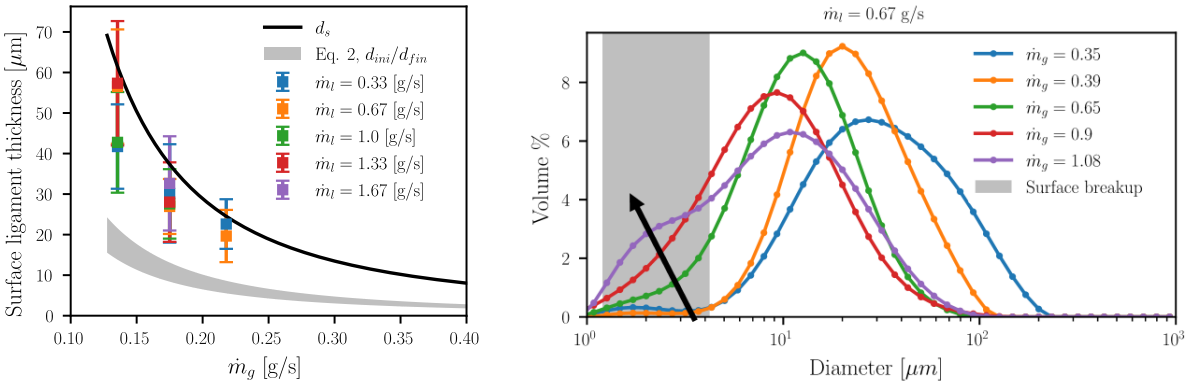

Figure B25: Comparison of theory of surface ligament thickness to measurements, and the effect of the surface breakup on the PSD.

The surface waves break at a characteristically small size. At low gas flow conditions, there is not enough surface breakup to dominate the volume distribution of the spray sizes. However, at higher flow rates, an additional mode in the PSD becomes apparent as the surface breakup begins to become important.

Understanding the balance between these three modes of breakup is crucial to understanding the proper operation of the spray. If there are too many large droplets due to intermittent core breakup, then the spray quality will be poor as too many large droplets will be produced. To counter this, the gas flow rate can be increased so that the core breaks up fully; however, at the extreme, too high of a gas flow rate also decreases the spray efficiency due to the over-production of fine droplets that do not settle in the drying air flow.

B.3. Elevated Temperatures

In typical spray-drying with two-fluid nozzles, the atomizing gas is not heated, and instead a secondary heated air flow is used to dry the resulting spray. Since the primary atomization occurs entirely before the atomizing air-stream mixes with the heated drying air-flow, there will be no effect of the heating drying air on the primary atomization. This is illustrated in Fig. B26.

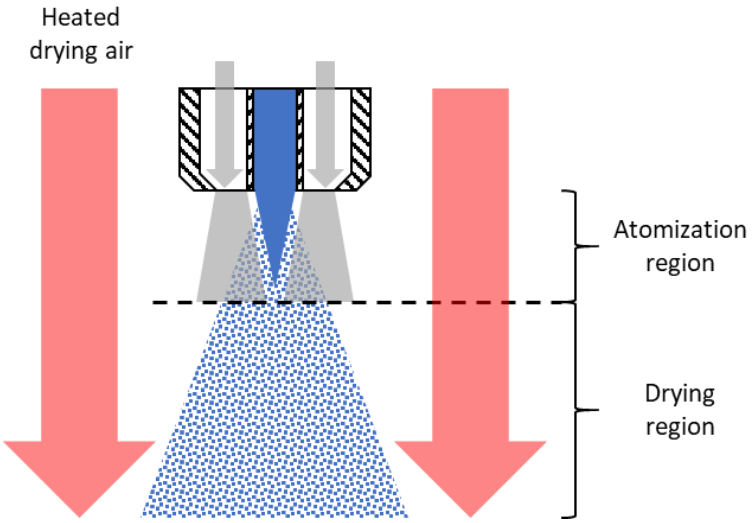

Figure B26: Illustration of the drying and atomizing air flow interaction with the primary atomization of the liquid jet.

While it would be possible to heat the atomizing air, the atomization time for two-fluid nozzles is so short that no significant heating of the liquid jet occurs. Using worst-case estimates for the heat transfer coefficient between the air and the liquid jet and the liquid jet diameter and atomization time, an atomizing air at 80°C above the liquid temperature would result in a heating of approximately 0.3°C of the liquid, which is not enough to significantly affect the evaporation rate or properties of the liquid. Furthermore, heating the atomizing air for a typical two-fluid nozzle is relatively wasteful, as the expansion of the air jet out of the nozzle results in a significant temperature drop in the air flow, substantially increasing the heating requirements to achieve the desired outlet air temperature. The main effect of doing so would be to allow for higher gas-flow speeds through the nozzle; however, this would be at the expense of a lower atomizing air density, which would partially negate any gain in performance from increasing the air speed. The effect of the heating on the air speed and density out of the nozzle is shown in Fig. B27. The heated air would likely have a greater effect over time on the nozzle body temperature, which would in turn heat the liquid and change its properties. However, it would be far more effective to simply heat the liquid directly to alter its properties; namely, lowering its viscosity.

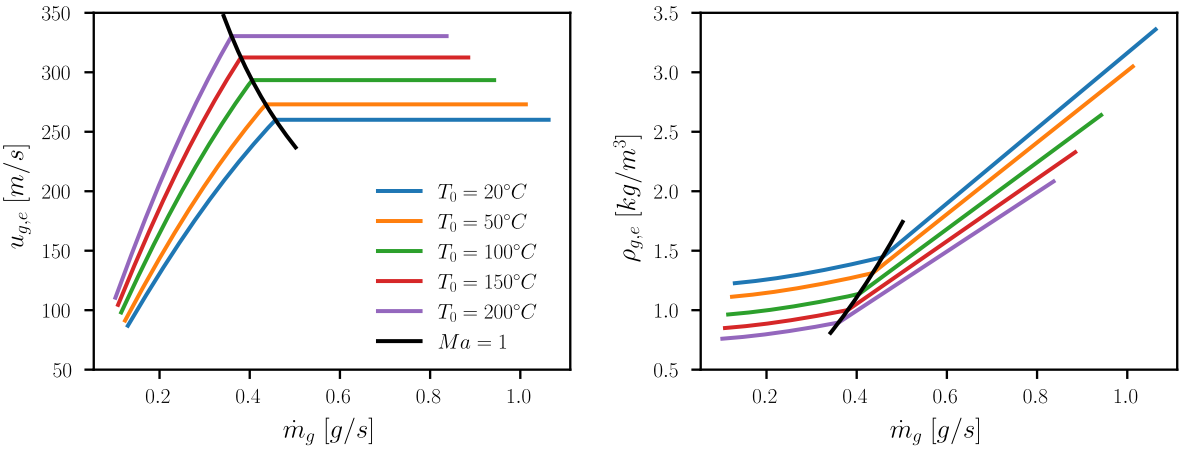

Figure B27: Effect of heating on the atomizing air speed and density.

Since the heated air flows are not expected to have a significant effect on the primary atomization of two-fluid nozzles, we have decided not to pursue this aspect of the investigation. However, for higher viscosity and polymeric fluids, the ligaments persist far downstream of the primary atomization region. In these cases, the effects of the heated airflow on the ligament breakup dynamics will be more important.

References

[1] Benchabane, A., and Bekkour, K., 2008, "Rheological Properties of Carboxymethyl Cellulose (CMC) Solutions," Colloid Polym. Sci., **286**(10), pp. 1173–1180.

[2] Chigier, N., and Farago, Z., 1992, "MORPHOLOGICAL CLASSIFICATION OF DISINTEGRATION OF ROUND LIQUID JETS IN A COAXIAL AIR STREAM," At. Sprays, **2**(2), pp. 137–153.

[3] Zhao, H., Liu, H. F., Xu, J. L., Li, W. F., and Cheng, W., 2012, "Breakup and Atomization of a Round Coal Water Slurry Jet by an Annular Air Jet," Chem. Eng. Sci., **78**, pp. 63–74.

[4] Varga, C. M., Lasheras, J. C., and Hopfinger, E. J., 2003, "Initial Breakup of a Small-Diameter Liquid Jet by a High-Speed Gas Stream," J. Fluid Mech., **497**(497), pp. 405–434.

[5] Aliseda, A., Hopfinger, E. J., Lasheras, J. C., Kremer, D. M., Berchielli, A., and Connolly, E. K., 2008, "Atomization of Viscous and Non-Newtonian Liquids by a Coaxial, High-Speed Gas Jet. Experiments and Droplet Size Modeling," Int. J. Multiph. Flow, **34**(2), pp. 161–175.

[6] Joseph, D. D., Belanger, J., and Beavers, G. S., 1999, "Breakup of a Liquid Drop Suddenly Exposed to a High-Speed Airstream," Int. J. Multiph. Flow, **25**, pp. 1263–1303.

[7] Joseph, D. D., Beavers, G. S., and Funada, T., 2002, "Rayleigh-Taylor Instability of Viscoelastic Drops at High Weber Numbers," J. Fluid Mech., **453**, pp. 109–132.

[8] Jackiw, I. M., and Ashgriz, N., 2021, "On Aerodynamic Droplet Breakup," J. Fluid Mech., **913**(A33).

[9] Zhao, H., Liu, H.-F., Li, W.-F., and Xu, J.-L., 2010, "Morphological Classification of Low Viscosity Drop Bag Breakup in a Continuous Air Jet Stream," Phys. Fluids, **22**(114103).

[10] Wang, Y., Dandekar, R., Bustos, N., Poulain, S., and Bourouiba, L., 2018, "Universal Rim Thickness in Unsteady Sheet Fragmentation," Phys. Rev. Lett., **120**(20), p. 204503.

[11] Guildenbecher, D. R., Gao, J., Chen, J., and Sojka, P. E., 2017, "Characterization of Drop Aerodynamic Fragmentation in the Bag and Sheet-Thinning Regimes by Crossed-Beam, Two-View, Digital in-Line Holography," Int. J. Multiph. Flow, **94**, pp. 107–122.

IFPRI Research Project Brief

Wetting and Dispersion of Organic and Biologically-Derived Powders

The International Fine Particle Research Institute (IFPRI) wishes to fund a project in the broad area of dispersion and dissolution of organic particles. The overall objective of the project is to develop systematic understanding of wetting, imbibition, dispersion, and dissolution to facilitate proactive design of powder formulations for optimal dispersibility.

The project should explore and demonstrate approaches to control, design, and engineer nano to meso scale particle surface topology and surface chemistry of organic and biologically-derived materials to promote wetting and dissolution, in concert with addition of surface modifiers (surfactants, ions, polymers, etc.). Dispersion by liquid incorporation into powders and powder addition to liquids should *both* be investigated. A mechanistic model for dispersion and dissolution should be developed and validated. This model should describe both modes of dispersion.

IFPRI's interest is in dispersion of powders common in food and pharmaceutical applications, with an emphasis on water dispersible, bio-derived materials of which, fully soluble particles and mixed soluble/insoluble particles are explored. A phenomenological mechanistic model of the particle/powder wetting, dissolution and dispersion kinetics should be developed and validated as a predictive tool for assessing wetting/dissolution issues of powders/powder beds in both confined and unconfined vessels. The model should address powder to liquid ratios that are representative of localized conditions in transforming a wetted bed of powder having capillary or even funicular wetting at liquid-particle interfaces to a fully dispersed suspension of particles in excess liquid. An understanding of the development of films, gelatinous layers, and fish eyes should be considered, as these are some of the most common issues encountered with reconstitution of powders. Systems where little to no agitation is available to promote wetting and dispersion, such as gravimetric liquid incorporation are of particular interest.

IFPRI Research project - ExPowSE

Exploring food powder surface under controlled environment

LIBio – Laboratoire d'Ingenierie des Biomolecules (Université de Lorraine, France)

Jennifer Burgain – Stéphane Desobry - Claire Gaiani

I. Proposal context, positioning and objective(s)

I.A. Objectives and research hypothesis

The current inability of most consumers to achieve the recommended daily intake of fruits and vegetables triggers food research toward the generation of new and improved fruit- and vegetable-based products and ingredients. The World Health Organization (WHO) recommends consuming at least 400 g each day to reap their health and nutrition benefits. In 2017, some 3.9 million deaths worldwide were attributable to the lack of fruit and vegetables in the diet (**WHO, 2019**). Actions are needed to **increase the production and consumption of fruit and vegetables and make them more economically accessible to consumers, while generating economic, social and environmental benefits in line with the Sustainable Development Goals**. In declaring 2021 as the international year of fruits and vegetables, the United Nations (UN) general assembly aims to raise awareness of the nutritional and health benefits of fruit and vegetables and their contribution to a balanced and healthy diet and lifestyle (**FAO, 2020**). The diverse range and characteristics of fresh fruit and vegetables and their inherently perishable nature warrants the deployment of conservation techniques in order to: (1) **guarantee their accessibility** throughout the year and in particular outside production periods, (2) **deliver stable products** in non-producing regions by exportation, (3) **reduce food waste** due to seasonality and report the consumption by using drying and powdering methods. However, these operation units govern powder structure and functional properties and it is of paramount importance to master them.

The overall scientific objectives of ExPowSE are:

- Preserving product stability and quality.
- Bringing knowledge in the technofunctionality of food powders using a multiscale approach with a focus on the particle surface. Even if the powder surface is one of the main players during the reconstitution or transport (powder flowability), it has been poorly studied in the literature for fruit and vegetables powders.
- Elucidating physical mechanisms occurring when materials reach the glass transition by increasing temperature and/or relative humidity (RH). Until now, only hypotheses were proposed as the techniques were not able to probe the progressive evolution. Atomic Force Microscopy (AFM) is the technique of choice to gather physicochemical and nanomechanical data during the glass transition phase.

A profound understanding of the **process–structure–function relations** to tailor the **functional properties** of fruits and vegetables powders is then required. A schematic representation of the key concept of the ExPowSE project is displayed in **Figure 1**.

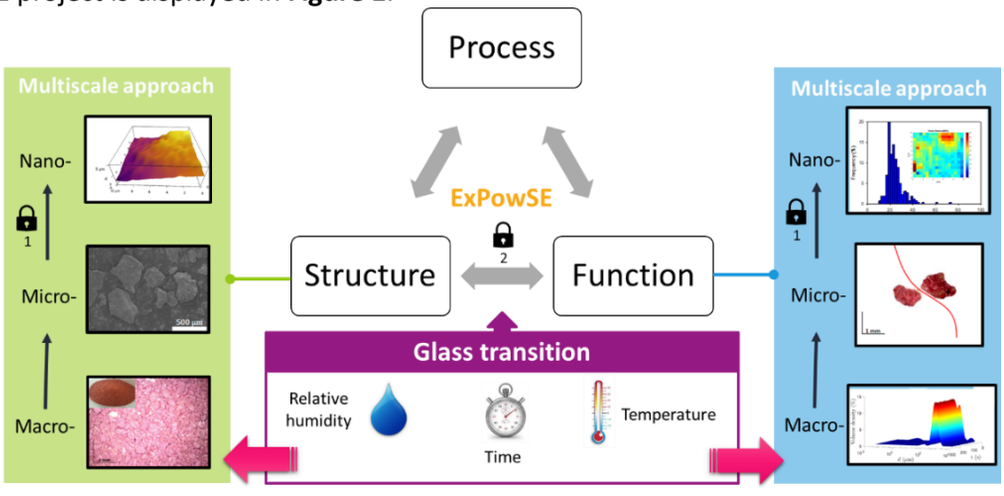

Figure 1: Schematic overview of the ExPowSE project: process–structure–function relations with a multiscale approach.

Research on this project will be performed at a nanoscopic, microscopic, and macroscopic level entailing particle surface investigations with the aim to answer to the following questions:

- How surface modification (topography, chemistry, nanomechanics) can impact the macroscopic behaviour (reconstituability and flowability) of the powder?
- What are the phenomena occurring at particle surface during the glass transition phase?
- How to improve powder stability and quality during shelf-life?

I.B. State of the art

Many types of fruit and vegetables are processed to increase their shelf-life, year-round availability, or to increase their value, which integrates structure-enabling and preservation techniques. Minimal processing includes drying and/or grinding (powdering process) of fruits and vegetables and guarantee that such foods are as nutritious as the food in its unprocessed form (**Fitzpatrick and Ahrné, 2005**). However, fruits and vegetables powders contain a high quantity of low molar mass sugars with low glass transition temperature (T_g) (**Fang and Bhandari, 2011**). The direct consequence is that fruit powders are highly hygroscopic and sticky at high temperatures but also at ambient temperature if the water content is not well mastered. This feature causes the powder adhesion to surfaces and powder caking during the storage, which affects the quality of the final product. **The T_g is one of the most important parameters to consider during powder storage.** Indeed, the phenomenon of glass transition is the gradual and reversible transition of amorphous materials from a hard and "glassy" state into a viscous and rubbery state as the temperature and/or the moisture content is increased. The glass transition is also linked to the water activity and water as a strong plasticizer decreases the T_g. Also, the glass transition temperature depends on the molecular mass as the T_g of monosaccharides, disaccharides, oligosaccharides and polysaccharides increases with increasing their molecular mass (**Roos, 2002**). If the glass transition is reached during powder storage, unexpected phenomena can happen that affect powder functionality such as reconstitution ability.

An important structure-determining component in this context is the particle surface. It should be noted that particle surfaces, in the case of fruits and vegetables powders, are essentially constituted by broken structures. Because of various origins, their particle size and shape distributions, chemical composition, surface composition, and physical properties are highly variable. Therefore, more than one analytical technique is often required to obtain a full set of information about a given scientific question (**Burgain et al., 2017**). Among these questions, the powders flowability and reconstitution are of upmost importance for the industry considering that most powdered ingredients are transported and dissolved or infused before use. For the past few years, numerous powder surface analysis techniques were used to further understand the role of powder surface on functionalities impairments. For example, microscopy techniques such as Scanning Electron Microscopy (SEM), Confocal Laser Scanning Microscopy (CLSM) or even chemical composition techniques such as X-ray Photoelectron Spectroscopy (XPS) are already widely used (**Burgain et al., 2017**). However, **AFM is currently a rising star in the food powder surface analysis field**, mainly for its resolutive capacity. AFM is a versatile tool compared to other surface analysis techniques. For example, AFM allows to study particle surface topography and roughness, surface chemistry and nanomechanics.

In a previous project, we were able to have a better understanding of surface modification after high temperature storage of whey protein isolate and micellar casein powders (**Burgain et al., 2016a, 2016b**). Surface hardening with the development of a poorly dispersible skin layer composed of aggregated micelles was evidenced to be the phenomenon responsible for the reconstitution impairment. However only punctual analyses were possible and the development of an environmental chamber around the AFM will allow for continuous measurements at nanometer scale. **By controlling the temperature and RH, their variation during time in the neighbouring of the sample will provide new insight in the elucidation of mechanisms occurring during powders storage or transport under unfavourable conditions, in particular when they reach the glass transition.** Even if AFM was already applied to dairy powder, application to fruits and vegetables powders is still missing while there is an important industrial stake with the growth of the plant products market and the development of vegetable formulations.

First experiments on fruits and vegetables powders provided hopeful results showing that when approaching glass transition, patches at the surface were crystallising by nucleation and the rest of the matrix presented a decreased elasticity (**Figure 2**). The glass transition event is accompanied by a physical change at the powder surface (modified topography) with a change in the Young modulus (modified nanomechanical

properties) (**Palzer, 2007).** Moreover, powder caking related to glass transition is promoted by moisture adsorption which create liquid bridges between hydrophilic groups at particle surface (modified physicochemical properties). **The strength of the technique is that it is now possible to follow the evolution of the same area during dynamic variation of temperature and RH**. These observations confirm the fact that a focus at particle surface is undeniably required to better understand macroscopic phenomenon such as powder flowability, caking or reconstitution. This is particularly true for fruit powders that are highly hygroscopic materials with low glass transition temperature and as a consequence easily affected by ambient temperature and RH. In a recent work, we evidenced that above T_g, a viscous layer around the particle limits water entrance and is the limiting step in the global reconstitution process (**Gaudel et al., 2022**). With AFM, surface structure and chemical properties will be correlated thanks to the combination of surface topography analysis and force measurements.

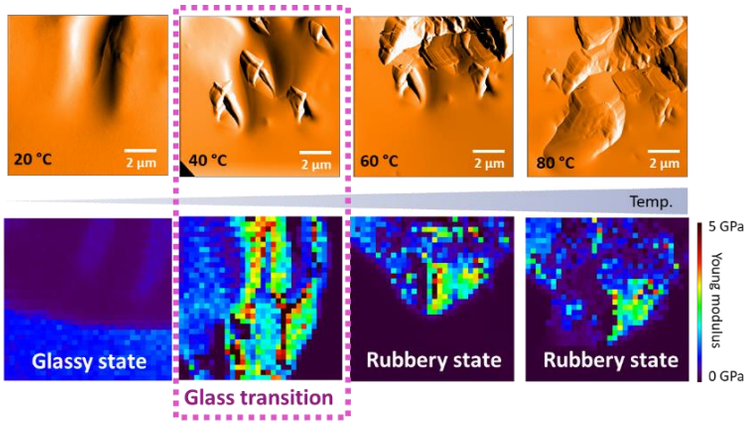

Figure 2: Use of AFM on maltodextrin powders with progressive temperature increase. The same area was analysed in situ during temperature increased (unpublished results from the team).

I.C. Project methodology

The project will be divided into three Work Packages (WP).

WP1: Fruits and vegetables powders screening (months: 0 – 12). The powder functional properties will be investigated at the macroscale by the evaluation of hygroscopicity, flowability and reconstituability. Powder thermal properties will also be determined and linked to powder proximate composition. In this WP, powders will be grouped as a function of their origin, T_g, solubility index, flowability index and only few powders of each group will be investigated in the WP2.

WP2: Probing surface physicochemical and nanomechanical properties by AFM-CE (months: 6 – 30). In this WP, a newly designed Controlled Environmental chamber around the AFM (AFM-CE where temperature and RH can be managed) will be employed. AFM-CE will be employed for the determination of particle surface topography and roughness and for the estimation of nanomechanics and adhesion forces. Even if process parameters define powder surface structure and functional properties, they can be impacted by environmental conditions. The technical and scientific challenge in the ExPowSE project will be to observe and quantify surface evolution during temperature and RH modulation (**Figure 1 - Locker 1**). In fact, the design of the environmental chamber was done in a way to recreate thermal and hygroscopic conditions that can be encountered by powders during transport and storage, but it is also possible to reach higher conditions in order to exceed the glass transition region. However, mechanical features of the AFM tip can evolve with increasing temperature or water droplet can deposit on the tip. All of these technical issues must be mastered to produce reliable data.

WP3: Modelling the process–structure–function relations (months: 24 – 36). Using mechanistic and statistical models, data will be processed in order to establish the process–structure–function relations and describe mechanisms at the basis of surface evolution (as a function of temperature and RH) and impacting powder reconstitution and/ or flowability. The second scientific challenge here will be to link powder surface structure with powder function and to get enough data to model the phenomena occurring and elucidate the underlying mechanisms (**Figure 1 - Locker 2**).

II. Team and link's with the actual IFPRI project

The work packages outlined above will be carried out by a dedicated full time PhD student 100 % funded by the IFPRI Consortium. Materials and consumables will be covered by the LIBio. This project can be leveraged to obtain local funds from the Grand Est region and the University of Lorraine Impact "Biomolecules" program leaded by a LIBio professor. These organizations provide 2-to-1 support for industrial cash grant. The PhD student will be embedded in the LIBio laboratory under the direct supervision of Prof. Claire GAIANI and Jennifer BURGAIN. They received more than of 2 000 k€ funding for projects on which they were principal investigators. Among other important activities, they successfully managed fundamental competitive programs including the French ANR and European projects. They also participated in international collaborations. Finally, they managed many industrial partnerships with leading international food companies (including Nestlé, Lactalis, Bel, Arla Food, and CNIEL).

Nowadays, their research thematic deals with the establishment of links between surface and functional properties of food powders. The objective will be to further develop, the work that was recently initiated into the IFPRI project managed by Claire GAIANI (more particularly in the WP2). The idea is to loop the approach process-structure-function and the development of AFM in controlled environmental.

The ExPowSE team will be managed by Claire GAIANI and Jennifer BURGAIN and composed of one PhD student, one technician (working mainly on the AFM technique) and a specialist of food glass transition (Pr Stephane DESOBRY). Therefore, four permanent staffs will be involved in the team plus one PhD student (IFPRI funds). The complementarity of the team members is clearly an asset for this project.

Finally, this project will be in close collaboration with the IFPRI members with regular meetings and reports. We will test powders of interest for the industry and if possible directly from the industrial partners.

III. References related to the project

Burgain, J., Scher, J., Petit, J., Francius, G., Gaiani, C., (2016a). Links between particle surface hardening and rehydration impairment during micellar casein powder storage. Food Hydrocolloids, 61, 277-285. DOI 10.1016/j.foodhyd.2016.05.021

Burgain, J., El Zein, R., Scher, J., Petit, J., Norwood, E.A., Francius, G., Gaiani, C., (2016b). Local modification of whey protein isolate powder surface during high temperature storage. Journal of Food Engineering, 178, 39-46. DOI 10.1016/j.jfoodeng.2016.01.005

Burgain, J., Petit, J., Scher, J., Rasch, R., Bhandari, B., Gaiani, C., (2017). Surface chemistry and microscopy of food powders. Progress in Surface Science, 92, 4, 409-429.

FAO. 2020. Fruit and vegetables – your dietary essentials. The International Year of Fruits and Vegetables, 2021, background paper. Rome. https://doi.org/10.4060/cb2395en

Fang, Z., Bhandari, B., 2011. Effect of spray drying and storage on the stability of bayberry polyphenols. Food Chem. 129, 1139–1147.

Fitzpatrick, J. J., & Ahrné, L. (2005). Food powder handling and processing: Industry problems, knowledge barriers and research opportunities. Chemical Engineering and Processing: Process Intensification, 44(2), 209-214.

Gaudel, N., Gaiani, C., Harshe, Y. M., Kammerhofer, J., Pouzot, M., Desobry, S., & Burgain, J. (2022). Reconstitution of fruit powders: A process–structure–function approach. Journal of Food Engineering, 315, 110800.

Palzer, S., (2007). Agglomeration of Dehydrated Consumer Foods, Granulation, 592-671. DOI 10.1016/S0167-3785(07)80048-0

Roos, Y.H., 2002. Importance of glass transition and water activity to spray drying and stability of dairy powders.

WHO, World Health Organization, 2019, Increasing fruit and vegetable consumption to reduce the risk of noncommunicable diseases.

IFPRI Research Project Brief

Rheology of Suspensions at High Solids Content: Bridging the Gap from Colloids to Grains

Pumping, flow, conveyance, and the long-term flow stability of highly concentrated particle systems remain and industrial challenge. Advancements in understanding surface turnover and chemistry-mediated particle interactions have improved our understanding of highly concentrated colloidal systems. Improvements in understanding of jamming phenomena, particle shape and inertial streams have similarly improved understanding of granular systems. A recent revolution has taken place in understanding the rheology of high-solid-content dispersions (HSCDs), viz., that at sufficiently high stress, particles are pressed into contact, so that many ideas from granular flow may become transferable to suspension flow in this regime. This project aims to explore how this new paradigm can be applied to optimize the processing of HSCDs by understanding how their rheology is controlled by many of the classic variables (e.g. morphology and size distribution) viewed under the new paradigm, and by some of the variables made relevant by these recent advances themselves (e.g. roughness, friction).

A key idea from recent advances is that HSCDs jam at a packing fraction ϕ_m substantially below random close packing, so increasing solid content involves increasing ϕ_m. *The overall objective is therefore to understand what controls* φ_m. Research themes under this heading may include:

- The friction coefficient matters, but how this can be systematically modified on the micro to nano scales is not yet mastered.
- Roughness almost certainly matters on some scale, but again, no systematic study yet exists.
- Badly packed aggregates lower ϕ_m, so that it may be fruitful to study wet milling in this context. In particular, wet milling applies stress to an HSCD at $\phi > \phi_m$ to break up aggregates, thereby lowering ϕ_m in the process; the new paradigm should give insight into how best to do this.
- Polydispersity is known to affect random close packing; how it affects ϕ_m is largely unknown.
- Identify key/dominant particle characteristics (e.g., morphology, surface friction, modulus, size distribution) that impact particle assembly, jamming and overall rheological behavior across the transition zone between low and high particle Peclet number concentrated (>40% vol) slurry systems for predictive modeling applications.
- Explore the link between system level and particle level characteristics on the packing/jamming transitions and corresponding rheology of concentrated suspensions across the transition regime between surface dominated interactions and inertially dominated particle systems.

To make progress, the contractor should be able to perform studies in well characterized systems using one or more of the following methodologies: monitor structure and dynamics under flow using a mixture of real-space and scattering methods; develop framework linking measured structure and dynamics to constitutive properties of suspension; develop toolkit for systematic variation of relevant parameters (friction, roughness, etc.).

IFPRI Project renewal: Erin Koos

1. State of the art

The structural properties of suspensions and other multiphase systems are vital to overall processability, functionality and acceptance among consumers. Therefore, it is crucial to understand the intrinsic connection between the microstructure of a material and the resulting rheological properties. In the previous portion of the project, we demonstrated how the transitions in the microstructural conformations can be quantified and correlated to rheological measurements. We found semi-local parameters from graph theory, the mathematical study of networks, to be useful in linking structure and rheology. Our results, using capillary suspensions as a model system, show that the use of the clustering coefficient, in combination with the coordination number, is able to capture not only the agglomeration of particles, but also measures the formation of groups [1]. A recent review paper outlines the various wetting-induced changes that occur in capillary suspensions [2].

1.1. Methodology

Capillary suspensions consisting of silica particles fluorescently labeled with rhodamine B isothiocyanate in a mixture of 1,2-cyclohexane dicarboxylic acid diisononyl ester (Hexamoll DINCH) and n-dodecane, with added aqueous glycerol. The three components are all index matched and the silica contact angle can be modified [3]. The attractive interaction strength can be modified by tuning the contact angle and fraction of secondary liquid. This lets us access both granular-like systems with weak interactions and strong attractive gels using the same model system. During the project, we switched from using porous silica particles to nonporous particles as there were problems noted with adsorption of the secondary liquid into the pores. This simplified the particle detection algorithm now includes a graphical user interface for both local detection and manual addition or removal of missing or misdetected particles improve the final detection efficiency.

Our initial goal of the project was to track microstructural changes in the network in response to external shear applied via a linear shear cell. These structural changes were correlated with the rheological response of the material. Application of external shear via the linear shear cell, however, was unsuitable. Due to the very low yield strain in capillary suspensions, the applied shear was often above the flow point and specific changes during yielding could not be adequately captured. Furthermore, the present setup only allowed for the deformation profile to be captured in one shear plane. While this has provided valuable information, proving that capillary suspensions tend to undergo solid-body movement, where the rotation of particles around their respective bridges is resisted through both the structure of the network and the extra torque provided by the contact angle pinning and/or the contact angle hysteresis, full 3D tracking is necessary. Therefore, a rheometer has now been mounted onto a high-speed confocal microscope. The improved setup will allow us to directly compare bulk, rheological changes with local, microscopic changes to the clusters and network.

1.2. Project results

Semi-local measurements capture rheological changes: Using both the coordination number and the clustering coefficient (Figure 1), we could rationalize the transitions in the structure and tie these changes to the rheological properties of the material. For instance, the transition from a pendular network, where particles are connected by binary bridges, to the funicular state, where larger clusters are formed, occurs at $\phi_{\text{sec}}/\phi_{\text{solid}} = 0.09$. This point corresponds to a peak in the coordination number and beginning of a plateau in clustering coefficient. While there is a slight shift in the distribution of coordination numbers, there is a large shift in the distribution of clustering. The number of particles with zero clustering drops significantly while there is an increase in intermediate and high clustering. These results are published in the journal Soft Matter [1].

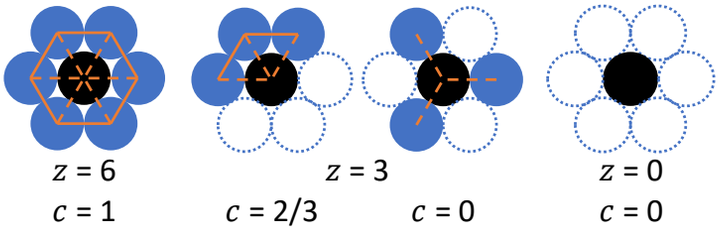

Figure 1: Difference between the coordination number z, the number of bonds per particle (dashed lines), and the clustering coefficient c. The clustering coefficient is defined as $c = \frac{2e}{z(z-1)}$, where the number of bonds between neighbors (solid lines) is e.

Particle volume fraction: Samples with particle volume fractions $\phi = 0.1 - 0.3$ were examined. Below $\phi = 0.15$, the flocs not fully percolated. The intracluster structure of all capillary suspensions was the same ($z \approx 5$ and $c = 0.33$), but the system becomes more dense with increasing particle volume fraction. This can be interpreted as a growing floc size with constant intrafloc structure. The microstructure after compression was examined for the higher particle volume fractions. The samples were compressed to a gap around 1 mm, equal to the measurement gap that was applied on the rheometer. The coordination number before and after compression remained constant, increasing at most by $z = 0.5$ for the $\phi = 0.3$ sample. The clustering coefficient was unchanged for all three samples.

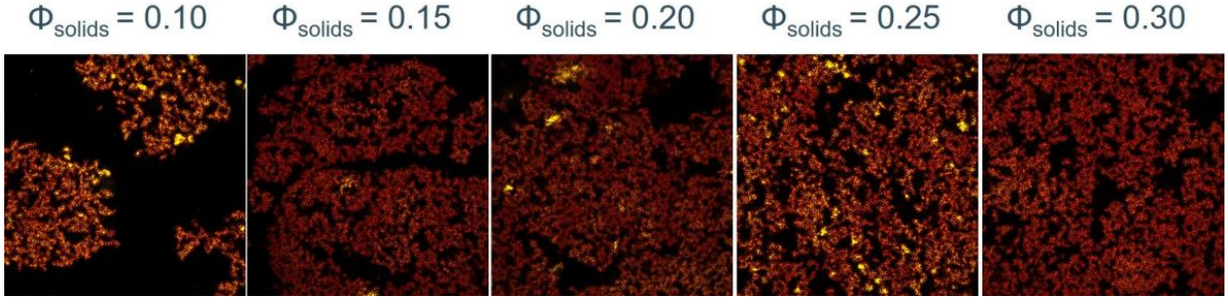

Figure 2: Confocal images of capillary suspensions with increasing particle volume fraction using non-porous particles.

Particle size: Samples with particles with sizes 3, 10 and 50 µm were prepared. The volume fractions are kept constant as is the contact angle and the mixing conditions. While it is expected that the particle size R should have an influence on the structure through the balance between the capillary and gravitational forces (Eötvös or Bond number),

$$\text{Eö} = \frac{\text{Capillary force}}{\text{Particle weight}} \approx \frac{2\pi R\Gamma\cos\theta}{\frac{4}{3}\pi R^3\rho} \sim \frac{1}{R^2}$$

no densification of the structure was observed. Changes to the bridge shape and distribution account for this relatively constant structure. In all three samples, a distribution of bridge

sizes, ranging from large, coalesced bridges connecting three or more particles, binary bridges connecting two particles, and very small drops and bridges between particle asperities are observed. These small bridges or patches of secondary fluid appear as a “uniform” film on the small particles whereas they form patches (with an apparent contact angle near 90°) on the particle surface of the large particles. This implies an influence of the particle roughness. Comparing the yielding behavior, we see that the stress at the end of the linear viscoelastic region increases with decreasing particle size, as would be predicted from $\sigma_y \sim F_c/R^2 \sim 1/R$. The flow point, on the other hand, is nearly identical for the small 3 µm particles as the large 50 µm particles and highest for the 10 µm. This change may be due to the changes in the bridge volumes and network structure of this sample.

Particle polydispersity: Adding a small percentage of larger 10 µm particles to the small 3 µm particles shows some influence on the network strength. The storage modulus shows no change with 1% 10 µm particles but does increase slightly with the addition 5% 10 µm particles. This increases G' towards the value with 100% 10 µm particles. The loss modulus shows no clear trend and the data for 100% 10 µm remains higher. We do not see a dramatic in the meniscus size that would be expected from large-large interactions. Instead, the structure is dominated by the interactions between the small particles with some small-large interactions. Preliminary image detection shows that the average network structure is the same with only local changes around the large particles. The large particles have a larger coordination number, owing to their larger size. We also see region, particularly around the large particles, where there are dense flocs consisting of many coalesced bridges. This may imply some change in the mixing conditions caused by the large particles.

Particle roughness: To directly test the influence of particle roughness on our system, silica nanoparticles are electrostatically adsorbed onto the surface of the larger microparticles and then smoothed with a Stöber silica layer [4]. By attaching differently sized NPs, we can tune the roughness. For samples with a constant secondary fluid volume, the increase in roughness results in several changes. First, for the attachment of 40 nm particles to the 3 µm primary particles, the storage modulus remains unchanged, but the loss modulus increases, shifting the yielding region and the flow point shifts to higher strain. With further increases in the roughness (attachment of 100 nm and 200 nm particles), a transition to asperity wetting – with corresponding decrease in the storage modulus – is observed. By adjusting the secondary fluid volume, the storage modulus in all samples can be matched. There remains, however, an increase in the yield strain and decreasing trend in z and c (Figure 3).

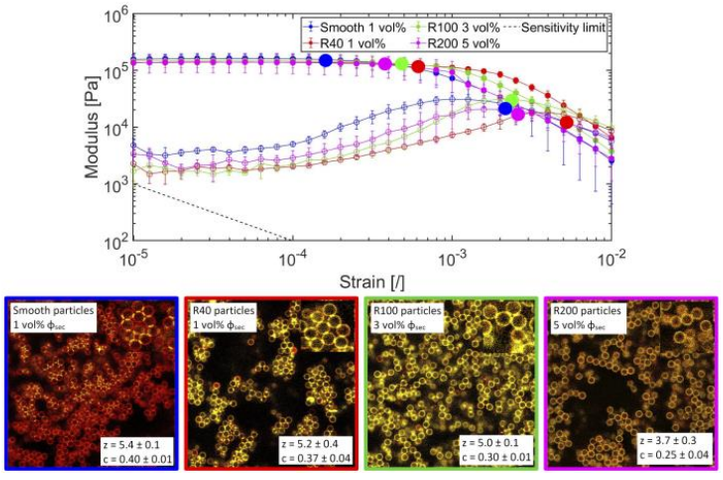

Figure 3: Influence of particle roughness for samples with secondary fluid volume adjusted to match the storage moduli. Increasing roughness increases the yield strain with very little effect on the flow point. The structure becomes less dense (decreasing both the coordination number and clustering coefficient) as the roughness increases.

The influence of particle roughness was further examined using information obtained from the medium amplitude (or asymptotically nonlinear) oscillatory shear regime. Previous research has shown that the third harmonic is non-integer and non-cubic [5] and the scaling of the third harmonic is sensitive to particle collisions [6]. The strength of the Hertzian contact is decreases with roughness as the samples transition from bridge to asperity wetting demonstrating the sensitivity of this rheological measure to the particle contact strength. The ratio of the elastic to viscous scaling is tied to the nature of the frictional contact and a transition from adhesion- to load-controlled friction may occur in these samples, but additional measurements must be conducted.

2. Proposed work

After discussion with project liaisons, we have decided to concentrate on the rheo-microscope in the project renewal. This will allow us to better connect the changes in the microstructure with the dynamics. The initial focus will be on the changes in the asymptotically nonlinear region to study both the bridging dynamics and yielding of the network. This will be supplemented by better detection of the bridge shape to determine changes to particle clustering and bridged contacts. A generalization of the particle detection algorithm will also allow us to investigate the influence of particle shape, integrating changes to the particle orientation and contact type (e.g. edge-edge or corner-edge).

2.1. Specific work packages

WP1: Yielding of capillary suspensions

We have now built a combined rheometer-confocal microscope setup that can be used to provide more accurate shear profiles while directly obtaining the resultant rheological properties. This new setup will allow us to better investigate the local, cluster-level changes to the structure and determine if yielding is the result of bond-breaking between a few, critical bridges or if general restructuring occurs. By tracking the individual particle deformation and that of the neighboring particles, we can correlate the motion of individual particles to the local clustering and local bridge strength. Of particular interest is the development of the coordination and clustering coefficient during shear.

To investigate the yielding dynamics, we will employ both oscillatory and step shear profiles. Our previous experiments showed how oscillatory shear in the asymptotically nonlinear regime is sensitive to particle collisions with little influence on the re-arrangement of the particles (resulting in network coarsening or compaction). Step shear profiles, however, can result in more pronounced re-arrangement and allow us to investigate the difference between inter- and intra-cluster bonds. We will also be able to directly track the different shear layers to investigate the influence of slip and shear banding.

WP2: Bridge sizes and asperity wetting

Previous experiments with both varying particle sizes and particle roughness have shown the importance of bridge size and size distribution on the structure and rheological properties. The transition between asperity wetting to particle bridging is associated with an increase in the storage modulus and decrease in the coordination number and clustering. This clustering can be highly inhomogeneous, however, as demonstrated for the mixtures of large and small

particles. There, mixing conditions leads to a local change in the bridge size near the added large particles. Changes in the local displacement of particles both close to and far away from these inclusions should be further investigated. The previous experiments using large and small particle mixtures should further be expanded to investigate intermediate fractions and larger differences between the sizes.

The experiments with rough particles also showed changes to the frictional contacts in the system with increased roughness. Despite matching the plateau storage modulus, the rougher particles had a lower clustering. There was scatter in the data between samples demonstrating adhesion- and load-controlled friction. This change should better be correlated to the local structure and the deformation of the particles. By modifying the particle hydrophobicity, we can include variations in the wetting to further investigate these changes.

WP3: Particle aspect ratio and cubic particles

The investigation of particles with a varying aspect ratio and/or angular shape is also viewed as of interest. Such particles can be printed using a Nanoscribe or particle stretcher. The strength of capillary suspensions varies with particle shape [7] and higher fractions of secondary fluid can induce changes from edge-edge contacts with high connectivity to hedgehog-like clusters formed through corner-corner contacts with low connectivity [8]. While these systems have been investigated rheologically, their structure remains largely unknown and of industrial interest. The local structure and aggregate behavior will be monitored as a function of the applied shear.

2.2. Gantt chart

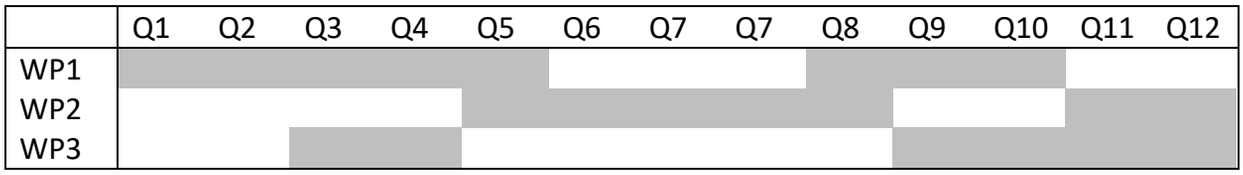

3. Leverage opportunities

I have already started to investigate the structure of capillary suspensions using these confocal microscopy techniques both within and outside of the present project. The project will also benefit from expertise added by a current doctoral student who is modeling capillary suspensions using the coarse-grained MD code ESPResSo. We recently improved the simulation methods so that pseudo-rheological experiments, mimicking the conditions present in the rheometer without the need for a biased shear, could be performed [9]. This can be further supplemented by the project “Computational Modeling of Particle Suspensions” currently in proposal stage.

I am also participating in a Marie Skłodowska-Curie Innovative Training Network “Dynamics of dense nanosuspensions: a pathway to novel functional materials” combining expertise from several European universities and companies to study the influence of combination of particles of different sizes and wettabilities as well as the properties of the liquid phases on the network structure and rheology of capillary nanosuspensions (capillary suspensions with nanoparticles both as the primary particles and with nanoparticles incorporated into the

bridges). The aim of this project is to fabricate and characterize porous bodies from capillary suspensions containing particles of at least two different wettabilities and nanoparticles.

The industrial expertise of the IFPRI members has also been invaluable in identifying areas of specific interest for this project. This research should be a platform that we can use to gain a clear understand the dynamics on a limited scale. Thus, the problems and test methods should be used as a starting point in this project. We can then identify the specific microstructural changes occurring during these tests or under these specific conditions. By highlighting the microstructural changes, especially in relation to the particle interactions, we can have a positive feedback loop with industry to suggest minor changes and tackle increasingly more complex problems.

4. References

1. Bindgen, S., Bossler, F., Allard, J., Koos, E. (2020). Connecting particle clustering and rheology in attractive particle networks. *Soft Matter*, *16* (36), 8380–8393.
2. Bindgen, S., Allard, J., Koos, E. (2021). The behavior of capillary suspensions at diverse length scales: from single capillary bridges to bulk. *arXiv*, 2107.14714.
3. Bossler, F., Koos, E. (2016). Structure of Particle Networks in Capillary Suspensions with Wetting and Nonwetting Fluids. *Langmuir*, *32* (6), 1489–1501.
4. Hsu, C. P., Ramakrishna, S. N., Zanini, M., Spencer, N. D., Isa, L. (2018). Roughness-dependent tribology effects on discontinuous shear thickening. *Proceedings of the National Academy of Sciences of the United States of America*, *115* (20), 5117–5122.
5. Natalia, I., Ewoldt, R. H., Koos, E. (2020). Questioning a fundamental assumption of rheology: Observation of noninteger power expansions. *Journal of Rheology*, *64* (3), 625–635.
6. Natalia, I., Ewoldt, R. H., Koos, E. (2021). Particle contact dynamics as the origin for non-integer power expansion rheology in attractive suspension networks. *arXiv*, 2104.05678.
7. Maurath, J., Bitsch, B., Schwegler, Y., Willenbacher, N. (2016). Influence of particle shape on the rheological behavior of three-phase non-brownian suspensions. *Colloids and Surfaces A: Physicochemical and Engineering Aspects*, *497*, 316–326.
8. Sun, H., Zhang, X., Yuen, M. M. F. (2016). Enhanced conductivity induced by attractive capillary force in ternary conductive adhesive. *Composites Science and Technology*, *137*, 109–117.
9. Bindgen, S., Weik, F., Weeber, R., Koos, E., de Buyl, P. (2021). Lees–Edwards boundary conditions for translation invariant shear flow: Implementation and transport properties. *Physics of Fluids*, *33* (8), 083615.

IFPRI Review Brief
Recent Developments in Dynamic Powder Flow

The International Fine Particle Research Institute wishes to commission a comprehensive critical literature review of recent developments in characterizing, modeling, and simulating dynamic flows of powders and grains. Decades of research on flows of powders and grains have produced a wide array of experimental data, models, and numerical simulations. Development of novel particle tracking experimental methods are providing particle-level characterization of flow kinematics and dynamics. Models range from highly complicated (kinetic theory) to deeply empirical (mu(I) rheology). Advances in numerical simulations offer a means of exploring the detailed granular dynamics as well as a glimmer of hope for design of practical industrial units. We would like this review to provide a synthetic view of the state-of-the-art in all these areas, which is not limited by the reviewers own interests.

The scope of the review includes Intermediate and rapid flow regimes. Quasistatic flow is out of scope. Free surface and confined flows should be considered, as should particle mixing and segregation.

The primary audience for this review is the IFPRI membership, i.e., industrial scientists and engineers who are familiar with some aspects of dry powder flow but not necessarily experts. Thus, it is important to discuss the underlying principles, assumptions, and limitations of each experimental, modeling, and simulation approach. We hope that the review will eventually be published in the open literature.

Recent developments in models, experiments, and simulation of dynamic flows of grains

Over the past fifteen years there has been a paradigm shift in the continuum modelling of granular materials; most notably with the development of rheological models, such as the $\mu(I)$ rheology. This rheology is based on experimental measurements and Discrete Particle Method/Discrete Element Method (DPM/DEM) simulation data from six different steady state flow configurations, which show that the friction μ is a monotonically increasing function of the nondimensional inertial number I. The inertial number itself is defined as $I = \dot{\gamma}d/(p/\rho_\star)^{1/2}$, where $\dot{\gamma}$ is the shear rate, p is the pressure, $\rho_\star$ is the particle density and d is the particle size. The $\mu(I)$ rheology is therefore a non-trivial generalization of the constant Coulomb friction coefficient, that introduces shear rate, pressure and particle-size dependence into the law. This paper reviews the experimental observations that led to the scalar $\mu(I)$ rheology and shows how it was generalized into tensorial form (Jop, Forterre & Pouliquen 2006 Nature vol. 44, pp. 727–730).

If the granular material is assumed to be incompressible then the $\mu(I)$ rheology has a similar mathematical structure to the Navier-Stokes equations of fluid mechanics. This is a useful analogy, which enables existing numerical methods to be relatively easily adapted to solve problems of practical interest. The challenge lies in the fact that the granular viscosity is not constant, but is linearly dependent on the friction and pressure, and is inversely proportional to the shear rate. This makes the equations much harder to solve. However, early simulations of granular column collapses and silo flow show that the rheology has the potential to solve real world problems using a relatively simple continuum theory. This is an exciting development, as continuum theories do not suffer from the computational restrictions of DPM/DEM in having to resolve every single particle in a large domain.

The original form of the $\mu(I)$ rheology is well-posed for a wide range of inertial numbers, but at high and low inertial numbers it is mathematically ill-posed. This means that the growth rate of linear instabilities is unbounded in the high number wave limit. This is a real problem, because it implies that numerical simulations will not converge to solution as a numerical grid is refined, and wave-like instabilities can grow catastrophically and break the numerical methods. One way of circumventing this is to use the partially regularized $\mu(I)$ rheology (Barker & Gray 2017 J. Fluid Mech. vol. 828, pp. 5–32.), which assumes that there is no yield stress, i.e. $\mu(0) = 0$, and uses the ill-posedness analysis to define a new frictional function $\mu(I)$ that is well-posed for all inertial numbers below a maximum threshold ($I_{\max} \simeq 17$). This theory enables reliable computations to be made with the incompressible $\mu(I)$ rheology that are grid converged over a wide range of inertial numbers. In particular, it is possible to couple the theory to recent models for particle-size segregation in multi-component mixtures (Gray

& Ancey 2011 J. Fluid Mech., vol. 678, pp. 353–588) and solve for segregating flows on chutes and in partially filled rotating drums. This is an important step towards simulating realistic granular materials that are composed of particles of differing sizes, as well as frictional and chemical properties. The resulting model is intimately coupled, because the inertial number is dependent on the particle size, so the local friction changes as the size distribution evolves during the flow. It is this fact that often leads to unexpected segregation in many industrial processes, which degrade the quality of the resulting products, and can cause severe flow problems.

A new class of granular rheologies have also recently been developed, which are called the Compressible I-Dependent Rheologies (CIDR). These essentially combine rate-independent Critical State Soil Mechanics (CSSM) with the rate dependence of the $\mu(I)$ rheology. In steady-state configurations these are designed to reduce to the classical $\mu(I)$ rheology, so they can capture the same steady-state behaviour observed in experiments and DPM/DEM simulations. However, by construction these theories are guaranteed to be mathematically well-posed and thermodynamically consistent. These models differ from the original $\mu(I)$ rheology in their transient response in time-dependent problems. The CIDR model is a framework, rather than a specific model, with considerable flexibility still available to design yield and dilatancy functions to match experiments and discrete particle simulations. Comparison of the inertial CIDR model (Schaeffer et al. 2019 J. Fluid Mech. 2019, vol. 874, pp. 926–951) with DPM/DEM simulations in one-dimensional time-dependent gravitationless shear, shows that it accurately captures the right transient response, whereas the compressible $\mu(I)$ rheology blows up catastrophically. The CIDR models include the important physical effect of compressibility, are mathematically well posed and probably show the greatest potential for the future, but at present a great deal of work needs to done to narrow down the appropriate yield and dilatancy functions, as well as develop robust numerical methods to solve the resulting equations in two and three dimensions.

The $\mu(I)$ rheology has also been incorporated into depth-averaged models. These exploit the shallowness of a flow in a particular direction to integrate through the flow depth and thereby remove one spatial dimension from the problem. Such models are potentially useful for computing flows in industrial transfer chutes, and are highly developed because of their application to large scale natural hazards, such as snow avalanches, rockfalls and debris flows. In particular, the depth-averaged $\mu(I)$ rheology naturally leads to the derivation of a dynamic basal friction law for chute flows that is dependent on the flow depth h and the Froude number $Fr = |\overline{\mathbf{u}}|/\sqrt{gh\cos\zeta}$, where $\overline{\mathbf{u}}$ is the depth-averaged velocity, g is the gravitational acceleration and ζ is the slope inclination angle. It is measurements of this basal friction law (Pouliquen 1999 Phys. Fluids vol. 11, 542–548) which actually led to the original development of the $\mu(I)$ rheology. Indeed, careful measurements of the depth-averaged flow velocity and thickness as a function

of slope angle still provides the primary means of determining the parameters in the $\mu(I)$ rheology. Tipping chute experiments should therefore become a routine rheological test to determine these parameters in future.

The $\mu(I)$ rheology is a very useful rheology that does a very good job of simulating many flows, however it is not a universal panacea. There are many flow features that it can not explain. For instance, when a steady uniform flow on a rough inclined plane is brought to rest by cutting off the supply, the grains do not all run off the chute, but they leave a deposit of thickness $h_{\rm stop}(\zeta)$. To get this material to flow again, the chute must be inclined to a steeper angle $\zeta_{\rm start}(h)$, which is the inverse function of $h_{\rm start}(\zeta)$. As a result, there is a metastable range of thicknesses $h \in [h_{\rm stop}, h_{\rm start}]$ within which flowing and static states can coexist. This leads to very rich flow behaviour, with the formation of (i) deposition waves, (ii) retrogressive failures, (iii) self-channelizing flows that are bounded by static levees and (iv) the formation of discrete wave pulses that progressively erode and deposit material as they propagate downslope. All of this behaviour can not be predicted by the $\mu(I)$ rheology alone, and are examples of non-local behaviour, i.e. the local behaviour of the flow is affected by motion, or otherwise, of the grains some distance away. In the case of these chute flow phenomena, it is the presence of the static basal boundary that is felt some distance away. Recent non-local models which capture some of these phenomena will be discussed.

Potential chapter titles

1. Experimental observations
2. The $\mu(I)$ rheology for granular flows
3. Simulation methods (Silos, rotating drums and column collapses)
4. Ill-posedness and partial regularization of the $\mu(I)$ rheology
5. Coupling rheology and segregation in granular flows
6. Well-posed Compressible I-dependent rheologies (CIDR)
7. Depth-averaged models incorporating the $\mu(I)$ rheology
8. Beyond the $\mu(I)$ rheology – weakly non-local behaviour

IFPRI Review Brief
Horizons in Dry Granular Modeling: Beyond DEM

The International Fine Particle Research Institute wishes to commission a comprehensive critical literature review of numerical methods for simulating the dynamics of dry particulate systems. IFPRI's membership is familiar with the discrete element method, and we have funded numerous projects and reviews of DEM, including an ongoing "round robin" project at the University of Birmingham that is exploring the accuracy of different DEM calibration approaches. However, for many of us, DEM is the *only* simulation method we know of for modeling kinematics and dynamics of granular systems. For this reason, we would like to commission a review of the state-of-the-art in modeling the dynamics of particulate systems *beyond DEM*.

The scope of the review is quite broad:

- Quasistatic through collisional flow regimes
- Soft through hard particles
- Non-cohesive through highly cohesive or adhesive particles
- Flows with and without interstitial gas
- General methods and techniques for particular scenarios, e.g., resistive force theory

Particle flows with interstitial liquids and Brownian systems are out of scope.

The primary audience for this review is the IFPRI membership, i.e., industrial scientists and engineers who are with some exceptions non-experts in simulations. Thus, the review should discuss the underlying principles, assumptions, and limitations of each technique. We hope that the review will eventually be published in the open literature.

Review outline

Horizons in Dry Granular Modeling: beyond DEM

By Farhang Radjai

22/12/2021

The **basic DEM** (Discrete Element Method) can be described as a method for the integration of equations of motion for a collection of simple (spherical) rigid particles interacting via frictional Hertz contacts. The motion of each individual particle is incrementally calculated from the forces acting on it by other particles and bulk forces such as gravity. In basic DEM scale separation is assumed between contacts and particles and the contact scale is resolved. However, since only particle motions are of interest, the contact scale is generally described by a *force law* involving overlaps and relative velocities (strain variables attributed to the contacts and calculated from rigid-body motions of the particles). For this reason, in close analogy with the Molecular Dynamics method, the DEM is defined in terms of two major ingredients: 1) Equations of motion, and 2) Contact force laws.

During the 1990s, the DEM evolved into a common simulation tool adopted by researchers and engineers in various fields. With rapidly increasing power and memory of computers, the DEM was subsequently extended to simulate particle clumps of arbitrary shapes, adhesion forces, electrostatic forces, solid bonding/debonding, and rolling resistance. This **extended DEM** is still the most common simulation tool for granular materials.

Radically new features have, however, been developed more recently and evolved into **advanced DEM** codes. These developments have been mainly driven by industrial applications, requiring realistic simulations of complex granular processes. These advanced features comprise *aspherical particle shapes*, *hybrid* discrete-continuous modeling, *liquid bridging*, coupling with a *fluid phase*, coupling with a *scalar field* (temperature, humidity, charge, chemical species…) or *vector field* (electrostatic, magnetic), highly *deformable* particles, and *comminution*. In contrast to the common lower-level DEM, these features are not generic, require specialized techniques and allied methods, and are based on more sophisticated data-handling procedures. They also raise hard efficiency, accuracy, calibration and validation challenges. The allied methods include FEM (finite element method), CFD (computational fluid dynamics), MPM (material point method), SPH (smoothed particle hydrodynamics), LBM (lattice Boltzmann method), LEM (lattice element method), and Peridynamics.

It is useful to represent the advanced features, often involving physics and techniques **beyond DEM**, with respect to the dynamics of a single particle, as illustrated in Fig. 1. Nearly all these features involve subparticle length scales ranging from contact scale to particle scale: pressure exerted by a fluid phase, internal stresses governing deformation and fracture, torques developed at cohesive extended contacts (face-face, face-edge…), interstitial liquid or solid

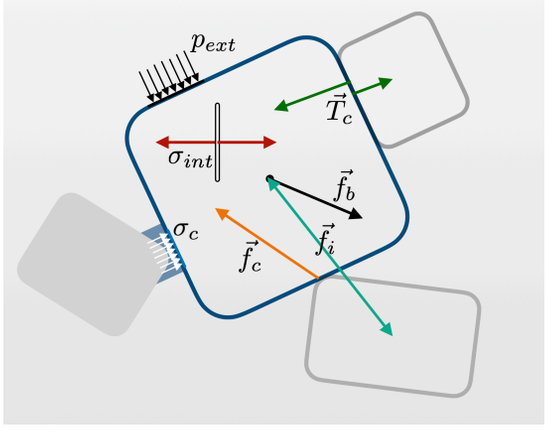

Fig 1. Schematic view of particle-scale and subparticle-scale forces acting on a particle.

phase stresses, long-range interbody forces (charged particles…), thermomechanical stress fields….

To account for multiple length scales and forces, four modeling strategies have been developed:

1) Subparticle resolution of particles, phases, fields and forces: The term DNS (direct numerical simulation) is often used for the methods of simulation of fluids at fine scales by solving Navier-Stokes equations or Boltzmann equation. This term can be generalized here to all other phases and fields such as cementing phase. Full resolution of particle shapes belongs to this category (for geometry).
2) Coarse-graining subparticle forces to the particle scale: Effects of subparticle forces are taken into account at the particle scale by averaging subparticle equations. The contact forces are excluded as they govern the collective behavior. Averaged subparticles forces become either contact forces or body forces acting on the particle centers. The interstitial phases can also be modeled at the pore scale and solved over the pore network.
3) Coarse-graining to a scale above the particle scale: The phase equations are solved on a grid containing several particles. Coarse-grained forces become body forces acting on the particles such as drag forces.
4) Coarse-graining both particles and forces to a scale above the particle scale: This leads to a continuum particle phase coupled with other continuum phases and fields.

The DEM refers essentially to the first three modeling strategies. Obviously, numerical efficiency increases from (1) to (4) at the expense of decreasing accuracy. The first strategy, despite its high computational cost, is needed for understanding the physical processes at fine scales and supports the elaboration of other strategies. The second strategy is closest to the spirit of DEM and it provides the best compromise between accuracy and efficiency. It can be compared to the *Potential of Mean Force* (PMF) used for mesoscopic simulations of nanoparticles (e.g. CSH cement particles and clay particles). For granular materials, this amounts to the elaboration of *enhanced force laws* based on both overlaps and interstitial or intercenter distance and involving stable minima (for cohesion), potential barriers (e.g. combination of capillary force and electric repulsion), evolving strength…, coupled with locally averaged fields (humidity, temperature, ionic species…). The four strategies have been extensively applied in powder technology for gas-particle flows. More recently, hybrid approached have been designed to describe different parts of a granular material alternatively as discrete or as a continuum depending on a criterion, allowing therefore to benefit from the advantage of accuracy for regions where high resolution is needed (for example at the outlet of a silo) and the advantage of efficiency where a spatial low resolution is sufficient (for example in the core of a silo flow).

Many recent developments concern *particle shape*. Different fully analytic particle shapes, digitalized real shapes and general representations based on spherical harmonics have been considered with smooth surface. However, common overlap-based force laws have mostly been used without properly accounting for the changes of curvature. Consistent contact force laws accounting for the geometry should be formulated based on energy considerations. A special case concerns force laws for extended contacts, e.g. face-face and face-edge contacts between polyhedral particles. Such contacts require at least two (for face-edge) or three (face-

face) contact points since a line is parametrized by two points and a surface by three points. Without this description adhesive extended contacts cannot transmit torques.

Simple reversible or irreversible *cohesive force laws* have been used to investigate the rheology of cohesive or cemented granular materials. It is often assumed that the effects of cohesion are uniquely controlled by the maximum tensile force sustained by the contact. However, it happens that the effective cohesive action of forces crucially depends on both contact stiffness and damping coefficients. This means that the contact stiffness cannot be downscaled (for the sake of numerical efficiency) raising therefore a difficult scaling problem for the simulation of cohesive powders. Such a dynamic effect is also relevant for *liquid bridges* in the pendular state where an approximate solution of the Young-Laplace equation in equilibrium is generally used. Extending the capillary force law to dynamic situations is necessary for the simulation of wet granular flows even in the pendular state.

Regarding rough particle surface states, the general understanding is that they can be coarse-grained into enhanced friction force. However, *elastic asperities* lead to enhanced stress concentration and significant deviation from the Hertz regime. The asperities can be fully included as part of particle shape (first strategy), but a coarse-grained contact force law accounting for roughness size and angles can provide an interesting shortcut for DEM simulations. This is more specifically important for *plastic asperities*. The effect of damageable asperities can even be more complex with effects depending on how debris particles move inside the granular materials. They can lead to enhanced dissipation or solid lubrication with adverse effects for friction.

Particle fracture and deformation involve *internal texture* and stresses inside particles. A fine treatment (first strategy) can be achieved by incorporating *fracture mechanics* in a continuum representation of each particle. This approach has been applied by means of FEM, MPM, LEM and Peridynamics in 2D and 3D. Two major issues arise for the simulation of contacts between meshed particles: 1) The usual overlap-based or penalization approach makes no more sense, and 2) fine meshing in the volume does not imply a fine meshing of the surface. Hence, a specifically fine meshing of particle surface is required and the contact needs to be enforced as a *unilateral constraint*. This aspect strongly moves the method away from the spirit of DEM, which is based on contact force laws, although the particles remain discrete entities and their contacts bear friction forces. A coarse-grained approach (second strategy) is possible to particle fracture and large deformations by “making soft from hard”, i.e. by subdividing each particle into rigid cells interacting through force laws. This *bonded particle method* has been applied and characterized, with several promising results. However, the interactions between primary particles should be further worked out in the light of what was discussed previously about the interaction laws between particles in order to implement correctly the material behavior (elastic, plastic…) and *dynamic fracture* (involving second law of thermodynamics).

Since for advanced DEM we are concerned with realistic simulations at the industrial level (and not only with a better understanding of physical mechanisms and qualitative description of phenomena), the calibration issues are of paramount importance. Clearly, the DEM is an intrinsically predictive method with physical parameters fed into the system at the particle scale to predict the overall behavior emerging from the collective interactions of the particles. This *bottom-top approach* faces the challenge of measuring the relevant parameters at fine scales. There are not many examples in the literature based on this type of calibration and validation. In contrast, in many examples can be found with a *top-down approach* based on

the adjustment of particle-scale and contact parameters to fit to a macroscopic descriptor of the material.

There are several major issues that need to be solved in this respect: 1) There has not been enough fundamental research reported on the sensitivity of macroscopic (or effective) properties to the micro-scale (particle-scale and contact) parameters. Most parameters considered so far describe static packings of grains rather than *dynamic properties*; 2) Some micro-scale parameters have no influence on the (known) macroscopic parameters. For example, the interparticle friction coefficient bears on the angle of repose only for values below 0.5; 3) Furthermore, some micro-scale parameters may well be ineffective in steady states or in static equilibrium but effective in dynamic transients. This is the case for the restitution coefficient, which controls the compaction rate but not the solid fraction in the final stages of compaction; 4) Last, but not the least, we are used to assume that the particles have well-defined parameter values. In practice, however, one often observes high *variability*. This variability is well known, for example, in the case of particle fracture and characterized by the Weibull distribution. For other parameters, such as friction coefficient, no information is available. Such a variability can be included in the DEM, but the corresponding parameters should be provided from measurements. It is also important to note that finite numerical precision is a source of variability in normal restitution coefficient.

As mentioned previously, *gas-particle flows* have been modeled through the four modeling strategies in connection with applications to chemical and pharmaceutical processes. The first approach is known as particle-resolved DNS. The multicomponent LBM is increasingly used as a volatile method with improved treatment of no-slip condition and momentum exchange at the particle surface using methods such as immersed boundary. The second approach consists in considering gas flow through the pore network and a *pore-scale finite volume* scheme. In the third approach (Euler-Lagrange or *CFD-DEM*) the equations of fluid are averaged and solved together with expressions of effective fluid stress and forces between particles and fluid in a Eulerian framework. In the fourth approach (Euler-Euler or two-fluid model) transport equations are applied to averaged variables of both fluid and particles. This approach needs models of phase stresses and the interface between the two phases.

Advanced DEM simulations with resolved or partially resolved fields and phases involve much larger numbers of degrees of freedom than the basic DEM. Fully resolved simulations even for a few thousands of particles are possible only with *parallelized codes* or *GPU* techniques. Moreover, the huge amount of simulation data requires smart strategies for storage, access and analysis. For example, a single gas-particle simulation using a coupled DEM-LBM approach produces several terabytes of information. Future developments can benefit from progress in data science and *Machine Learning* techniques to manage both run-time data flows and post-processing procedures to extract meaningful information from raw data.

This review will expand and illustrate all the aspects mentioned in this brief outline. Here is a list of major topics that will be covered:

Gas-particle flows
Highly deformable particles
Particle fragmentation
Particle shapes and contacts

Generalized force laws
Cohesive interactions
Tribocharging
Cementing bonds
Capillary bridges
Transport of scalar and vectorial variables by particles and contacts

Coarse-graining
Data-driven approaches
Hybrid discrete-continuum approaches
Upscaling particle size
Calibration issues
Validation strategies